UNIVERSITA' DEGLI STUDI DI PADOVA

Sede Amministrativa: Università degli Studi di Padova

Dipartimento di Scienze Cliniche Veterinarie

SCUOLA DI DOTTORATO DI RICERCA IN : Scienze Veterinarie

INDIRIZZO: Scienze Cliniche Veterinarie

CICLO XXI

Comparison of a 3-dimensional model and standard radiographic evaluation of femoral and tibial angles in the dog

Direttore della Scuola : Ch.mo Prof. Massimo Morgante

Supervisore : Prof. Maurizio Isola

Dottorando : Silvia Meggiolaro

ABSTRACT

MEGGIOLARO SILVIA, Comparison of a 3-dimensional model and standard radiographic evaluation of femoral and tibial angles in the dog.

Bone deformities are a common problem in veterinary medicine. These problems are frequently related to the main hind limb pathologies that commonly affect our animals, such as hip dypslasia, cranial cruciate ligament rupture and patellar luxation. It has been demonstrated that a precise and accurate preoperative planning is crucial to the success of the corrective surgeries.

The assessment of hind limb deformities has been studied in the past years and up till now there is still a lot of confusion in understanding what could be the best method to apply for a correct evaluation of the deformity. Several methods have been suggested to measure femoral and tibial angles, some studies suggested even an assessment using computed tomography and magnetic resonance imaging. During the last years new methods combining traditional images with reverse engineering technique have been suggested too but although the use of different techniques have been described, radiographic measurement still represents the most common method used for the interpretation of hind limb deformities.

This study aimed to compare a 3-dimensional model with standard radiographic evaluation of femoral and tibial angles.

Cadavers of eight adult dogs, deceased for reason unrelated to this study, were obtained. Radiographs were obtained using four standard projections: an elevated-torso/hip-extended radiograph, a mediolateral radiograph of the femur, a caudocranial view of the stifle joint and a mediolateral radiograph of the stifle. All radiographs included in the study were made by two single individuals and reviewed and approved in terms of quality and positiong by three different examiners.

Evaluation of the neck-shaft angle, the aLPFA, mLPFA, aMDFA and mMDFA, the angle of version and the varus angle for the femur and of the mMPTA, mMDTA and MAD for the tibia, was performed applying the main methods available in literature.

After femoral and stifle radiographs were made of each cadaver, the femurs and tibia were harvested and freed of all of the soft tissues sparing the articular cartilage. Every bone was then scanned to create a 3-dimensional computed model.

Using RAPIDFORM 2006 (Inus Technology INC.) we could manipulate the shell to evaluate all of the angles previously determined in the 2-dimensional model.

The average error in assessing mLPFA , mMDFA , mMPTA and mMDTA, was less than 5% comparing the 2-dimensional method with our 3-dimensional model. Based on these findings, we feel that the reported radiographic methodologies and values may be used to diagnose and quantify hindlimb deformities with a good accuracy.

aLPFA and aMDFA values were acceptable for three of the four methods and neck-shaft angle was better represented from the combination of Symax method for the neck axis and Kowalesky's method for the anatomic one.

RIASSUNTO

MEGGIOLARO SILVIA, Confronto tra un modello 3-dimensionale e il metodo radiografico standard nella valutazione degli angoli femorali e tibiali del cane.

Le deformita' ossee rappresentano un problema relativamente comune in mediacina veterinaria. Queste alterazioni sono frequentemente associate ad alcune delle principali patologie ortopediche dell'arto posteriore che comunemente affliggono i nostri animali, come per esempio la displasia dell'anca, la rottura del legamento crociato craniale e la lussazione di rotula. E' stato dimostrata la necessita' di eseguire planning preoperatori accurati e precisi, cio' risulta fondamentale per il successo di eventuali chirurgie correttive.

Le principali linee guida per la misurazione delle deviazioni ossee sono state studiate nel corso degli anni e ad oggi persiste un ampio dibattito su quale possa essere considerato il metodo migliore per una valutazione delle deformita'. Sono stati suggeriti diversi metodi per la misura degli angoli femorali e tibiali, alcuni lavori suggeriscono l'impiego di tac e risonanza magnetica. Durante gli ultimi anni sono stati proposti metodi innovativi che combinano le metodologie tradizionali con l'impiego di elaborati software ingegneristici per la rielaborazione delle immagini e creazione di modelli tridimensionali. Nonostante sia stato suggerito l'impego di diverse tecniche, nel panorama odierno la radiografia continua a rappresentare il metodo piu' comunemente utilizzato per l'interpretazione delle deformita' scheletriche dell'arto posteriore.

Questo studio vuole confrontare un modello 3-dimensionale e il metodo radiografico standard nella valutazione degli angoli femorali e tibiali.

Sono stati ottenuti otto cadaveri di cani adulti, deceduti per cause esterne allo studio. Tutti i soggetti sono stati sottoposti a studio radiografico di entrambi gli arti posteriori, eseguendo quattro proiezioni standard: una proiezione ventrodorsale “a cane seduto”, una proiezione mediolaterale del femore, una caudocraniale ed una mediolaterale del ginocchio e della gamba. Tutte le radiografie incluse nel presente studio sono state selezionate in termini di qualita' e posizionamento da tre diversi operatori.

E' stata quidi eseguita la valutazione dell'angolo cervico-diafisario, dell'aLPFA, mLPFA e mMDFA, l'angolo di versione e l'angolo di varismo femorale per il femore, e

dell'angolo mMPTA, mMDTA e MAD, per la tibia, utilizzando alcuni dei principali metodi descritti in letteratura.

Dopo l'esecuzione delle proiezioni radiografiche, sono stati scheletrizzati i femori e le tibie risparmiando la cartilagine articolare. L'immagine di ogni osso e' stata quindi acquisita tramite l'impiego di uno scanner per creare successivamente un modello tridimensionale.

Usando il programma RAPIDFORM 2006 (Inus Technology INC.) abbiamo potuto lavorare con il nostro modello per valutare tutti I valori precedentemente calcolati nell'immagine radiografica.

L'errore medio nella valutazione del mLPFA , mMDFA , mMPTA and mMDTA, e' stato inferiore al 5% confrontando il modello bidimensionale con quello tridimensionale. Basandoci su questi risultati ci sentiamo di suggerire che le metodologie radiografiche descritte possono essere utilizzate per diagnosticare e quantificare le deformita' degli arti posteriori con una buona accuratezza.

I valori ottenuti per gli angli aLPFA e aMDFA sono stati accettabili in tre dei quettro metodi applicati mentre il metodo che meglio ha rappresentato l'angolo crevico-diafisario e' risultato dalla combinazione dell'utilizzo dell'asse cervicale Symax con l'anatomico di Kowalesky .

I metodi utilizzati per il calcolo degli angoli di varismo femorale, verione e MAD sono risultati non accettabili con un valore del parametro p significativamente > 0.1 in tutti I casi.

TABLE OF CONTENTS

TABLE OF ABBREVIATION iii

1. INTRODUCTION 1

2. LITERATURE REVIEW 3
   - 2.1 Introduction to hind limb pathologies related to misalignment 3
     - 2.1.1 Common orthopedic disease 4
   - 2.2 Biomechanic of the hind limb 9
     - 2.2.1 Biomechanic of the normal hip joint 9
     - 2.2.2 Biomechanic of the stifle joint 12
   - 2.3 Radiographic assessment of hind limb deformities 19
     - 2.3.1 Radiographic study of the femur 19
     - 2.3.2 Radiographic study of the tibia 21
     - 2.3.3 Femoral radiographic measurement 23
     - 2.3.4 Tibial radiographic measurement 33

3. MATERIALS AND METHODS 37
   - 3.1 Inclusion criteria 37
   - 3.2 Radiographic measurements 37
   - 3.3 3-dimensional measurements techiques 39
     - 3.3.1 3D evaluation of the femur 40
     - 3.3.2 3D evaluation of the tibia 46

4. RESULTS 49
   - 4.1 Femoral evaluation 49
   - 4.2 Tibial evaluation 52

5. DISCUSSION 54

6. CONCLUSION 61

7. REFERENCES 63

APPENDICES 69
Appendix A 70
Appendix B 87

TABLE OF ABBREVIATIONS

Table 1: abbreviations used in this paper

aLPFA	anatomic lateral proximal femoral angle
aMDFA	anatomic medial distal femoral angle
AP	anteroposterior
CaCL	caudal cruciate ligament
CAD	computer aided design
CrCL	cranial cruciate ligament
CrTT	cranial tibial thrust
CT	computed tomography
DFLA	distal femoral long axis
Fa	abductor muscle force
Fh	hip reaction force
FHNA	femoral head and neck axis
Fk	ground reaction force
Fo	body weight
FTA	femoral torsion angle
FVA	femoral varus angle
MAD	mechanical axis of deviations / mechanical angle of deviation
ML	mediolateral
mLPFA	mechanical proximal femoral angle
mMDFA	mechanical medial distal femoral angle
mMDTA	mechanical medial distal tibial angle
mMPTA	mechanical medial proximal tibial angle
Mo	spinal torque
OCD	ostechondritis dissecans
PFLA	proximal femoral long axis
ROM	range of motion
TCA	transcondylar axis
TPA	tibial plateau angle
TPLO	tibial plateau levelling osteotomy
TPS	tibial plateau slope

1. INTRODUCTION

Angular deformities of the canine pelvic limb are relatively common and related to the main pathologies that commonly affect our animals. During the last decades biomechanic factors involved in the pathogenesis of hip dysplasia, patellar luxation and cranial cruciate ligament rupture have been studied trying to understand failures of common surgeries. It has been demonstrated that an inadequate correction of femoral or tibial deformities can be a cause of postoperative recurrence of medial patellar luxation or implant failures in case of cranial cruciate ligament rupture [29; 38; 63].

Corrective osteotomies are generally performed to treat limb misalignment: altough it is crucial to perform a precise and accurate preoperative planning when approaching this kind of surgery.

Evaluation of hind limb alignment is usually accomplished by radiographic projection of both limbs but there are some limits such as the lack of informations due to the by dimensionality of radiography instead of the three dimensionality of the bone.

Recently, the measurement of some angles in dogs using magnetic resonance imaging have been reported, as well as the description of the use of CT [24; 65]. During the last years new methods combining traditional images with reverse engineering technique have been suggested too [25-28; 34; 62]. Although the use of different techniques have been described, radiographic measurement still represents the most common method used for the interpretation of hind limb deformities. Unfortunately there is not a real standardization in ranging values and radiographic measurements still can be confusing due to the existence of several methods.

Measurements obtained in a real bone or a 3-dimensional model could be more realistic offering a good chance to perform an adequate assessment of the deformity.

The purpose of this research is to compare the available radiographic methods with a new 3-dimensional model that we designed through the collaboration with a team of engineers at the university of Padua.

All the measurements will be performed in 8 dogs of different breeds deceased for reasons unrelated to this study, a total number of 16 femurs and 16 tibiae will be

evaluated with both radiographic and 3D method for assessment of femoral and tibial angles.

It is hypothesized that the 3-dimensional method is the most accurate in the assessment of hind limb deviations.

2. LITERATURE REVIEW

2.1 Introduction to hind limb pathologies related to misalignment

Bone deformities are relatively common in both humans and animals. To understand deformities and limits of normal alignment, the exact anatomy of the femur, tibia, hip, knee, and ankle is of great importance. Anatomic planes are crucial in studying misalignment of the long bones as deformities can be referred to either the frontal, sagittal, or transverse anatomic planes [5; 44].

Angular deformities that occurs in the coronal (frontal) plane are the most common deformities of the hind limb and are better known with the terms of varus and valgus. In orthopedics, a varus deformity represents the inward angulation of the distal segment of a bone or a joint (in this case it always refers to the direction that the distal segment of the joint points). Varus deformity of the hip is called coxa vara, it is a reverse where the neck-shaft angle is reduced .

Varus/valgus deformities can be either referred to other joints such as stifle and ankle joints. Varus deformity of the knee is called genu varum characterized by medial angulation of the leg in relation to the thigh, an outward bowing of the legs, giving the appearance of a bow (that is why it is also known as bowleg). Usually there is an outward curvature of both femur and tibia. In human medicine it is distinguished from Blount's disease because this affects only the tibia with no femur involvement.

Alternately, a valgus deformity is a term for the outward angulation of the distal segment of a bone or joint. Valgus deformity of the hip is called coxa valga, in this case the shaft of the femur is bent outward in respect to the neck of the femur, on the other hand, genu valgum, commonly called “knock-knees”, is a condition where the knees angle in and touch one another when the legs are streightened.

The terminology may be confusing by the etymology of these words: in Latin, varus actually means “knock-kneed” and varus means: bowlegged”. In human medicine, a knock-kneed person is a person which femur is deviated inward in relation to the hip (varus deformity of the hip) but in the same knock-kneed person, the opposite situation is found at the knee, with the distal segment now being deviated outward, so the term

valgus is used for the knee. It is correct for a knock-kneed deformity to be called both a varus deformity at the hip/femur and a valgus deformity at the knee/tibia, although the common terminology is to refer to it as genu valgum.

Sagittal plane deformities usually occurs more often in the front limb, they can be either referred to a recurvatum or a procurvatum deviation.

Transverse plane deformities can be divided into two groups: torsion and rotation. Torsion is a rotation of a portion of an extremity with relationship to the long axis of the entire extremity; rotational deformity is slightly different as it is referred to a bone in relation to another. Torsion and rotation can be either internal or external [67].

Most deformities are developmental and can be treated early, in skeletally immature patients. Adults also have deformities that may result from metabolic diseases, malunions, or untreated developmental deformities. Either way understanding hind limb deformities is crucial as misalignment can cause some of the most common orthopedic disease. The overall alignment, and thus biomechanics, of an entire weight-bearing are likely to be affected even if the deformity is isolated to a single bone. It has been established that malalignment of a bone results in degenerative changes of the associates joints over time. Further, developmental angular deformities of a single bone within the pelvic limb of dogs can result in compensatory angulation of the other bones within the limb.

In humans, femoral varus and torsional abnormalities have been reported in patients with various congenital or developmental disorders, including Blount's disease, and fracture malunion. Secondary effects and torsional abnormalities in human include miserable malalignment syndrome or “anterior knee pain”, and progressive osteoarthritis of the knee and hip joints [53]. In veterinary medicine, pathologic femoral varus and/or torsion abnormalities have been implicated in the pathogenesis of patellar luxation and canine hip dysplasia [24; 37; 46].

2.1.1 Common orthopedic diseases

Canine hip dysplasia is a developmental disorder characterized by instability of the hip joint that mainly affects medium- and large-breed dogs. It has been reported that hip

dysplasia can be related to some hind limb deformities. An internal torsion of the femur or either an excessive anteversion can be involved in the pathogenesis of hip dysplasia.

As we will see, in a normal situation the hip reaction force (vector sum of the body weight and the abductor muscle force) is distributed over a large articular area which reduces cartilage stresses; factors such as an increased neck-shaft angle (coxa valga) and excessive femoral anteversion will result in increased abductor demand and therefore increased joint loading. Increased abductor demand can cause hip subluxation and excessive loading in small areas of the femoral head with consequent cartilage erosion [5; 68].

Furthermore an excessive femoral anteversion may cause an external rotation of the proximal femur with a compensatory internal rotation of the pelvic limb. This internal rotation displaces the origin of the quadriceps muscle group medially in relation to the long axis of the femur, plus compensatory rotation of the foot. In order for the foot to be placed properly,the dog must externally rotate the tarsal joint, which results in external torsion on the distal tibial growth plate [5].

Alternately a retroversion may cause an external rotation of the hip and a consequent tibial internal rotation, this can be followed by a lateral torsion of the femur due to abnormal forces.

Coxa valga and excessive anteversion may also determine genu valgum and inward hocks, this can be observed even with ostechondritis dissecans (OCD) of the lateral femoral condyle.

OCD can have additional limb alignment pathology associated with the longer limbed dogs, for example, the Great Dane puppy who has developed OCD of the lateral condyle may create a genu valgus secondary to the loss of the cartilage surface. Genu valgus allows a craniomedially rotary instability at the stifle. Due to this instability an excessive pressure at the stifle will occur stretching the anteromedial joint capsule just cranial to the medial horn of the meniscus along the medial margin of the tibial plateau. This deformation creates greater pressure on the lateral portion of the physis and a proximal tibial valgus or distal femoral valgus may result. In addition a lateral patellar luxation or a lateral placement of the tibial tubercle may be a response to the abnormal forces created by this valgus growing limb [59; 60].

Furthermore OC creates a loss of femoral length on the medial femoral condyle (genu varum) and a lack of bony spacer (due to the loss on the joint space with the OCD

lesion) that allows a laxity of the cruciate ligaments which may be mistaken for a rupture of the cranial cruciate ligament. Both the genu varum and the ligamentous laxity allow an excessive internal rotation at the stifle. The consequence is deviation of the quadriceps mechanism at the patella and stretching of the lateral fabellopatellar ligament and joint capsule. Naturally, medial patellar luxation follows [59; 60].

Patellar luxation is one of the most common orthopaedic conditions encountered in dogs [14; 15; 39; 49].

Medial patellar luxation is much more common than the lateral one [38]. A grading scheme for medial patellar luxation is presented in Table 2.1.

	Grading System for Medial Patellar Luxation
Grade 1	Patella can be luxated medially when the stifle joint is held in full extension. There is no crepitation or bony deformity. Clinical signs are not present or occur infrequetely
Grade 2	Spontaneous luxation occurs with clinical signs of a nonpinful, “skipping” type of lameness. Mild deformities develop, consisting of internal rotation of the tibia nad abduction of the hock. This condition may progress to a grade 3 luxation with associated cartilage erosion on patellar and trochlear surfaces
Grade 3	Patella is luxated permanently but can be reduced manually. More severe bony deformities are present, including marked internal tibial rotation and an S-shaped curve of the distal femur and proxiaml tibia. A shallow trochlear groove may be palpable. The clint often complains of an abnormal “crouched” gait rather than intermittent lameness because the dog often uses the leg in a semiflexed, internally rotated position. This condition is often bilateral
Grade4	This is a severecondition with permanent, nonreducible luxation of the patella. The tibia is rotated from 60° to 90° relative to the sagittal plane. If not corrected early in life, severe bony and ligamentous deformities develop and often are not reparable.

Table 2.1 From Singleton WB: The surgical correction of stifle deformities in the dog. J Small Anim Pract 1969; 10:59.

The aetiopathogenesis of canine patellar luxation has been extensively reviewed and many factors have been related to the development of this condition [21; 22; 41; 59; 60].

1. Valgus of the Proximal Tibia: this is an an outward deviation of the tibia that displaces the foot lateral to the stifle causing an external rotatory force which produces external rotation at the stifle. This conformation may deviate the quadriceps mechanism laterally and result in craniomedial rotatory instability of the stifle and a lateral patellar luxation.
2. Medial Displacement of the Tibial Tubercle: it is important to remember that the normal alignment of the hindlimb is present when the patella, the tibial tubercle, the hock and the foot are all in the sagittal plane. If the tibial tubercle is pathologically positioned medial to the sagittal plane, the quadriceps mechanism will have a medial deviation beginning at the patella that eventually will luxate medially.
3. Internal tibial torsion: this is an internal twisting of the tibia around its functional long axis that causes the entire stifle to be lateral to a line between the femoral head and the foot.
4. Retroversion of the Femoral Head: this conformation causes the patient to externally rotate the hip in order to achieve a proprioceptively neutral joint. This necessitates the internal rotation of the stifle to allow the foot to be in the sagittal plane. In this situation the quadriceps mechanism is deviated at the patella stretching the fabellopatellar ligament and retinaculum.
5. Distal femoral varus: it has been reported that values greater than 10 degrees create an internal rotatory force which is inadequately opposed by the biceps femoris muscle. This may cause e a medial patellar luxation due to capsular stretching.
6. Crouch and External Rotation of the Hip: Springer spaniel hunting crouch is a characteristic of the breed. The crouch is accomplished by externally rotating the hip, internally rotating the stifle, and lowering the center of gravity of the dog by flexing its joints. The crouch position will develop extremely large biceps femoris muscles. The rectus femoris is the only head of the quadriceps which arises on the pelvis and inserts on the tibial tubercle. The other three heads arise on the femur. With the dog in the crouch position, the straight-line pull of the

rectus femoris is deviated medially beginning at the patella. The consequence is a medially directed force on the patella that may stretch the lateral fabellopatellar ligament and joint capsule.

It has been suggested that medial patellar luxation increases the stress on the cranial cruciate ligament predisposing to degeneration and rupture [69], however it is proved that the prevalence of cranial cruciate ligament injury in dogs with patellar luxation is not different when compared with dogs with other orthopaedic conditions [20]. Furthermore it has been suggested that cranial cruciate ligament tears may facilitate patellar luxation. Ruptures of the cranial cruciate ligament allow cranial displacement of the tibia with respect to the femur and that translation reduces the femoropatellar compression. This often results in a medial patellar luxation which will continue until the cranial cruciate ligament rupture is treated.

Some of the deviations involved in the pathogenesis of patellar luxation can either contribute to cranial cruciate ligament rupture. For example the internal rotatory force at the stifle, related to the distal varus deformity of the femur, may rupture of the caudal half of the cranial cruciate ligament followed by rupture of the cranial half of the cranial cruciate ligament. For the same reason, internal tibial torsion and medial displacement of the tibial tubercle may damage the cranial cruciate ligament too.

A particular deformity that can involve the proximal epiphysis of the tibia is the high inclination of the tibial plateau [56; 57; 58; 61].

It has been suggested that slope of the tibial plateau greater than 30 degrees cause an internally generated force (cranial tibial thrust) that forces the tibia to displace cranially. The cranial tibial thrust caused by axial compression of the tibia on that sloped tibial plateau can be sufficient to stretch or rupture the cranial cruciate ligament.

Ruptures of the cranial cruciate ligament allow cranial displacement of the tibia with respect to the femur and that translation reduces the femoropatellar compression. This type of patient often lacks the cranial prominence created by the patella on the lateral silhouette of the hindlimb. The cranial translation of the tibia and the straight-line pull of the quadriceps mechanism to the tibial tubercle causes this peculiar long thigh appearance. In addition these patients are characteristically bandy-legged secondary to internal tibial torsion which creates internal rotation at the stifle. This often results in medial patellar luxation.

2.2 2.2 Biomechanic of the hind limb

Several studies have been made to evaluate the hindlimb angles and the results are extremely various due to the different morphology in the canine population.

In general we can assume that the pelvis has a cranial inclination of around 40° in the horizontal plane, the femor has a caudal angle of around 105° and an abduction angle of 10°; the tibia has a cranial angle of 105° related to the ground. The femor is proximally related to the acetabulum with a cranial angle of around 110° and distally with the tibia with a caudal angle of around 130° [5].

In the past years many Authors have tried to define the normal Range of Motion (ROM) of the different joints in the canine population. Jagger et al have demonstrated that the normal hip ROM in Labrador Retrievers can be considered between 50° and 162°, instead a normal stifle ROM is around 41° in flexion and 162° in extension [23].

2.2.1 Biomechanic of the normal hip joint

The normal anatomy of the hip joint is a classic ball and socket joint. A ball and socket joint has the ability to rotate about the three orthogonal (XYZ) axes. With respect to the hip, the femur can rotate back and forth (flexion/extension), medial and lateral (adduction/abduction), and can rotate "toe in"/"toe out" (internal/external rotation).

The biomechanic of the hip joint is strictly related to the anatomy of the joint, the integrity of the ligaments, tendons, muscles and cartilage and to the distribution and the intensity of the forces acting on the hip. The forces exerted on the hip have their biological expression in the form of the femur and acetabulum, particularly in the location and orientation of the trabecular pattern.

A theoretical model in dogs was developed to analyze the biomechanic of the normal and diseased canine hip and the effect of various therapeutic procedures on the forces acting on the hip [4]. Dogs have the ability to develop a spinal torque that acts with the abductor muscles to balance the pelvis during three-legged stance. As a result of this addictional torque, forces at the hip joint are relatively smaller in dogs than in humans.

As in humans, this force increases with the coxa valga, abduction, and subluxation of the joint but decreases with varization of the femoral neck and with hip adduction. It is important to understand that in general the center of the femoral head is extended medially and proximally by the femoral neck so that the center of the femoral head is at the level of the tip of the trochanter. The effect of the overhanging head and neck is to lateralize the abductors, which attach to the greater trochanter, from the center of rotation (center of the femoral head). This increases the torque generated by the abductors and reduces the overall force necessary to balance the pelvis during single leg stance (in humans) or three leg stance (in quadrupeds). Reducing this level arm (coxa valga) increases total load across the hip, and coxa vara reduces it to the extent it increases the lever arm [47].

Arnockzy et al. developed a biomechanical model to study the different forces acting about the canine hip. It has been shown that the hip reaction force (Fh) is the summation of several vectors. As the center of gravity lies medially to the center of the coxofemoral joint, body weight will exert a turning motion around the center of the femoral head so the fulcrum effect of the body weight results in a level arm (Lg) that is equal to the difference between the center of gravity and the center of the femoral head. This turning motion must be offset by the combined abductor forces inserted into the lateral femur (in particular the gluteus muscles). Hip reaction force is the vector sum of the body weight and the abductor muscle force [4; 5; 17; 68] (figure 2.1).

It has been demonstrated in both humans and dogs that the orientation of the hip force closely coincides with the orientation of the medial trabecular system of the femoral neck, thus optimizing its resistance to bending stresses.

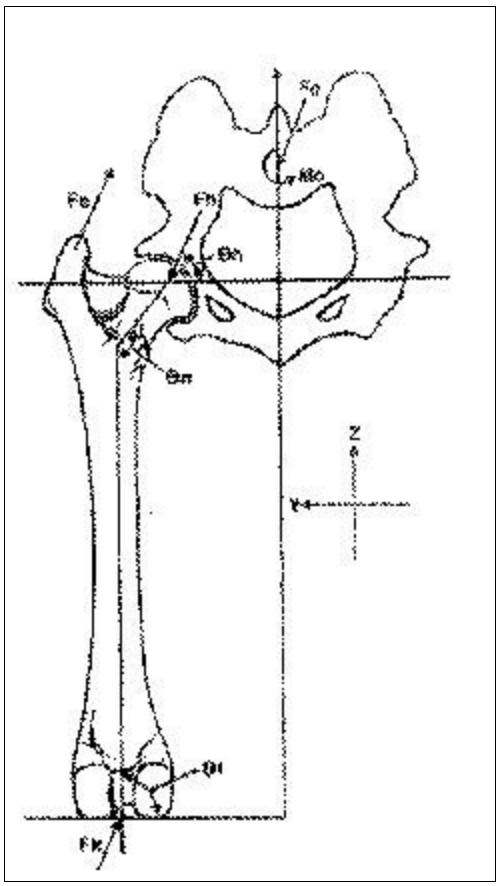

Figure 2.1 Schematic drawing illustrating the main frorces acting about the hip in the transverse (zy) plane. Fa: abductor muscle force; Fo: body weight; Fk: ground reaction force; Fh: hip reaction force; Mo: spinal torque balancing the pelvis. Important angles: hip reaction force angle (θh), neck shaft angle (θn) and abduction-adduction angle (θf). (Arnockzy SP, Torzilli PA. Biomechanical analysis of the forces acting about the canine hip. Am J Vet Res, 1981. 42:1581-1585.)

The combined force of the abductors is strong enough to keep the femoral head into the acetabulum. This function is preserved when a normal containment (related to the configuration of the hip) and congruity are guaranteed.

In a normal situation the hip reaction force is distributed over a large articular area which reduces cartilage stresses.

The factors influencing both the magnitude and the direction of the compressive forces acting on the femoral head are 1) the position of the center of gravity; 2) the abductor lever arm, which is a function of the neck-shaft angle; 3) the magnitude of body weight; 4) the length of the femoral neck; and 5) the position of the throcanter. Shortening of the abductor lever arm through coxa valga or excessive femoral anteversion will result in increased abductor demand and therefore increased joint loading.

Understanding of the forces that cross the hip and of the details of the anatomy leads to a better understanding of some of the failures of the past and helps to better

make a decision for a surgical treatment of hind limb pathologies such as hip dysplasia [4; 47; 68].

2.2.2 Biomechanic of the stifle joint

The stifle joint is a complex hinge joint with two functionally distinct articulations. Weight bearing occurs primarily through the articulation between the femoral and tibial condyles. The femoropatellar articulation greatly increases the mechanical efficiency of the quadriceps muscle group and facilitates extensor function.
Different movements can be performed: because of ligamentous constrains and the complex geometry of the articulations involving the femoral and tibial condyles and the menisci, in particular, the irregular contours of the femoral condyles, simple uniplanar rotation about a stationary axis does not occur [3]. Flexion and extension occurs in the sagittal plane, with the normal range of motion being about 140° [35] but with flexion the lateral collateral ligament relaxes and allows the lateral femoral condyle to displace caudally, resulting in internal rotation of the tibia; conversely, during extension, the lateral collateral ligament tightens and causes the lateral femoral condyle to move cranially, resulting in external rotation of the tibia (Figure 2.2).

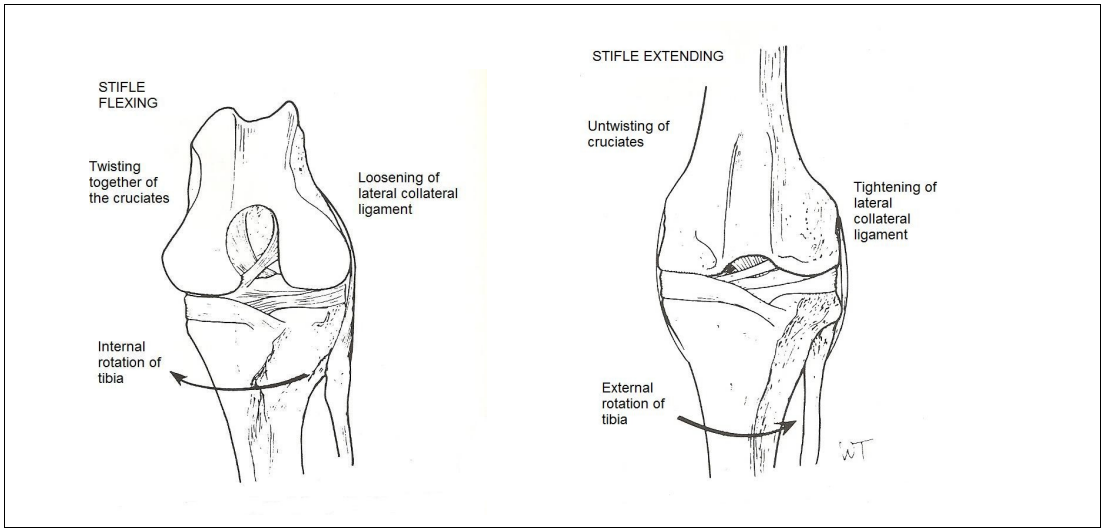

Figure 2.2 Frontal view of the stifle. Note that in flexion the lateral collateral ligament allows an interrnal rotation instead in extension this ligament is tight causing an external rotation.
(Arnoczy S.P.: Meccanica patologica dei traumi a carico dei legamenti crociati e dei menischi. In: Boyrab M.J. *Le basi patogenetiche delle malattie chirurgiche nei piccoli animali.* S. Lazzaro di Savena-Bologna: Giraldi Editore, 2001, 1023-1038)

In general, we can assume that the normal range of motion is 40° in flexion and 148° circa in extension. The allowed rotation degree is strictly connected with the flexion/extension movements: the intrarotation is around 6° with extension and 19° with flexion, the external rotation is 5° with extension and 8° with flexion [3].

A small amount of craniocaudal motion also occurs in the sagittal plane as a result of the cam shape of the femoral condyles: these roll caudally with flexion and cranially with extension, relative to the tibial plateau [22].

Slight varus and valgus movement of the tibia occurs in the transverse plane. The collateral ligaments are responsible for limiting this motion in the extended joint; with flexion the cruciate ligaments also contribute to the control of these movements [22; 66].

The ligaments that mainly play role in the biomechanic of the stifle are the cranial cruciate ligament (CrCL) and the caudal cruciate ligament (CaCL).

With complete tears of the CrCL, abnormal cranial drawer motion is noted in the extended and the flexed positions. Often the craniomedial band of the ligament is torn, leaving the caudolateral portion intact. The caudolateral portion in taut in extension, preventing cranial tibial displacement. Abnormal cranial drawer motion is evident in flexion because the caudolateral portion is relaxed. Isolated rupture of the caudolateral portion occurs and can confuse diagnosis because the intact craniomedial portion is taut both in flexion and in extension [3; 22] (Figure 2.3).

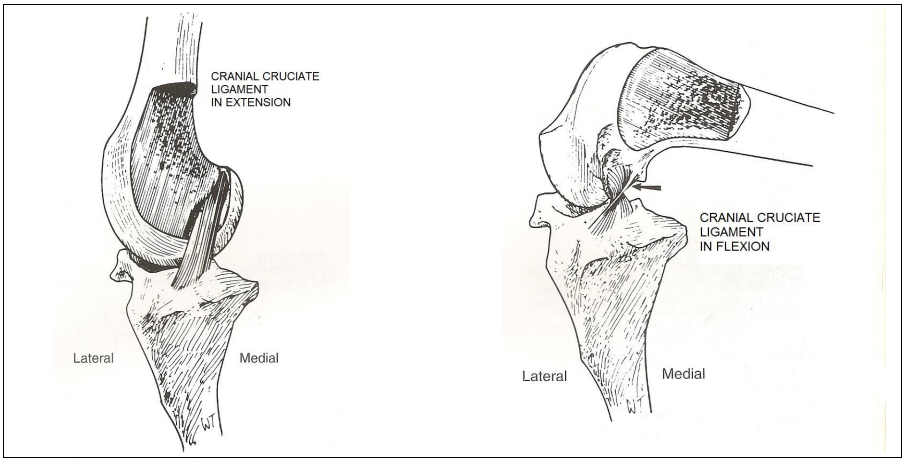

Figure 2.3 Drawing showing the CrCL with stifle felction and extension. Note that in flexion the craniomedial portion is taut (see the arrow) instead the caudolateral portion is not. With stifle extension both portions are taut. (Arnoczy S.P.: Meccanica patologica dei traumi a carico dei legamenti crociati e dei menischi. In: Boyrab M.J. *Le basi patogenetiche delle malattie chirurgiche nei piccoli animali.* S. Lazzaro di Savena-Bologna: Giraldi Editore, 2001, 1023-1038)

The cranio-caudal stability is guaranteed even by the caudal cruciate ligament. This ligament has two portions as the cranial one. The cranial portion is taut only with stifle flexion, the caudal portion is taut only with stifle extension.

Excessive joint motion is prevented not only by the ligamentous constrains of the stifle joint, but also by the major muscle groups around the stifle.

The anatomical and physiological basis of the theories previously described are strictly connected with the so called *traditional model* of the stifle [57]. This model considers only structure in and around the stifle as important to the cranial cruciate ligament.

The traditional model represents the stifle as a two-dimensional, single-degree-of-freedom linkage moving in a single plane. There are four components that basically influence the stifle motion: the CrCL, the CaCL, the portion of the femur between the proximal ends of the ligaments, and the portion of the tibia between the distal ends of the ligaments (Figure 2.4). Ligaments limits the distance between their attachments by their length.

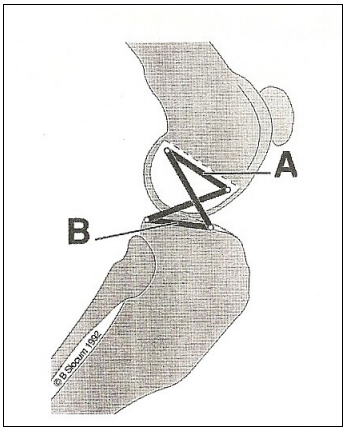

Figure 2.4 Four-bar linkage to control stifle motion:
A: femoral connection of the proximal part of the cranial and caudal cruciate ligaments
B: tibial connection of the distal part of the cranial and caudal cruciate ligaments
(Slocum B, Slocum TD.: Tibial plateau leveling osteotomy for repair of cranial cruciate ligament rupture in the canine. Vet Clin North Am Small Anim Pract. 1993; 23 (4): 777-795.)

The stifle is 100% dependent on the ligaments to determine the stable relationship between the femur and the tibia as these ligaments passively limit any other motion from occurring: flexion of the stifle is limited by contact between the thigh and the crus and extension is limited by contact between the cranial cruciate ligament and the cranial intercondylar notch of the femur. If hyperextension of the stifle occurs, the CrCL can fail or the femur must crush, as the distance between the femoral and tibial attachments of the CrCL exceeds its length (Figure 2.5).

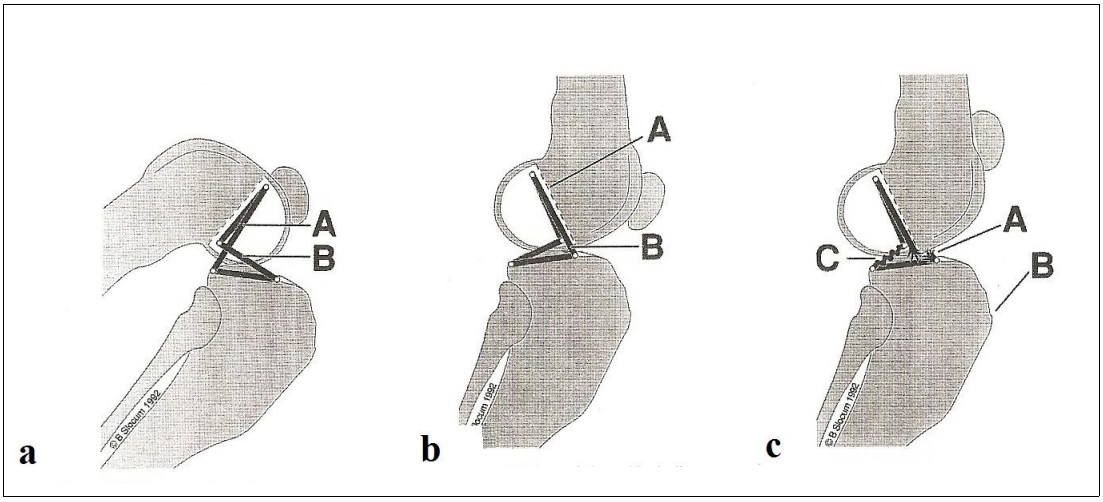

Figure 2.5 **a.** Flexion of the stifle is limited by contact between the thigh and the crus; **b.** Extension of the stifle is limited by contact of the cranial portion of the intercondilar notch (A) with the cranial cruciate ligament (B); c. Hyperextension can cause CrCL failure because the distance between the femoral and tibial attachments become greater than the length of the ligament.
(Slocum B, Slocum TD.: Tibial plateau leveling osteotomy for repair of cranial cruciate ligament rupture in the canine. Vet Clin North Am Small Anim Pract. 1993; 23 (4): 777-795.)

It is important to understand that the traditional model is a passive model: the cranial drawer sign, typical of the cranial cruciate ligament rupture, find an explanation in the traditional model but it is not until the veterinarian applies an external force that the tibia will translate cranially. Under this passive restraint model it is impossible for the CrCL to fail in the absence of the hyperextension: the traditional model is a passive model that cannot explain CrCL rupture with no external trauma happen while performing routine activities of daily living. The traditional model also recognizes the mechanism of impingement and rupture of the caudal horn of the medial meniscus, but offers no explanation for it. Finally it also fails to explain the wide range of both success and failure of several traditional surgeries.

To better understand these unknown features of the CrCL rupture, Slocum evaluated the *active model* of the stifle that gives some new informations about the biomechanic of the joint, including the fundamental role that muscles and weight bearing plays in it.

In 1983 the Author evaluated the tibial compression test and in studying the mechanism of this test he came to recognize the *Cranial Tibial Thrust* (CrTT), a force generated in the stifle that, during weight bearing, acts to thrust the tibia cranially.

The main things that play a fundamental role in the genesis of the cranial tibial thrust are: the position of the contact point between the femur and the tibia in the stifle joint, that lies cranial to the line that connects the center of the hock and the stifle joint; the slope of the tibial plateau with respect to the line between the center of motion of the stifle and hock; and the amount of compression.

Since the tibial plateau is inclined to the functional axis of the tibia, and the point of contact of the articular surfaces is cranial to this axis, a cranial tibial thrust is generated by tibial compression [56] (Figure 2.6).

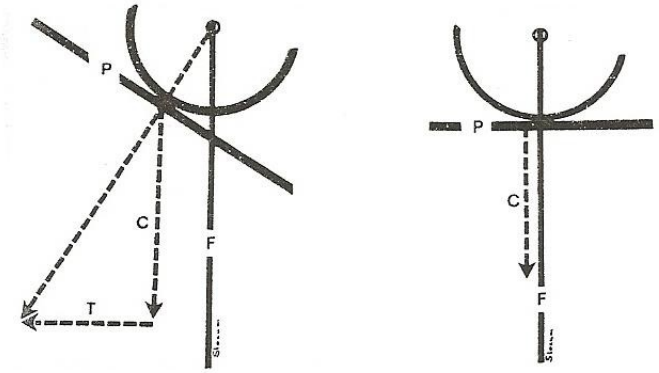

Figure 2.6 The tibial plateau (P) is inclined to the functional axis of the tibia (F) and the point of contact of the articular surfaces lies cranially to F, the result is a compressive force that acts between the femur and the tibia divided in two vectors: the CrTT (T) and the ground reaction force (C). If the tibial plateau were perpendicular to the fucnctional long axis, and if the point of contact were on this axis, compressive forces alone would be generated on tibial compression.
(Slocum B., Devine T.: Cranial Tibial Thrust: a primary force in the canine stifle. *J Am Vet Med Assoc* 1983; 183: 456-459.)

In 1993 Slocum propose the active model of the stifle [61].

The active model combine the first founding on the genesis of the CrTT and the traditional model with the dynamic component due to the the forces generated by weight bearing and muscles.

The cranial tibial thrust is an internally generated force created by weight bearing (Figure 2.7).

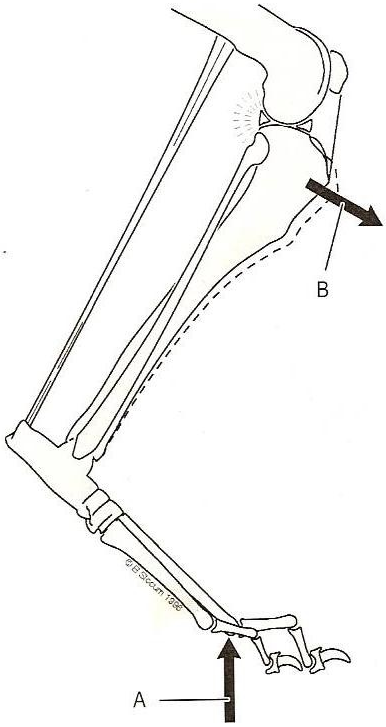

Figure 2.7 Cranial tibial thrust take place as the dog walks and it is due to the weight bearing. In the cranial cruciate ligament is ruptured there is a cranial translation of the tibia. An audible click can be heard as the caudal horn of the medial meniscus becomes impinged between the femur and the tibia. (Slocum B, Slocum TD.: Tibial plateau leveling osteotomy for repair of cranial cruciate ligament rupture in the canine. Vet Clin North Am Small Anim Pract. 1993; 23 (4): 777-795.)

The muscle forces of stifle flexion and extension create stifle stability through a balance of the moments around the instant center of motion. For the stifle to maintain a constant angle of flexion during the weight bearing phase of the stride, the moments of flexion and extension about the center of motion of the stifle must sum to zero. In this way the stifle is in muscular balance (Figure 2.8). The prevention of the limb from collapsing is due to the extensor muscles of the stifle (primarily the thigh muscles) and hock (primarily the calf muscles) plus the tarsal tendon. The caudal thigh muscles stabilize the stifle, but act mainly as extensor of the hip to create forward propulsion of the dog.

Tibial compression is created by the extensors of the limb, plus the force of weight bearing (Figure 2.9). As long as the elements compressed are on a line between the center of the hock and stifle joints, the compressed components will be in equilibrium. As the contact point between the femur and the tibia is cranial to that line, additional active (hamstring and biceps femoris) or passive forces (CrCL and caudal horn of the medial meniscus) are necessary to provide equilibrium and prevent the tibia from projecting cranially.

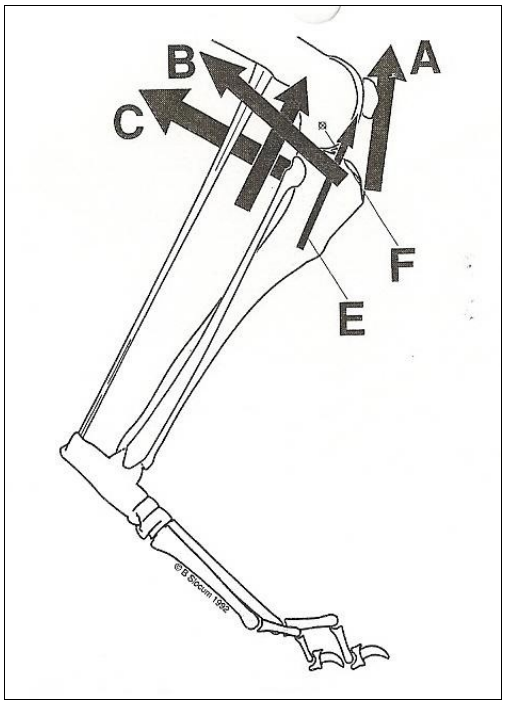

Figure 2.8 Moments about the center of motion of the stifle joint (F). They are in balance when the extensor moments (A: quadriceps and E: digital extensor) are equal to the flexor moments (B: biceps femoris , C: pes anserinus group and tibial head of the semomembranosus and C: gastrocnemius and superficial digital flexor muscle). (Slocum B, Slocum TD.: Tibial plateau leveling osteotomy for repair of cranial cruciate ligament rupture in the canine. Vet Clin North Am Small Anim Pract. 1993; 23 (4): 777-795.)

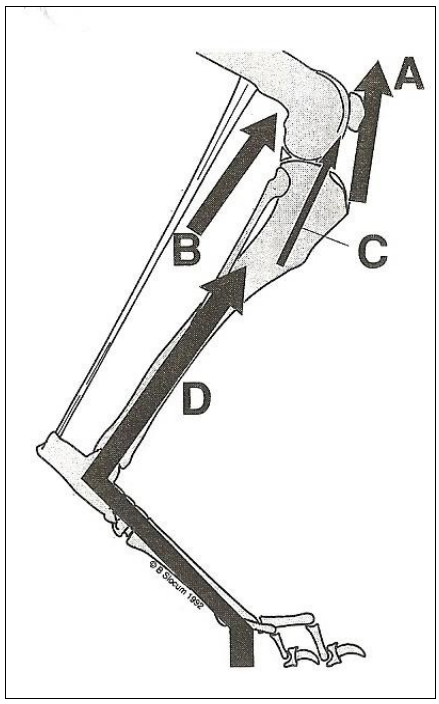

Figure 2.9 Tibial compression is created by the extensors of the stifle (A: quadriceps and C: long digital extensor muscle) and the extensors of the hock (B: gastrocnemius and superficial digital flexor) plus the forse of weight bearing (D). (Slocum B, Slocum TD.: Tibial plateau leveling osteotomy for repair of cranial cruciate ligament rupture in the canine. Vet Clin North Am Small Anim Pract. 1993; 23 (4): 777-795.)

The magnitude of tibial thrust is dependent not only on the amount of compression, but also on the slope of the tibial plateau with respect to the line between the center of motion of the stifle and hock. The compression is variable as strictly related to the amount of force generated at the ground by the dog but the slope of the tibial plateau can be controlled changing the presence or absence of cranial tibial thrust [57; 58; 61].

2.3 Radiographic assessment of hind limb deformities

The magnitude of the hind limb deviations may impact the surgical treatment of some important syndromes such as patellar luxation and canine hip dysplasia. In veterinary medicine descriptions of some measurements, such as femoral varus and torsion, have been limited primarily to radiography [6; 13; 37; 40]. Recently, the measurement of the anteversion angle in dogs using magnetic resonance imaging have been reported, as well as the description of the use of computed tomography (CT) [24; 65]. Although the use of different techniques have been described, radiographic measurement still represents the most common method used for the interpretation of hind limb deformities.

A precise and repeatable radiographic study of the femur and the tibia is fundamental to better understand the hind limb anatomy.

The main problem related to radiographic techniques is that there is a lack of informations due to the by dimensionality of radiography instead of the three dimensionality of the bone. Strict guidelines for patient positioning are essential when attempting to make accurate measurements [2; 5; 30; 59].

2.3.1 Radiographic study of the femor

A current, clinically practiced, method for measurement of radiographic femoral axes and angles involves either dorsally recumbent/hip extended or torso-elevated/hip extended patient positioning under general anesthesia [29; 57; 63].

For dorsally recumbent/hip extended radiographs the dog has to be positioned in dorsal recumbency within a foam trough, the spine has to be straight. One person has to extend the hips to get the femora parallel to the radiographic table, parallel to the pelvic long axis and applying a little internal rotation. The beam has to be centered at the mid-point between the two coxofemoral joints and the final image has to show the entire pelvis, the femors, the stifle and a little part of the proximal tibia.

For elevated-torso/hip extended radiographs, the dog's torso has to be elevated ~45° from the radiographic table, this position can be easily obtained with the aid of a wooden or a large foam wedge while a technician grabs the dog and another one

positions the hind limb as previously described (figure 2.10). This projection is particularly useful in case of dogs with a lot of muscle mass or with a decreased hip extension due to articular disease. Recently some Authors define this positioning as “sit dog positioning” [36].

A proper positioning is necessary to an accurate evaluation of the hind limb deformity: both the obturator foramina have to be parallel, femora have to be parallel to the long axis of the pelvis, patella centered within the trochlear solcus, fabellae bisected by the respective femoral cortex and the lesser throcanter protruding from the medial aspect of the femor [30; 59] (figure 2.11).

Fig. 2.10 Positioning for elevated-torso hip radiograph. A wooden edge can be helpful in obtaining a standard inclination of 45°.

Fig. 2.11 Ventrodorsal radiograph of canine pelvis. femora are parallel to the long axis of the pelvis, patella is centered within the trochlear solcus, and fabellae are bisected by the respective femoral cortex and the lesser throcanter protrudes from the medial aspect of the femor.

The need to establish the validity of a radiograph is clear because a positioning that does not satisfy the selection criteria may compromise the study suggesting erroneous alterations of skeletal alignment measurements, for example small internal rotation or stifle extension may cause an apparent distal femor deformity as the farther is the bone segment from the table the larger it seems in the final image.

Fig. 2.12 Mediolateral radiograph of the femur. Note that the border of the femoral head is visibible enough to be underlined. Femoral condyles are superimposed.

For a complete evaluation of femoral alignment a standard mediolateral (ML) projection of the femur is necessary too. The dog lies in a lateral recumbency with the pelvic limb of interest placed on the table and the other one cranially extended. The greater trochanter, head of the fibula, and lateral malleolus have to be all in contact with the film cassette. Positioning is judged satisfactory if both femoral condyles are superimposed and the intertrochanteric crest is superimposed on the femoral head (figure 2.12).

The mediolateral projection of the femur has to be compared with the craniocaudal view of the same bone as an apparent deformity (valgus/varus) can be easily confused with a minor malpositioning [59; 65].

2.3.2 Radiographic study of the tibia

Two different radiographs are necessary to determine tibial malalignment or deformities: a mediolateral projection of the stifle and a standard caudocranial view of the limb.

The mediolateral projection is very useful to evaluate either the inclination of the tibial plateau (TPA) or torsional deformity. For the mediolateral projection the dog is positioned in a lateral recumbency on the affected limb and the opposite limb slightly displaced cranially to avoid overlap of the stifle joints; the greater throcanter, lateral condyle, and lateral malleolus are placed in contact with the table. The position of the radiographic beam is controversial as it is equivocal if a displacement of the

radiographic beam from the stifle joint to the midshaft of the tibia decreases the accuracy of tibial plateau slope (TPS) measurements [7].

Positioning is judged satisfactory if both femoral condyles are superimposed on lateral projections and the radiograph includes the entire tibia, stifle, and tarsus with the tarsus and stifle both at 90° of flexion (figure 2.13)

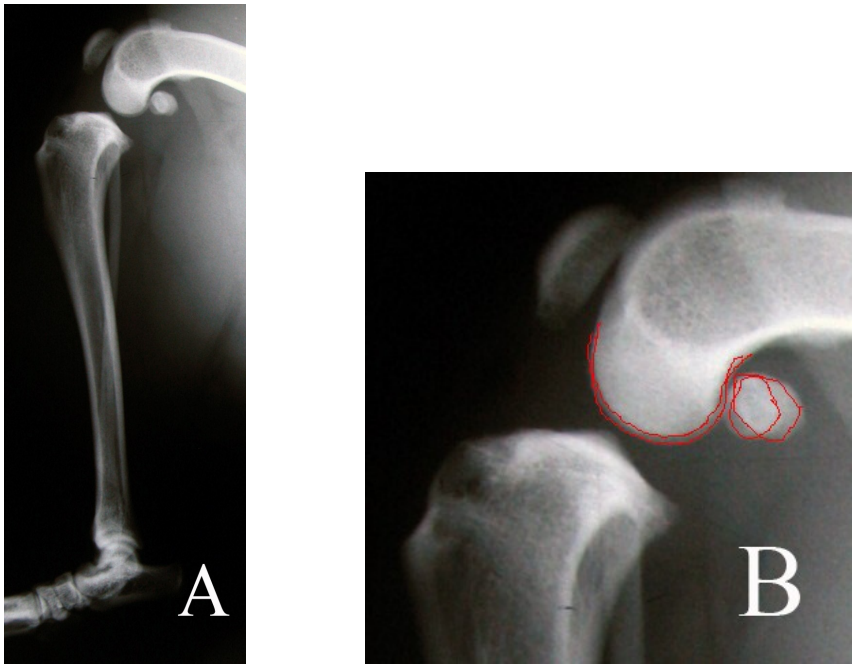

Figure 2.13 A) Mediolateral radiograph of canine stifle. B) Particular showing the two femoral condyles and fabellae that are superimposed.

Caudocranial radiographs are obtained placing the dog in a sternal recumbency and the stifle joint locked in extension. The position of the radiographic beam is centered over the stifle joint. The tibia has to be positioned in a neutral position, such that the medial aspect of the calcaneus has to be aligned with the base of the sulcus of the talus [2] (figure 2.14). If no tibial torsion exists, the patella is centered in the trochlear groove of the femur, the fabellae bisected by the distal femoral cortices and the medial aspect of the calcaneus aligned with the base of the sulcus of the talus (figure 2.15).

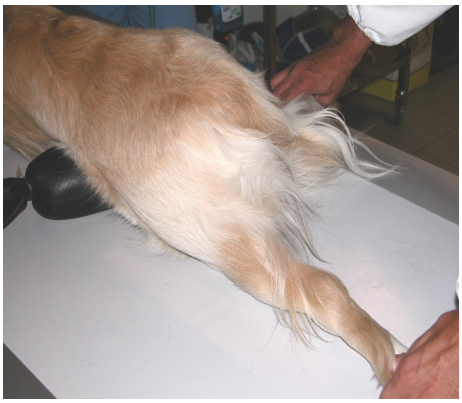

Figure 2.14 Positioning for caudocranial view of the tibia.

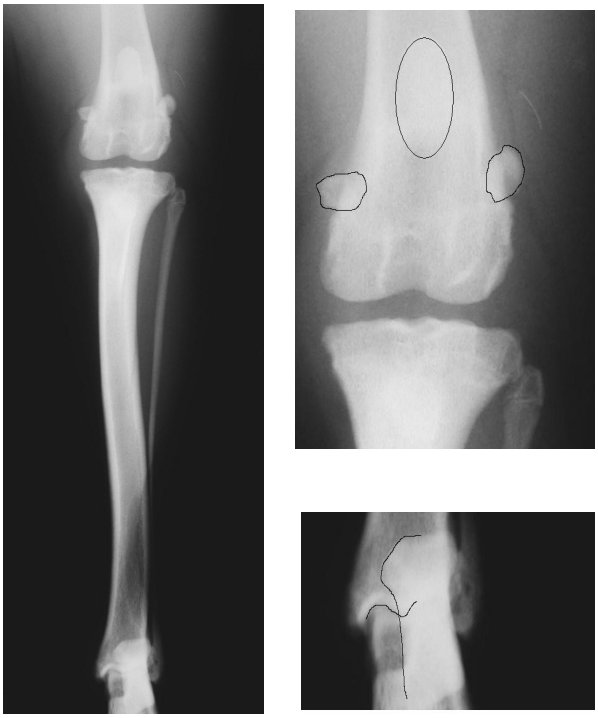

Figure 2.15 Caudocranial radiograph of canine tibia. One the right it is shown the correct posittion of patella and fabellae. The medial aspect of the calcaneus has to be aligned with the base of the sulcus of the talus as shown on the right particular.

2.3.3 Femoral radiographic measurement

To understand deformities of the hind limb, it is important to first understand and establish the parameters and limits of normal alignment. The exact anatomy of the femur, tibia, hip, knee and ankle is of great importance to the clinician when examining the hind limb and to the surgeon when operating on the bones and joints. To better understand alignment and joint orientation, the complex three-dimensional shape of bones and joints can be simplified to basic line drawings. Furthermore these line drawings should refer to either the frontal, sagittal, or transverse anatomic planes.

Standard terminology and method of measurement for femoral angles of limb alignment are routinely used in human orthopedic surgery. In human medicine reference ranges for normal angles have been reported. Values for the inclination angle for the femoral head and neck and the anteversion angle in dogs have been reported too [19; 37; 52; 64].

Unfortunately the morphology of the femur is hard to be represented in a bidimensional image as a radiograph. First of all, there is not a real hip joint orientation plane, and femoral head and neck lie on a sagittal plane that is different from the one which the femoral shaft lies on; plus the femoral physiologic torsion is hard to be represented in a bidimensional image [67].

Landmarks on the femur must be taken into consideration too: the problem is that we do not have enough points on the proximal femur for the evaluation of the positioning. Most of the points that are used to establish the validity of a radiograph are part of the distal femur but this part of the bone is the one most commonly affected by the orthopedic pathologies and limb deformities so that these reference points are frequently missed in the radiograph [5; 30; 46].

The limits of measurements on the radiograms are well-known and related to the subjectivity of drawing points and lines and to the different methods that still exists in veterinary medicine: during the years different Authors suggested several methods for the evaluation of the femoral axis and angles and up till now there is not a real standardization for the evaluation of femoral deformities; this makes comparison difficult.

Multiple measurement techniques address the evaluation of hind limb deformities to different lines placed over an anteroposterior (AP) view and ML view of the femur, these lines represent the forces exerted on the bone during either stance or movement.

As regards to the femur, the main lines that are used and well known in literature are:

- Hip joint orientation line
- Mechanical axis
- Anatomic axis
- Axis of the head of the femur
- Axis of the neck
- Distal femoral joint orientation line or transcondylar axis

Because the femoral head is round, it is necessary to use the femoral neck or the greater trochanter to draw a joint line for hip orientation in the frontal plane. **Hip joint orientation line** was defined in 1992 by Paley and Tetsworth as a line from the tip of the greater trochanter to the center of the femoral head [44] (figure 2.16).

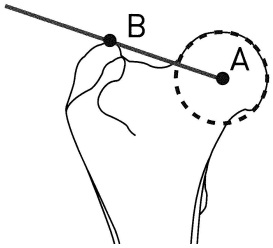

Figure 2.16 Hip joint orientation line. A: center of the femoral head; B: tip of the greater trochanter

This is not a real axis but it important in the evaluation of the orientation angle of the femoral joints as much as it is important the distal femoral joint orientation line.

The **mechanical axis** of a bone is defined as the straight line connecting the joint center points of the proximal and distal joints, so the femoral mechanical axis is that line that joins the center of the femoral head with the center of the most proximal aspect of the intercondylar fossa of the femur [44; 48; 67] (figure 2.17).

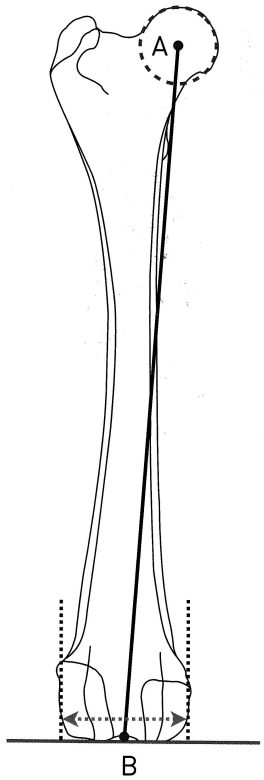

Figure 2.17 Femoral mechanical axis. A: center of the femoral head; B: center of the most proximal aspect of the intercondylar fossa of the femur

The **anatomic axis** of a bone is the mid-diaphyseal line, this axis is not straight due to the anatomy of the femur and this is why many Authors described different methods to draw this line.

In 1985 Montavon et al. described the anatomical axis of the femur as a line connecting the central points of the femoral diaphysis at each of three levels: 1) the femoral isthmus and two other points 2 cm under and over the previous one [37] (figure 2.19) .

In 1990 Rumph and Hathcock studied the Symax method. This method, based on the principles of symmetric axis (Symax) shape analysis is used to study complex shapes using several circles drawn interior to the object of the study, these circles have

to touch the sides of the object in two or more points. After several studies the Authors defined this axis as that line joining the center of the two circles inscribed in the proximal and distal femoral metaphisys [50] (figure 2.19).

Figure 2.18 Craniocaudal radiograph of canine femur. PFLA: Proximal Femoral Long Axis; FVA: Femoral varus angle; DFLA: Distal femoral Long Axis; TCA: Transcondylar Axis. (Dudley RM, Kowaleski MP, Drost WMT Dyce J. Radiographic and computed tomographic determination of femoral varus and torsion in the dog. Vet Radiol Ultrasound 2006; 47(6): 546-552)

The problem related to these two techniques is that 1) the line representing the anatomic axis is curved due to the femoral shape; and 2) they were studied for the determination of femoral head and neck-shaft angle and torsion; it is not proved their utility in the evaluation of femoral varus and joint orientation angles. If we consider these problems we understand why other methods have been suggested drawing two different anatomic axes, a proximal anatomic axis and a distal one.

The distal anatomic axis or **distal femoral long axis** is defined as a line bisecting the intercondylar notch, perpendicular to the transcondylar axis [13; 30; 48] (figure 2.18).

The **proximal femoral long axis** can be drawn in two different ways. Recently Kowalesky determined this axis by first identifying the center of the proximal femoral diaphysis at three points distal to the lesser trochanter, approximately 1 cm apart; these points are connected with a line which represents the proximal femoral long axis [48; 67] (figure 2.19).

Tomlinson has modified this last technique. Firstly the length of the femur is measured from the most proximal aspect of the center of the intercondylar fossa to the most distal aspect of the dorsal aspect of the femoral neck; the proximal femoral long axis is defined as that line that connects the two midpoints of the two lines drawn at one-third and one-half of this length from the most distal aspect of the dorsal aspect of the femoral neck [64] (figure 2.19).

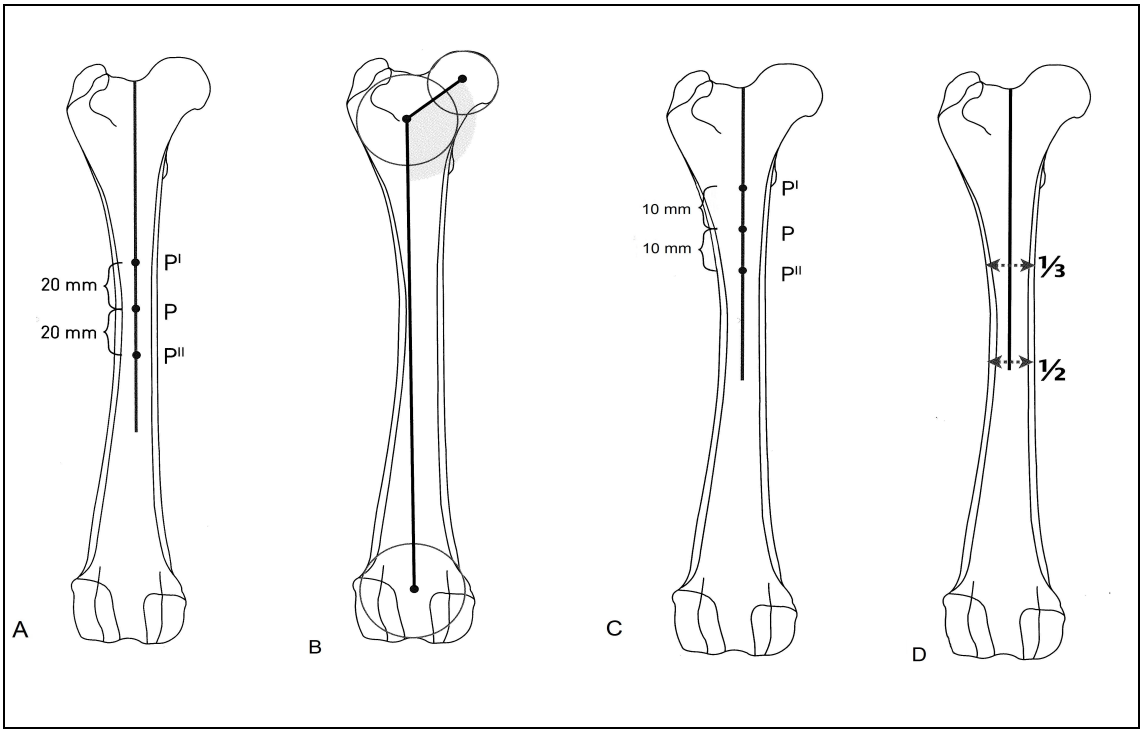

Figure 2.19 Schematic drawing of several methods to measure the anatomic axis. A) Montavon method; B) Symax method; C) Kowalesky method; D) Tomlinson method (Petazzoni M., Atlante di goniometria clinica e misurazioni radiografiche dell'arto pelvico. 2008)

Dealing with the proximal femoral epiphysis we can draw two different axis: axis of the head of the femur and axis of the neck.

The axis of the neck is crucial studying the hind limb alignment, it is defined as a line connecting the center midpoints between cranial and caudal cortical margins of the femoral neck. These margins can be hard to find that is why several methods have been suggested in the determination of this line.

Rumph and Hathcock used Symax method as for the anatomic axis: the neck axis is the line joining the center of the two circles inscribed in the femoral head and proximal epiphysis [50] (figure 2.20).

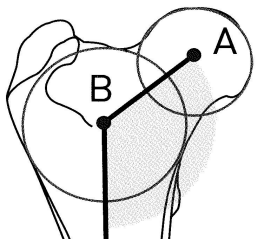

Figure 2.20 Femoral neck-shaft angle – Symax method

In 1979 Hauptman suggested two different techniques to describe the neck axis [18; 19].

The first method describes the neck axis as the line that joins the center of the femoral head with the midpoint of the perpendicular to the shaft axis connecting the intertrochanteric area and the medial cortex (figure 2.21).

The second method connects the center of the femoral head with the midpoint of the istmus of the neck (figure 2.21).

Montavon suggested another method to determine the femoral neck axis using three circles which radial represents the distance between the center of the femoral head and the intertrochanteric area as shown in figure 2.21 [37].

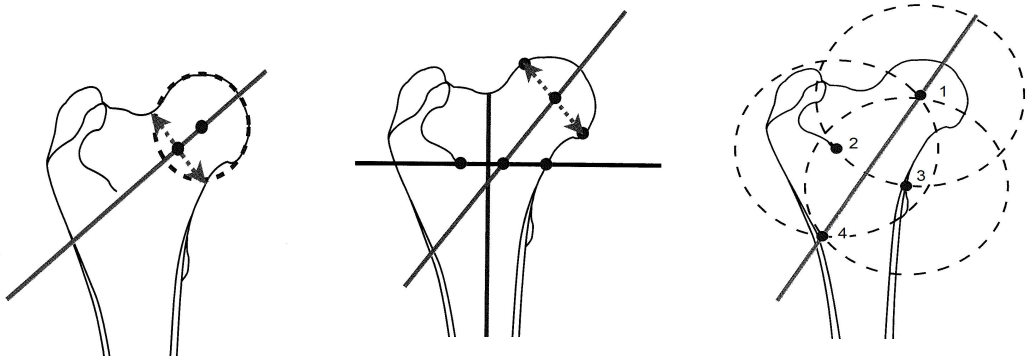

Figure 2.21 Schematic drawing showing different methods to measure the axis of the neck. From left to right it is shown Hauptman's method A and B. On the right Montavon's method. (Petazzoni M., Atlante di goniometria clinica e misurazioni radiografiche dell'arto pelvico. 2008)

The **transcondylar axis** is defined as a line drawn tangential ti the distal articular surface of the femoral condyles (figure 2.18).

The axes are crucial in the study of limb alignment. In human medicine the evaluation of pelvic limb alignment is accomplished by standing, full-limb horizontal-beam radiography performed in the same plane. These radiographic studies are used to determine joint reference angles of the femur and tibia. In veterinary medicine the evaluation of limb alignment is a little different: standing radiography has been used to determine normal adduction-abduction angles of the hip, stifle, and tarsal joints of normal dogs. These techniques were performed without sedation, requiring a high level of cooperation from the dogs. Obviously this technique is likely patient dependent; in addiction, patients with angular limb deformity often presents clinical pain which could

prohibit the dog from standing in a normal position for radiography. These considerations are crucial to understand why the method used in human medicine in the evaluation of lower limb alignment (calculation of mechanical axis deviation and tibiofemoral angle) has to be modified in veterinary medicine [11].

Part of the methodology and terminology used in human medicine to describe the joint reference angles and axes of the femur and tibia can be used either in veterinary medicine.

The most important angles that can be used in the evaluation of hind limb alignment are:

- aLPFA (anatomic lateral proximal femoral angle)
- mLPFA (mechanical proximal femoral angle)
- aMDFA (anatomic medial distal femoral angle)
- mMDFA (mechanical medial distal femoral angle)
- Neck-shaft angle
- Angle of version
- femoral varus angle

As we previously said, in the frontal and sagittal planes, a joint line can be drawn for the hip and knee. The angle formed between the joint line and either the mechanical or anatomic axis is called joint orientation angle. The name of each angle specifies whether it is measured relative to a mechanical or an anatomic axis. The angle may be measured medial or lateral to the axis in the frontal plane and may refer to proximal or distal joint orientation angle of a bone. mMDFA is the medial angle formed between the mechanical axis line of the femur and the knee joint line of the femur in the frontal plane (transcondylar axis). Similarly the aMDFA is the medial angle formed between the anatomic axis of the femur and the knee joint line of the femur in the frontal plane. Schematic drawings of the mechanical and anatomic frontal plane joint orientation angles are shown. (figure 2.22)

The **mMDFA** and **aMDFA** are both normally less than 90° and are different from each other. Some Authors provided normal values for distal femoral joint angles in the frontal plane, aMDFA should be around 83° [64].

Other Authors suggested normal aMDFA values around 85° [33] or between 82° and 86° [67]. The mMDFA is around 80° [33] with a physiologic range between 80° and 83° [67].

The **mLPFA** and **aLPFA** have been recently described and only few ranges of normal values have been suggested [64].

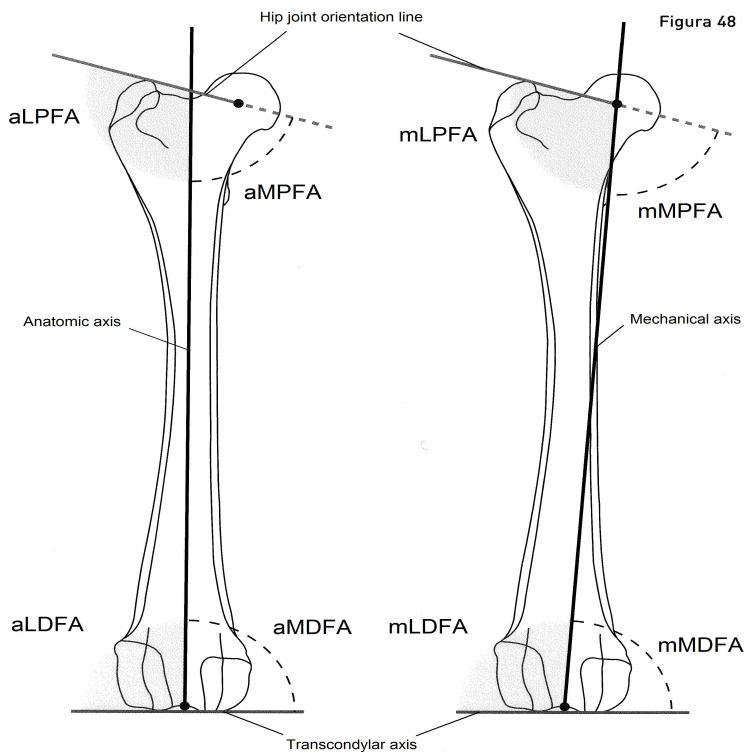

Figure 2.22 Shematic drawing representing aLPFA (anatomic lateral proximal femoral angle), mLPFA (mechanical proximal femoral angle), aMDFA (anatomic medial distal femoral angle), mMDFA (mechanical medial distal femoral angle)
(Petazzoni M., Atlante di goniometria clinica e misurazioni radiografiche dell'arto pelvico. 2008)

Hip joint orientation can be either evaluated using neck shaft angle. The **neck-shaft angle** is the angle formed between the axis of the neck and the anatomic axis. Due to the different modalities that have been previously described in the evaluation of these axes, the Authors suggested either normal values around 130° and 140° or around 140° and 150° [37; 48; 50; 67].

The angulation between the femoral neck and the diaphysis can be either described by the angle of torsion. The angle of torsion is that between the plane of the

femoral condyles and the axis of the femoral neck. Femoral torsion, expressed as **angle of version**, can be evaluated using two different techniques: a distal-proximal axial femoral radiograph (direct method) and a comparison betweed a mediolateral projection of the femur and a rcaniocaudal view of the same bone (undirect method).

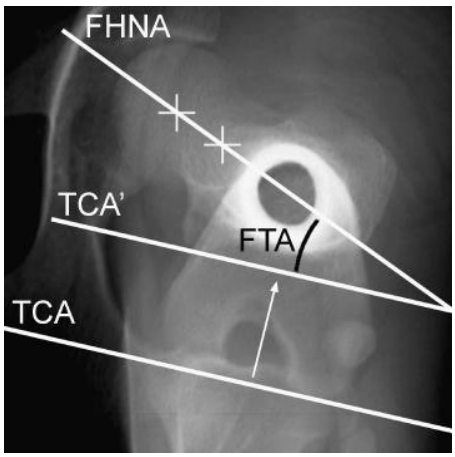

Figure 2.23 Distal-proximal axial femoral radiograph. FHNA: femoral head and neck axis, TCA: transcondylar axis, FTA: femoral torsion angle. ((Dudley RM, Kowaleski MP, Drost WMT Dyce J. Radiographic and computed tomographic determination of femoral varus and torsion in the dog. Vet Radiol Ultrasound 2006; 47(6): 546-552)

For the axial projection, the limb has to be positioned such that the long axis of the femur is perpendicular to the table and parallel to the x-ray beam. This allows visualization of the femoral head, neck and condyles with the femoral shaft forming a concentric ring. The femoral torsion angle is defined as the angle formed by the femoral head and neck axis and transcondylar axis at their intersection [13; 40] (figure 2.23).

The axial projection of the femur is hard to be obtained, that is why a direct method have been suggested comparing the sagittal and frontal view of the femur as shown in figure 2.24 [48].

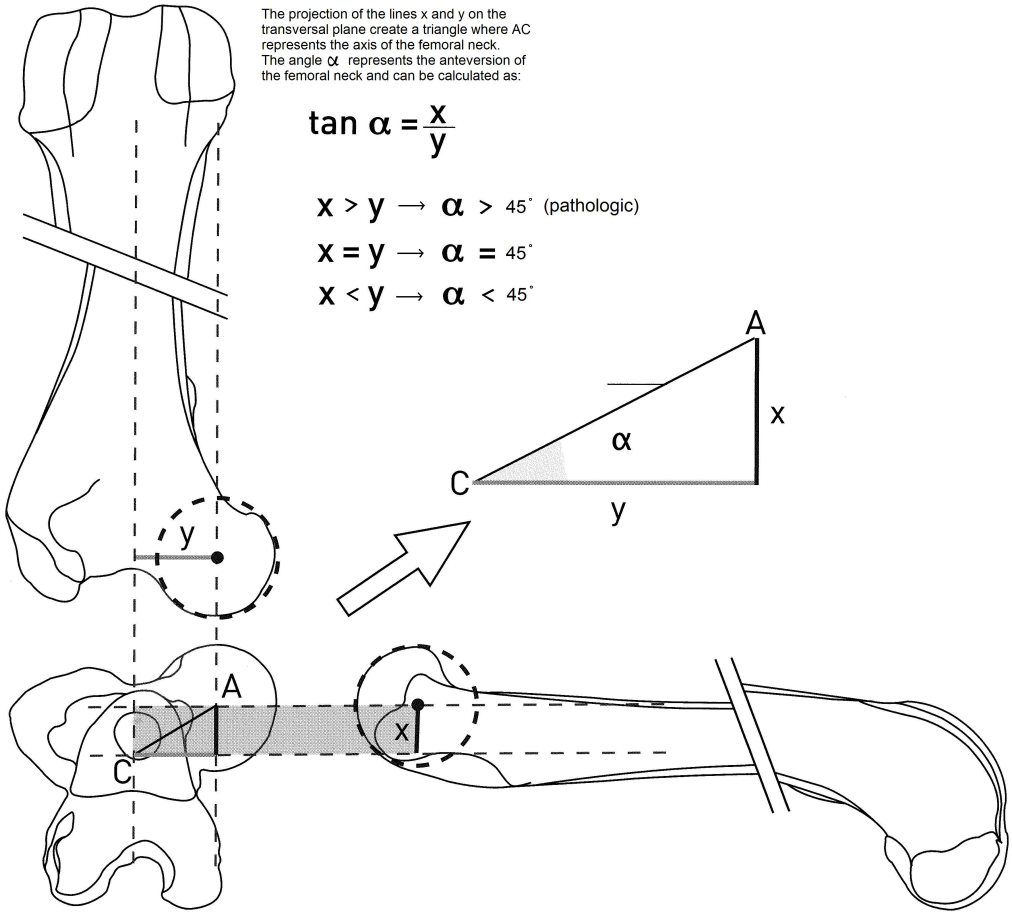

Figure 2.24 Graphic identification of the angle of version using the length of x and y (distance of the center of the femoral head from the femoral anatomic axis in two radiographic projection) (Petazzoni M., Atlante di goniometria clinica e misurazioni radiografiche dell'arto pelvico. 2008)

A positive angle of torsion, with the head and neck directed cranially, is referred to as anteversion; a negative angle, with the head and neck directed caudally, is referred to as retroversion. A zero angle is referred to as normoversion.

In puppies normal version angle is around 0° but it increases until a normal value around 27°. The normal angle of torsion ranges from +12° to +40° with a mean of 27° [24; 40; 54].

Another crucial angle in the evaluation of hind limb alignment is the **femoral varus angle**. For measurement of femoral varus angle the proximal femoral long axis, the transcondylar axis and the distal femoral long axis of the femur are determined. The femoral varus angle is defined as the angle formed between the proximal femoral long

axis and the distal femoral long axis at their intersection [13; 67] (figure 2.18). Ranges are around 0° and 10° but a real magnitude of this angle has not been reported yet. [13; 63].

2.3.4 Tibial radiographic measurement

As all of the other long bones, tibia has a mechanical and an anatomic axis but, in this bone, the frontal plane mechanical and anatomic axes are very similar and only few millimeters apart that is why it is common to draw just one line that represents both of these axes [48].

Landmarks established for the mechanical axis of the tibia are the halfway point between the two intercondilar tubercles and the most distal point of the subchondral bone of the distal intermediate tibial ridge (figure 2.25).

Some Authors prefer to consider the center of the proximal most aspect of the intercondylar fossa of the femur as the proximal point of reference for the mechanical axis [12].

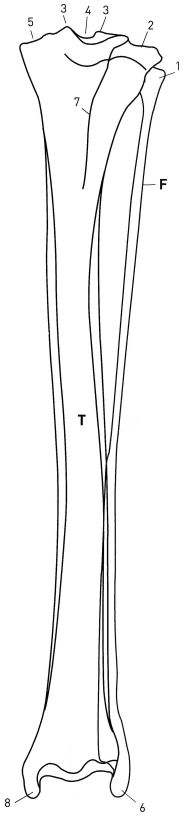

Figure 2.25
(Petazzoni M., Atlante di goniometria clinica e misurazioni radiografiche dell'arto pelvico. 2008)
F: fibula; T: tibia. 1: fibular head; 2: lateral condyle; 3: medial and lateral intercondylar eminence; 4: intercondylar area (fossa); 5: medial condyle; 6: lateral malleous (fibular); 7: tibial crest; 8: medial malleolus (tibial)

The mechanical axis is crucial in the evaluation of joint angles. Joint angles of the canine tibia determine the amount of varus or valgus associated with the angular deformity. Landmarks established for the proximal tibial joint orientation line are the most distal points of the subchondral bone concavities of the medial and lateral tibial condyles. Landmarks established for the distal tibial joint orientation line are the most proximal points of the subchondral bone of the two arciform grooves of the cochlea tibiae (figure 2.25).

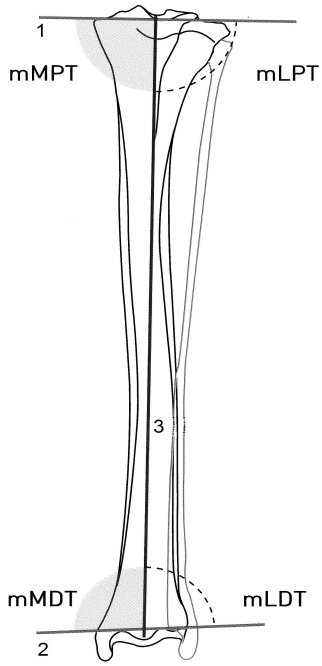

Figure 2.26 Proximal and distal tibial joint angles in the frontal plane. (Petazzoni M., Atlante di goniometria clinica e misurazioni radiografiche dell'arto pelvico. 2008)

The landmarks of the tibial joint surface are connected for both the proximal and distal surfaces to create the proximal and distal joint orientation lines.

As for the femur, the angle formed between the joint line and either the mechanical or anatomic axis, is called joint orientation angle. The angle may be measured medial, lateral, anterior, or posterior to the axis line. The angle may refer to the proximal or distal joint orientation angle of the bone. Therefore, in veterinary medicine it is common to consider the mechanical medial proximal tibial angle (mMPTA) and the mechanical medial distal tibial angle (mMDTA) (figure 2.26).

Mean mMPTA and mMDTA values have been recently reported. Mean mMPTA is 93.3° ± 1,78°; so that it can be considered pathologic a mMPTA deviation over 94° or under 92° [12; 48; 67]. Recently Lozier has cosidered normal even angles between 90°-93° [32; 33].

Mean mMDTA is 95.99° ± 2.70°; angles over 97° or under 92° are abnormal [12; 48; 67].

There is another angle that can be measured in the frontal plane: the mechanical angle of deviation (MAD). The issue of MAD is highly controversial: in human medicine MAD is defined as mechanical axis of deviation and it represents the distance between the mechanical axis line (the mechanical axis of the lower limb is the line from the center of the femoral head to the center of the ankle plafond) and the center of the knee in the frontal plane (figure 2.27). It can be either medial or lateral and referred to as varus or valgus malalignment.

The full-lenght standing radiograph is considered the gold standard for assessment of mechanical axis deviation and joint line orientation of the knee.; but while less full-lenght radiographs of the femur or tibia can be used to measure joint orientation angles of the knee (femur: lateral distal femoral angle; tibia: medial proximal tibial angle), the mechanical axis deviation can only be measured on a long film that includes the hip, knee, and ankle [43; 51].

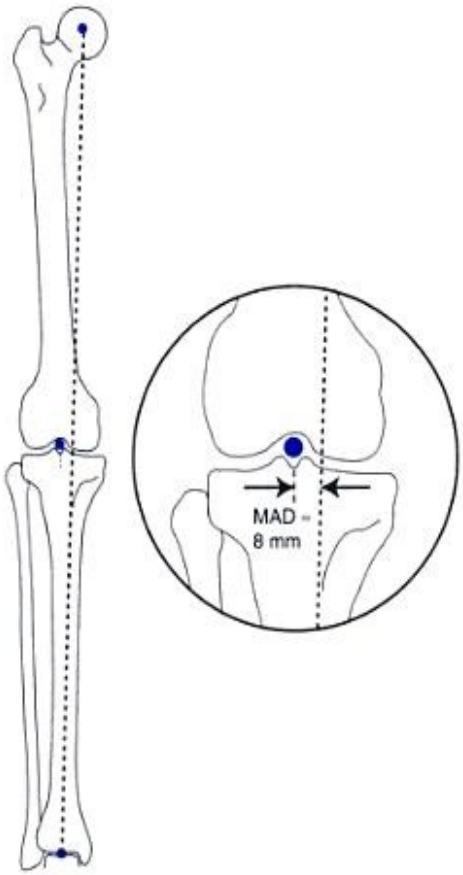

Figure 2.27 Mechanical axis of deviation (MAD). In human medicine MAD is the perpendicular distance from the mechanical axis line to the center of the knee joint line. The frontal plane mechanical axis of the lower limb is the line from the center of the femoral head to the center of the ankle plafond. Normally the mechanical axis passes 8±7 mm medial to the center of the knee joint line.
(Paley D, Herzenberg JE. Principles of deformity correction. (ed 1) Springer-Verlag. Berlin Heidelberg, 2002.)

In veterinary medicine MAD is not a lenght but an angle (mechanical angle of deviation) and it is measured in a frontal view of the tibia [67]. MAD is normal between 2° and 4° and it is directly related to the mMPTA.

A very important angle to take into consideration is the tibial plateau angle (TPA) (figure 2.28). Recently it has been demonstrated that an increase of the tibial plateau slope can predispose to a cranial cruciate ligament rupture. Slocum developed a procedure that decrease the angle of the tibial plateau by performing a cylindrical proximal tibial osteotomy and rotating the proximal tibial component, thereby leveling the articular surface of the tibia. The success of the tibial plateau leveling osteotomy (TPLO) procedure relies, in part, upon neutralizing the detrimental effects of cranial tibial thrust [56-58; 61].

Determining the slope of the tibial plateau is s prerequisite to the tibial plateau levelling osteotomy (TPLO) procedure. The TPA determination is made on a mediolateral radiograph and it is measured as the angle between the tibial plateau line (a line joining the small, discreet cranial margin of the tibial plateau and the point of insertion of the caudal cruciate ligament) and a line drawn perpendicular to the tibial long-axis line (line joining the intercondilat eminence and a point equidistant to the cranial and caudal aspects of the throclea of the talus [1; 9].

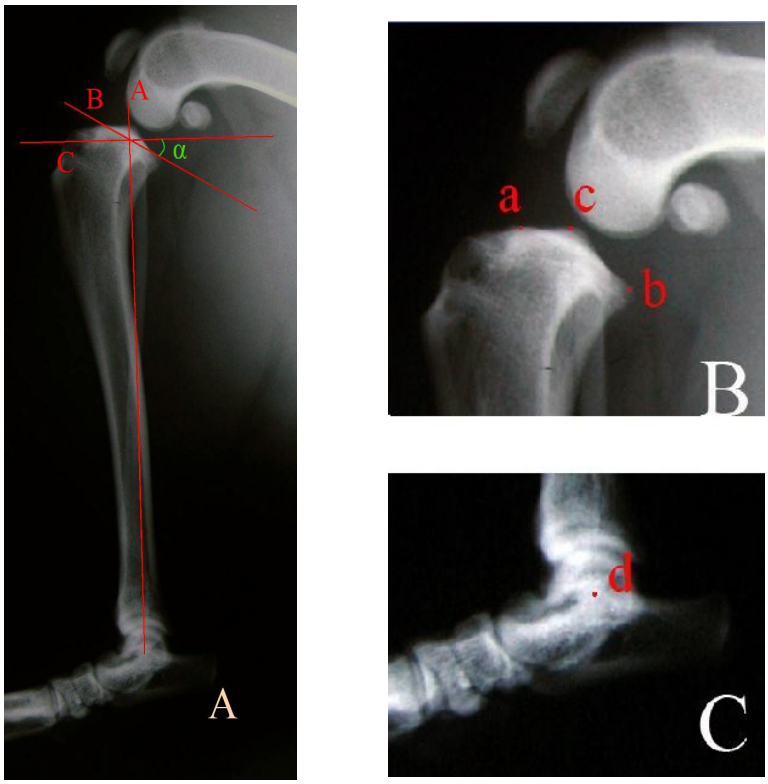

Figure 2.28 A: Mediolateral radiograph of canine tibia: axes to measure the angle of tibial plateau (TPA) are red (**A** : tibial functional axis , **B** : tibial plateau, **C** : perpendicular to the tibial axis); B: Particular showing landmarks for drawing the axes and the tibial plateau(**a** cranial cruciate ligament origin, **b** caudal cruciate ligament insertion, **c** intercondylar eminence); C: **d** center of the the trochlea of the talus.

3. MATERIALS AND METHODS

3.1 Inclusion Criteria

Cadavers of eight adult (skeletally mature) dogs were obtained after euthanasia or death for reason unrelated to this study. All dogs were medium to large, mixed-breed dogs weighting between 20 and 40 kg. Exclusion criteria included: adolescent dogs (any radiographically open physis), limbs with radiographically or palpably evident orthopedic disorders of the hip and stifle joint (including hip dysplasia, degenerative joint disease, cranial drawer or cranial tibial thrust and patellar luxation), or dogs with gross angular limb deformity detected on visual inspection.

All radiographs included in the study were made by two single individuals and reviewed and approved in terms of quality and positiong by three different examiners. Those radiographs that did not satisfy the selection criteria were exluded from the study.

3.2 Radiographic measurement

Radiographic examination included mediolateral projections of each femur and each tibia, caudocranial projection of the tibia and extended ventrodorsal projection of the pelvis including 2/3 of the tibia.

For ventrodorsal projection of the pelvis an elevated-torso/hip-extended radiograph was performed. Each cadaver was positioned in dorsal recumbency elevating the dog's torso ~ 45° from the radiographic table with the aid of wooden wedge within a foam trough. Radiographs were reviewed for proper positioning: femora parallel to the long axis of the pelvis, patella centered within the trochlear solcus, fabellae bisected by their respective femoral cortex and the corticocancellous tip of the lesser trochanter protruding from the medial aspect of the femur.

For mediolateral radiograph of the femur the dog was positioned in a lateral recumbency with the pelvic limb of interest placed on the table and the other one cranially extended. The greater trochanter, head of the fibula, and lateral malleolus

were all in contact with the film cassette. The mediolateral projection was considered acceptable when the femoral condyles were superimposed and the border of the femoral head sufficiently visible for accurate measuring.

For caudocranial view of the stifle joint, cadavers were positioned in sternal recumbency on the radiographic table with the pelvic limb of interest placed in full extension of the hip, stifle, and tarsus. This positioning was achieved without placing any tension, compression, angular, or torsional forces on the limb itself thus allowing passive full extension of the joints. The beam was centered over the stifle joint.

Mediolateral radiograph of the stifle were made including the entire tibia, stifle, and tarsus, with the tibia parallel to the radiographic film cassette and the beam centered on the mid-tibial diaphysis with the tarsus and stifle both at 90° of flexion. The greater trochanter, head of the fibula, and lateral malleolus were all in contact with the film cassette, ensuring that a true lateral radiographic view of the stifle and hock joints was obtained.

For the tibial evaluation, positioning was judged satisfactory if both femoral condyles were superimposed on lateral projections and both fabellae symmetrically bisected the femoral cortices in cranial views and the patella was centered over the trochlear groove; this positioning resulted in the medial edge of the calcaneus aligning close to tali of the tibia. Dogs were included in this study if the lateral projection of the stifle extended to the diaphysis of the tibia and to the tarsus, allowing all the measurement required.

Radiographs were scanned. A transparency was superimposed on each radiograph for determination of the anatomical landmarks (ex. femoral head and cortex) for the evaluation of all of the axis.

Regarding the femoral measurements, hip joint orientation line, mechanical axis, anatomic axis, axis of the neck and the transcondylar axis were drawn applying all of the methods known in literature and previously described (see chapter 2.3.3 Femoral radiographic measurements). In particular we evaluated femoral anatomic axis using Symax, Montavon, Kowalesky and Tomlinson method and the femoral axis of the neck using the classic method applied in human medicine, Symax, Hauptman A and B, and Montavon method.

Measures of the following values were collected:

- LPFA (anatomic lateral proximal femoral angle) calculated in 4 different ways using the four previously drawn anatomic axis
- mLPFA (mechanical proximal femoral angle) obtaining a single value
- aMDFA (anatomic medial distal femoral angle) calculated in 4 different ways (four anatomic axis)
- mMDFA (mechanical medial distal femoral angle) obtaining a single value
- Neck-shaft angle calculated in 20 different ways comparing all of the method to draw the femoral axis of the neck with every single method to measure femoral anatomic axis
- Angle of version obtaining a single value applying the indirect method
- Femoral varus angle obtaining a single value

The main tibial axes were drawn too (mechanical axis, proximal and distal tibial joint orientation line). Three angles were evaluated: the mechanical medial proximal tibial angle (mMPTA), the mechanical medial distal tibial angle (mMDTA) and the mechanical angle of deviation (MAD).

3.3 3-dimensional measurement techniques

After femoral and stifle radiographs were made of each cadaver, the femora and tibia were harvested and freed of all soft tissues sparing the articular cartilage.

Figure 3.1 KONICA MINOLTA VI-910 (Konica minolta Sensing Inc.

Every bone was then scanned with KONICA MINOLTA VI-910 (Konica minolta Sensing Inc.) (Fig 3.1).

The VI-910 is a non-contact 3-D digitizer, offering precise capture of 3-D shapes. This device is invaluable for “reverse engineering” or creating CAD (computer aided design) data from physical models and design mock-ups.

The VI-910 employs laser-beam light sectioning technology to scan workpieces using a slit beam. Light reflected from the workpiece is acquired by a CCD camera, and 3D data is then created by triangulation to determine distance information.

We obtained several scans of each bone from different angles (at least eight different scans in the sagittal plane and at least six for each femoral epiphysis and four for each tibial epiphysis). Using polygon Editing Tool ver 1.22 (Konica minolta Sensing Inc.) we aligned and combined the 3D data sets. Multiple scans were registered and merged into a single watertight polygonal mode (figure 3.1)

Having reconstructed a complete 3D model by optical scanning, the following part of the project was to create different axes in the 3-dimensional model to measure all of the angles previously calculated in the 2-dimensional image.

Using RAPIDFORM 2006 (Inus Technology INC.) we could manipulate and prepare polygon mesh models for all of the required applications.. The Polygon Workbench allowed us to fill in missing data, and smooth the surface to repair common errors in 3D scan data. The same program was used to obtain axis, reference points and plane to measure the main femoral and tibial angles.

3.3.1 Femoral 3D evaluation

- HIP JOINT ORIENTATION LINE

To compute this line three steps were necessary:

1. Recognition of the center of the femoral head: The femur head was approximated into sphere. To find the best fit sphere we selected the faces and limits of the femoral head excluding the fovea of head of femur as this is a depression that could create an underestimated sphere (smaller than the real femoral head).

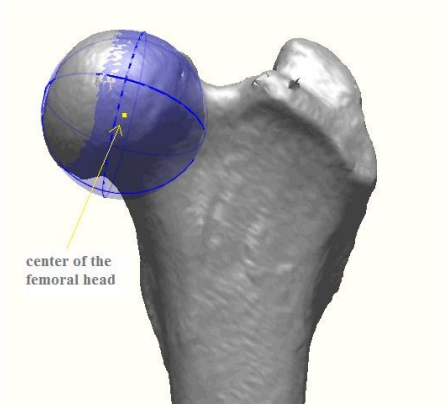

Figure 3.2 Center of the femoral head. This point is the cenetr of the best fit sphere created from a fit region through previous selection of the articular cartilage of the femoral head

The selected area was used as a reference for fitting the sphere and the center of sphere was referred as the center of the femoral head (figure 3.2).

2. Identification of the tip of the greater trochanter as an anatomical landmark: The point was created on the surface of the greater trochanter subjectively, identifying the area of the trochanter that most likely represented the top of the structure.

3. Creation of vector "hip joint orientation line" through the command "pick reference points".

3. MECHANICAL AXIS

To compute mechanical axis we used the anatomic definition of this line as that line that joins the center of the femoral head with the center of the most proximal aspect of the intercondylar fossa of the femur [44; 48; 67]. To draw this axis several steps were necessary:

1. Recognition of the center of the femoral head as previously described

2. Recognition of the center of the stifle joint: Due to the complex biomechanic of the stifle, this point could not be simplified as the center of a single best fit geometric figure that most likely represented the distal femoral epiphysis as for the femoral head. For this reason we suggested a method to find this point that took into consideration the fundamental biomechanic concepts.

First of all we hypothesized that the two femoral condyles could be well represented by a cylinder. To create the best fit cylinder we selected the surface and limits of the articular cartilage of the condyles as shown in figure 3.3.

The axis of the cylinder was computed and a plane from this line to the middle point of the most proximal border of the articular cartilage,on lateral femoral condile, was created. This plane was then cranially rotated with an angle of 95° from the previous position (figure 3.3).

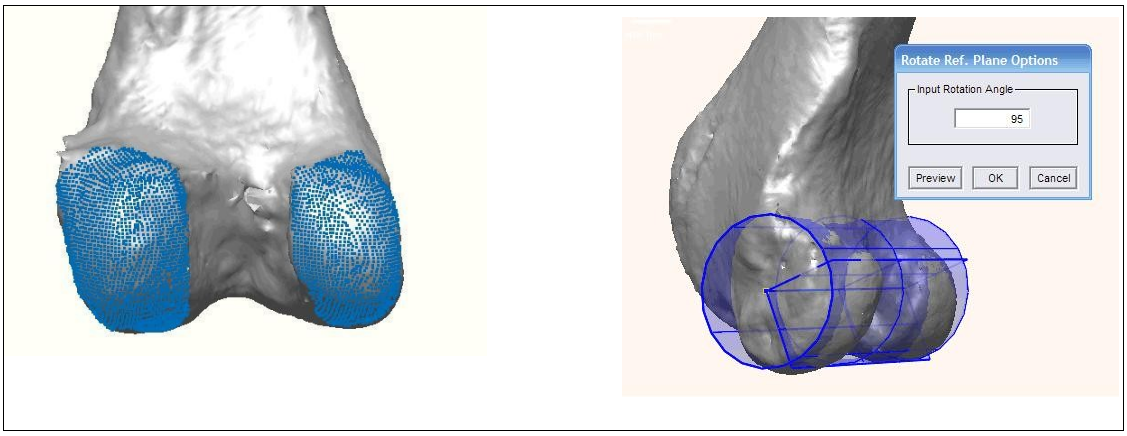

Figure 3.3 Creation of the best fit cylinder through selection of the articular cartilage of the femoral condyles. In our model the best fit cylinder represented the best geometric figure in representing fthe shape of emoral condyles. Note the plane passing throgh the most proximal aspect of the articular cartilage; this plane has been cranially rotated with an angle of 95°

The explanation in creation of this plane is in the biomechanic of the stifle joint: normal range of motion of this joint is around 40° and 150° [22; 64]; the most proximal border of the articular cartilage corresponds with a good chance to the point of maximum flexion (40°). In a standing position the stifle joint usually has an average angle around 135° (95° more than the maximum flexion) so the rotated plane most likely represents the surface of contact between femur and tibia in a normal standing position.

The following step was to measure the cross section of the distal epiphysis using this plane as a reference. The connecting line between the most distal point of each (medial and lateral) condyle was created using this cross section (figure3.4 A e B); this line represented the transcondylar axis.

To better represent the anatomy of the distal femoral epiphysis we decided to find another geometric figure representing the intercondilar fossa; this best fit geometric figure was a toroid and its reference plane was created to represent the plane where the forces are excited on the femur during station and motion (figure 3.4 C).

The center of the stifle joint was defined as that point created from the intersection of the toroid plane and the transcondylar axis (figure 3.4 D).

3. Creation of mechanical axis through the comman “pick reference points”

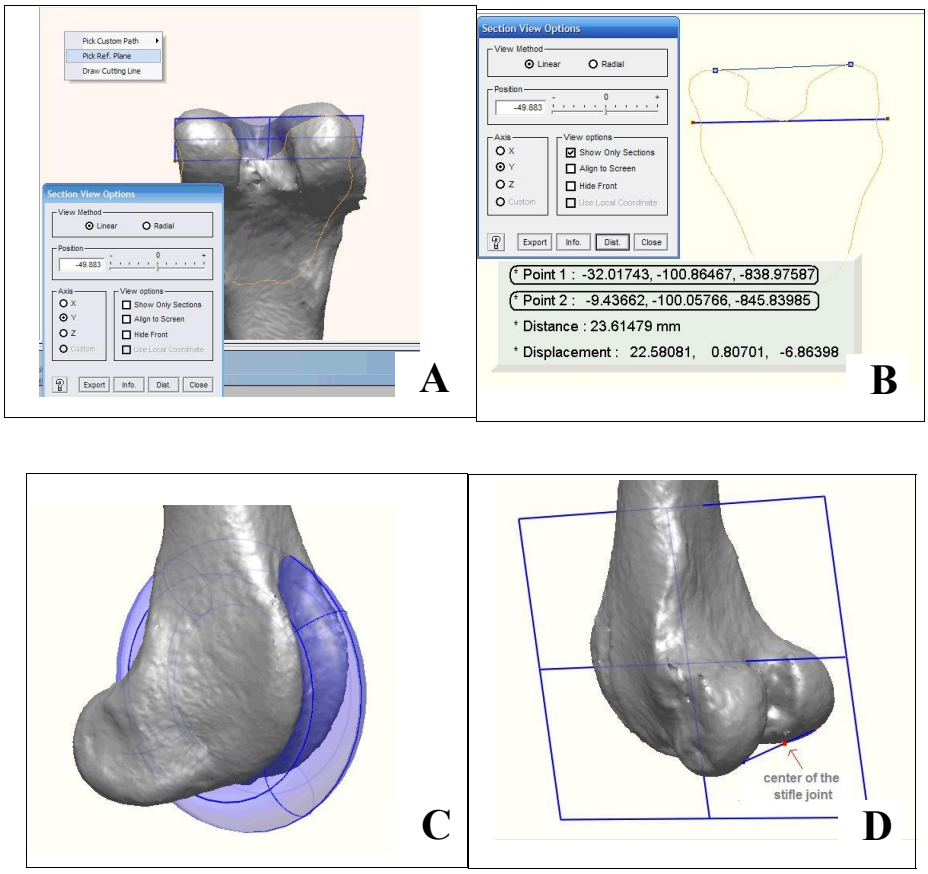

Figure 3.4 Steps in creation of the center of stifle joint necessary to create the mechanical axis.
The transcondylar axis (see fig.B) is detected through the cross section obtained using a reference plane showon in fig. A. The best fit toroid is created (fig.C). The center od stifle joint is the point obtained from the intersection of the toroid plane and the transcondylar axis.

- ANATOMIC AXIS

This axis passes through the middle of the bone structure. To compute this line the steps were:

1. Orient and divide the femur model into sections (at least 10 sections, 10 mm apart starting from the less trochanter)
2. Collect the centroid coordinate of each section
3. Connect the centroids
4. Fit a best curve for locating the axis

- AXIS OF THE NECK OF THE FEMUR

The geometric definition of this axis is a line that passes through the neck joining its center and the center of the femoral head [6]. We decided to compute this line following this definition. The measurement of the neck axis required three steps:

1. Recognition of the center of the femoral head as previously described (see hip joint orientation line)
2. Creation of a "pre-axis": We firstly created the cylinder that best fit the shape of the femoral neck. The axis of this cylinder was the "pre-axis" (figure 3.5 A e B)
3. Creation of the "final-axis": We used the "pre-axis to create a sequence of cross sections of the neck (1mm distant one from the other starting from the section intersectin the center of the femoral head with the exclusion of the cross sections that included the greater trochanter). Connecting the centroids of each section we obtained our final neck axis (3.5 C e D).

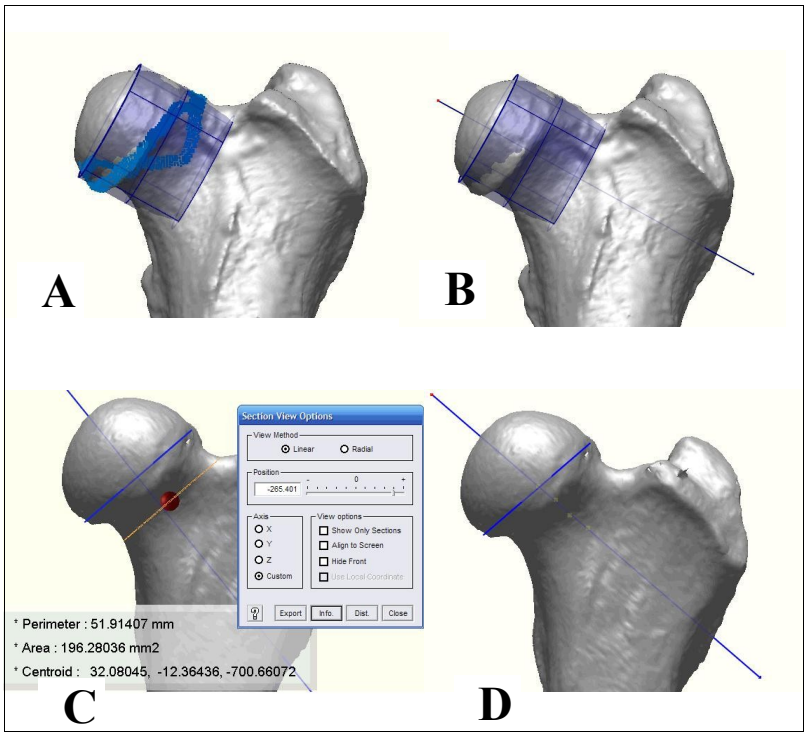

Figure 3.5 Steps in creation of neck axis
The best fit cylinder is detected through the selection of the cranial border of the neck (see fig.A). The axis of this cylinder represents the "pre-axis" of the neck.
Several cross section of the neck are obtained (fig.C). The "final" neck axis is the one that joins all of the centroids of the cross sections (fig.D).

- TRANSCONDYLAR AXIS

This line was created as we previously described in the section “mechanical axis”

- DISTAL FEMORAL LONG AXIS

This axis represents that line that bisects the intercondylar fossa. We detected this line selecting the surface of this anatomic area and creating, on this refernce area, the best fit cylinder. The axis of the cylinder represents the distal femoral axis.

Once all of the axis were created we could easily measure the neck-shaft angle, the aLPFA, mLPFA, aMDFA and mMDFA with the command “Measure_angle” (RAPIDFORM 2006), between two reference vectors.

For the evaluation of the angle of version and the varus angle, two more steps have been necessary to create two additional planes:

- PLANE FOR THE EVALUATION OF THE ANGLE OF VERSION

- Step 1: Creation of a reference point (P) between the anatomic axis and the axis of the cylinder that best fit the femoral condyles.
- Step 2: Creation of a plane intersecting the midpoint (P) which normal was represented by the anatomic axis
- Step 3: Creation of a point (P2) created from the intersection between the plane that was created in step 2 and the anatomic axis
- Step 4: Connection of point P and P2
- Step 5: Creation of the plane for the evaluation of the angle of version (figure 3.6) intersecting P2 which normal was represented by the line created in step 4.

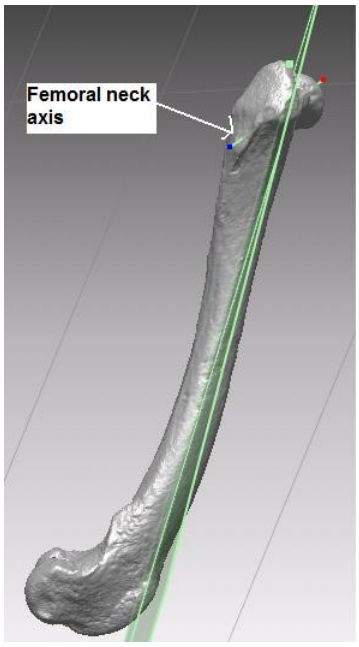

Figure 3.6 3D method for the evaluation of the angle of version. The angle of version is the angle between the axis of the neck and the plane shown in the picture.

- PLANE FOR THE EVALUATION OF VARUS ANGLE

The method to evaluate femoral verus angle is shown in figure 3.7.

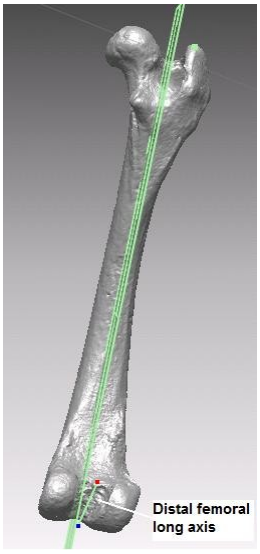

Figure 3.7 3D method for the evaluation of varus angle.
A point is created on the distal femoral long axis. The plane intersecting ths point and the anatomic axis is created. Varus angle is the angle between the plane of reference and the distal lfemoral long axis

3.3.2 Tibial 3D evaluation

- PROXIMAL TIBIAL JOINT ORIENTATION LINE

In the radiograph this axis is represented by that line that joins the two concavities (medial and lateral) of the tibial condyles in the frontal plane.

Dealing with the 3-dimensional model we had to apply this definition to the creation of a plane representing the orintation of the entire articular surface.

The surface of the articular cartilage of medial and lateral condyles was selected to create a plane fitting this reference region as shown in figure 3.8. In the determination of this plane we decided not to take into consideration the intercondylar fossa that could create an underestimation of the plane.

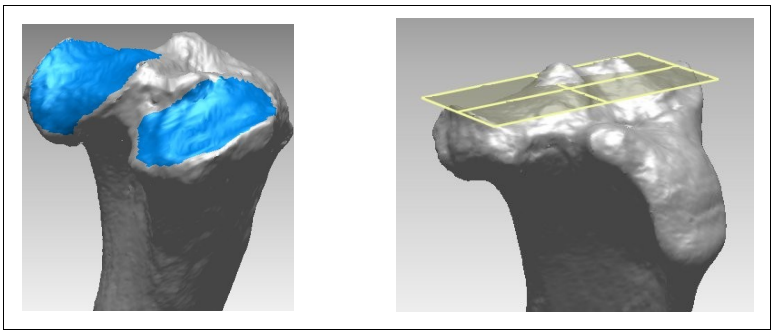

Figure 3.8 Creation of the best fit plane through selection of the articular cartilage of the tibial condyles. In our model the best fit plane represented the proximal tibial joint orientation plane. Note thet the intercondylar area has not been selected.

- DISTAL TIBIAL JOINT ORIENTATION LINE

As previously said for the proximal tibial joint orientation line, even the distal axis could not be represented with a line in the 3-dimensional model.

The plane representing the distal joint was measured as shown in figure 3.9.

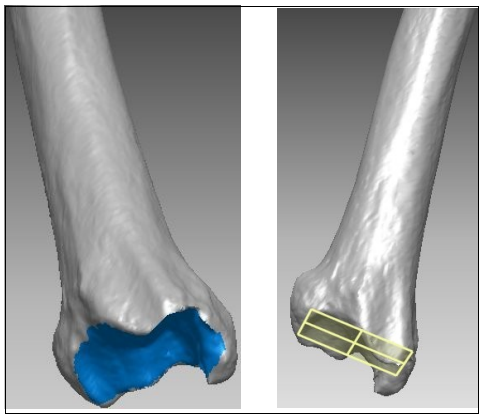

Figure 3.9 Creation of the best fit plane through selection of the articular cartilage of the distal tibial epiphysis

- MECHANICAL AXIS

The mechanical axis is the line joining the center of the proximal joint with the center of the distal joint. In the radiographic method this line usually can represent also the anatomic axis in the frontal plane but in the 3-dimensional method these lines are separated. A plane representing both of these axes was created then throgh several steps:

1. Creation of the anatomic axis: We oriented and divided the tibia model into sections (at least 14 sections, 10 mm apart starting from the distal point of the tibial crest). We connected all of the centroids of each section and finally fit a best curve for locating the axis

2. Recognition of the center of the intercondylar area: We randomly chose two points on the top of the medial and lateral intercondylar eminences. To diminish the risk of error we repeated the same measure five times and the final point of interest was the mean value of the five measurements

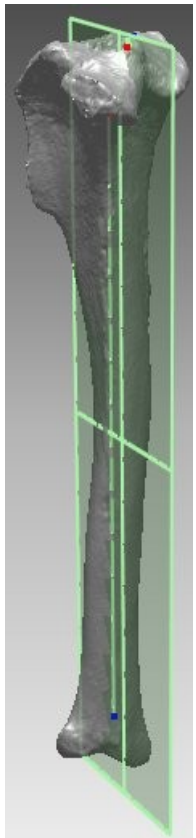

Fig. 3.10 Tibial mechanical plane

3. Creation of the mechanical plane: This plane was represented by that plane joining the center of the intercondylar area and the anatomic axis (figure 3.10).

Once all of the axis were created we could easily measure the mMPTA and the mMDTA with the command “Measure_angle” (RAPIDFORM 2006), between the two refence planes.

For the evaluation of the mechanical angle of deviation one more step was necessary: we created the vector perpendicular to the proximal tibial orientation plane intersecting the center of the intercondylar area. MAD was the angle between this vector and the mechanical plane.

4. RESULTS

4.1 Femoral evaluation

A total of 16 femora were evaluated. The values for aLPFA, aMDFA, mLPFA, mMDFA, femoral varus, femoral torsion and neck-shaft angles were collected.

The values for each radiologic method and the 3-dimensional evaluation are reported in Table 4.1 and Table 4.2 Data collected from all of the femora can be found in Appendix A.

	Anatomic axis SYMAX	Anatomic axis MONTAVON	Anatomic axis KOWALESKY	Anatomic axis TOMLINSON	Mechanical axis	Angle of version
Hip joint orientation line	109,87	107,43	114,60	107,26	104,16	28,76
Transcondylar axis	92,26	89,92	96,99	90,80	86,55	
Distal femoral long axis	2,25	0,18	6,98	0,35		
Neck axis-CLASSIC	131,42	133,86	126,69	134,03		
Neck axis-SYMAX	129,37	131,81	124,64	131,98		
Neck axis-HAUPTMAN A	150,83	153,26	146,10	153,43		
Neck axis-HAUPTMAN B	133,37	135,81	128,64	135,98		
Neck axis-MONTAVON	152,44	154,88	147,71	155,05		

Table 4.1 Right femur n.1: 2-dimensional values of the angles obtained with different methods. Blue: Anatomic Lateral Proximal Femoral Angle (aLPFA); grey: Mechanical Lateral Proximal Femoral Angle (mLPFA); green: Anatomic Medial Distal Femoral Angle (aMDFA); light blue: Mechanical Medial Distal Femoral Angle (mMDFA); yellow: Femoral Varus Angle; red: Angle of version; orange: Neck-Shaft Angle

A comparison between the 2-dimensional method and the 3-dimensional one was performed and the value called “Standard Difference” (absolute value). A p-value of less than 0.05 indicates evidence of statistically acceptable difference between the compared values, this means that the maximum error allowed was 5%. Maximum distance allowed for each method in each femur are shown in Appendix A

	Neck-shaft angle	Femoral varus angle	aMDFA	aLPFA	mLPFA	mMDFA	Angle of version
	129,48	4,43	93,96	115,16	109,53	90,65	19,21
5% of the value	*6,47*	*0,22*	*4,70*	*5,76*	*5,48*	*4,53*	*0,96*

Table 4.2 Right femur n.1: 3-dimensional values of the angles obtained with different methods. Blue: Anatomic Lateral Proximal Femoral Angle (aLPFA); grey: Mechanical Lateral Proximal Femoral Angle (mLPFA); green: Anatomic Medial Distal Femoral Angle (aMDFA); light blue: Mechanical Medial Distal Femoral Angle (mMDFA); yellow: Femoral Varus Angle; red: Angle of version; orange: Neck-Shaft Angle.
5% of the value was calculated to determine the maximum difference allowed between the 2-dimensional and the 3-dimensional value. "Standard difference" has to be less than 5% of the 3-D value.

As evidenced in Table 4.3, neck-shaft angle values obtained through Hauptman A and Montavon methods (cervical axis) were almost never less than 5% compared with the 3-dimensional method.

	Anatomic axis SYMAX	Anatomic axis MONTAVON	Anatomic axis KOWALESKY	Anatomic axis TOMLINSON	Mechanical axis	Angle of version
Hip joint orientation line	11	11	12	9	14	1
Transcondylar axis	16	16	13	16	15	
Distal femoral long axis	0	0	0	1		
Neck axis-CLASSIC	8	8	7	8		
Neck axis-SYMAX	8	10	8	10		
Neck axis-HAUPTMAN A	1	0	1	0		
Neck axis-HAUPTMAN B	6	7	9	7		
Neck axis-MONTAVON	0	0	0	0		

Table 4.3 Frequency table of the "Standard difference" in 16 femora. Blue: Anatomic Lateral Proximal Femoral Angle (aLPFA); grey: Mechanical Lateral Proximal Femoral Angle (mLPFA); green: Anatomic Medial Distal Femoral Angle (aMDFA); light blue: Mechanical Medial Distal Femoral Angle (mMDFA); yellow: Femoral Varus Angle; red: Angle of version; orange: Neck-Shaft Angle.
Note that frequencies referred to Hauptman A and Montavon methods are zero or either 1.

Mean of the "Standard Difference" was calculated (Table 4.4 and compared with the values of each femur (shown in Appendix A) to obtain Standard Deviation (Table 4.5) and Variance (Table XLVII Appendix A). Values of Standard Deviation and Variance were calculated to average the distance of our variable from the expected value.

	Anatomic axis SYMAX	Anatomic axis MONTAVON	Anatomic axis KOWALESKY	Anatomic axis TOMLINSON	Mechanical axis	Angle of version
Hip joint orientation line	4,74	4,67	3,95	5,21	3,07	7,89
Transcondylar axis	1,65	1,81	2,65	1,76	2,42	
Distal femoral long axis	4,16	4,30	4,62	4,01		
Neck axis-CLASSIC	6,44	6,31	6,39	6,68		
Neck axis-SYMAX	5,71	5,64	5,68	5,91		
Neck axis-HAUPTMAN A	25,88	26,08	23,96	26,59		
Neck axis-HAUPTMAN B	8,28	8,26	8,46	8,12		
Neck axis-MONTAVON	28,46	28,67	26,55	29,17		

Table 4.4 Mean of the "Standard difference" in 16 femora. Blue: Anatomic Lateral Proximal Femoral Angle (aLPFA); grey: Mechanical Lateral Proximal Femoral Angle (mLPFA); green: Anatomic Medial Distal Femoral Angle (aMDFA); light blue: Mechanical Medial Distal Femoral Angle (mMDFA); yellow: Femoral Varus Angle; red: Angle of version; orange: Neck-Shaft Angle.
The underlined values are the best values, those that are closer to zero, so that the 2-dimensional value is closer to the 3-dimensional one (we accepted the best four values for the neck-shaft angle and the best three for aLPFA, aMDFA and femoral varus angle)

	Anatomic axis SYMAX	Anatomic axis MONTAVON	Anatomic axis KOWALESKY	Anatomic axis TOMLINSON	Mechanical axis	Angle of version
Hip joint orientation line	2,32	2,56	2,45	2,91	2,06	5,51
Transcondylar axis	1,16	1,05	2,91	1,15	1,55	
Distal femoral long axis	3,57	3,09	3,16	2,82		
Neck axis-CLASSIC	4,18	3,90	3,52	3,59		
Neck axis-SYMAX	3,91	3,56	2,97	3,59		
Neck axis-HAUPTMAN A	9,34	8,85	9,85	8,81		
Neck axis-HAUPTMAN B	5,17	4,99	6,88	4,88		
Neck axis-MONTAVON	8,03	7,61	8,82	7,52		

Table 4.5 Standard Deviations in 16 femora. Blue: Anatomic Lateral Proximal Femoral Angle (aLPFA); grey: Mechanical Lateral Proximal Femoral Angle (mLPFA); green: Anatomic Medial Distal Femoral Angle (aMDFA); light blue: Mechanical Medial Distal Femoral Angle (mMDFA); yellow: Femoral Varus Angle; red: Angle of version; orange: Neck-Shaft Angle.
The red underlined values are the best values, those closer to zero that most likely represent the correct method that has to be used to measure the angle. (we accepted the best two values for the neck-shaft angle)

4.2 Tibial evaluation

Dealing with tibial angles we had some difficulties in evaluating data as we did not have any parameter to compare with. The reason was that there is just one method to calculate tibial angles and our 3-dimensional method has never been used before so we decided to compare the 2-dimensional measures (see Table I Appendix B) with the 3-dimensional method (see Table II Appendix B) to see if the difference was low enough to consider the 3-dimensional approach statistically acceptable.

First of all we calculated the difference between the 3-dimensional model and the radiographic data in each bone. This difference was called "standard difference" and results are reported in table 4.6

	DISTANZA STANDARD < 10%							
	TIBIA 1dx	TIBIA 1sx	TIBIA 2dx	TIBIA 2sx	TIBIA 3dx	TIBIA 3sx	TIBIA 4dx	TIBIA 4sx
mMPTA	0,20	0,80	3,20	5,50	1,70	3,20	2,60	1,00
mMDTA	2,30	1,50	0,80	4,70	3,10	3,80	3,00	0,60
MAD	0,20	0,80	3,20	5,50	1,70	3,20	2,60	1,00

	TIBIA 5dx	TIBIA 5sx	TIBIA 6dx	TIBIA 6sx	TIBIA 7dx	TIBIA 7sx	TIBIA 8dx	TIBIA 8sx
mMPTA	0,70	1,54	6,33	3,94	0,17	6,22	2,24	1,43
mMDTA	7,52	7,27	0,88	1,29	9,60	3,41	0,89	3,11
MAD	0,70	1,54	6,33	3,70	0,17	6,22	2,24	1,43

Table 4.6 "Standard difference" in 16 tibiae.

We accepted those standard differences with a p value < 0.1. The Table of frequencies has been reported (see Table 4.7)

	FREQUENZE
mMPTA	16
mMDTA	16
MAD	2

Table 4.7 Frequency table of the "Standard difference" in 16 femora.
Note that frequencies referred to Hauptman A and Montavon methods are zero or either 1.

We took into consideration also the mean “standard difference” and the standard deviation to see which values were closer to zero so that they could be acceptable (See table 4.8 and 4.9)

MEDIE DELLE DIST. ST.	
mMPTA	2,35
mMDTA	3,07
MAD	2,35

Table 4.8 Mean of “Standard difference” in 16 tibiae.

DEVIANZA STANDARD	
mMPTA	1,94
mMDTA	2,43
MAD	1,94

Table 4.9 Standard Deviations in 16 tibiae.

We can easily see that frequencies in MAD data are close to zero (2) that is why we cannot consider this value statistically acceptable.

5. DISCUSSION

Hind limb pathologies related with bone deformities are relatively common in both humans and animals; most deformities are developmental and are treated early but adults may have deformities too. Corrective osteotomies are generally performed to treat limb misalignment.

It is crucial to perform a precise and accurate preoperative planning when approaching to a corrective osteotomy: preoperative planning is critical to the success of these procedures.

Evaluation of lower limb alignment in humans is accomplished by standing, full-limb, horizontal beam radiography performed in the same plane [43], unfortunately this is difficult to apply in veterinary medicine. Furthermore the morphology of the femur is hard to be represented in a bidimensional image as a radiograph. Several methods have been suggested to measure femoral and tibial angles, some studies suggested even an assessment using CT and magnetic resonance [1; 9; 11-13; 18; 19; 31; 32; 37; 48; 50; 64; 67] but still there is not a real standardization for the evaluation of hind limb deformities.

During the last years several studies have been suggested to solve all of these problems. New methods combining traditional images with the innovation of the reverse engineering technique have appeared in the medical field [25; 26-29; 34; 62]. Three-dimensional models can be reconstructed from the computerized tomography images and approximated with 2D and 3D fitting algorithms based on reverse engineering methods.

Teams of software engineers and orthopedic surgeons have worked together with the objective of providing the orthopedic community with advanced software solutions capable to improve efficiency in the orthopaedic field [25;26;34; 42].

Recently rapid prototyping has been suggested as one method to solve some problems related with evaluation of hind limb deformities [16], it is becoming a very popular technology in surgical medicine allowing for surgery planning and simulation like never before but even if biomodels can be very usefull to plan and reharse complex

osteotomies of severe deformities, routine cases would probably not benefit as much from use of biomodels.

The main objective of this study was to determine the accuracy of the conventional 2-dimensional methods (based on radiography) to measure femoral and tibial angles comparing the results with a new 3-dimensional model. Our hypothesis was that the 3-dimensional model is more realistic and can be considered a correct evaluation of femoral and tibial angles instead of the radiographic method. Our goal was also to determine which method available in literature best fit the real 3-dimensional axis or angle.

To the authors' knowledge there are only few other reports on the use of 3-dimensional models for determining femoral and tibial angles and most of them are in the human field and in particular they just deal with tibial and femoral torsion or femoral anteversion. Previous studies obtained 3D models from CT images. Our study obtained 3D models from 16 dried femurs and tibiae.

In our study the mean aLPFA angle measured on radiography using Kowalesky's anatomic axis was 112,21°. The average "Standard difference" was 3.95° (<5% of the value), DS was 2.45 and the frequency was high (12/16); the confidence interval was 3.95±2.45 so that the range of the error is not high (1.5 to 6.4). and the 2D value can range from 105.81 to 118.61. As the 3D mean value was 114.62, we can say that this method is acceptable. We decided to accept this method instead of Symax method or Montavon method (even if the mean "Standard difference" and DS were acceptable as shown in fig 5.1 and 5.2 and table 4.4 and 4.5) because Kowalesky method was the one with the highest frequency (table 4.3).

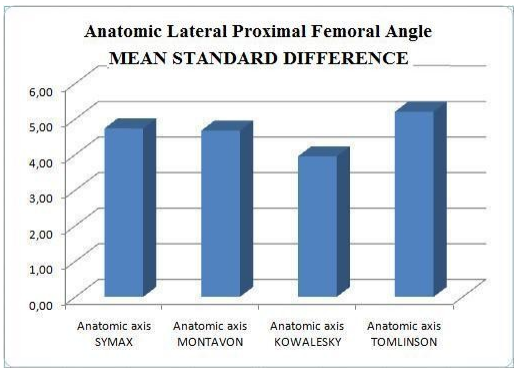

Figure 5.1 Mean of "Standard difference" in 16 femors. Note that Kowalesky method is definately lower than all of the other methods

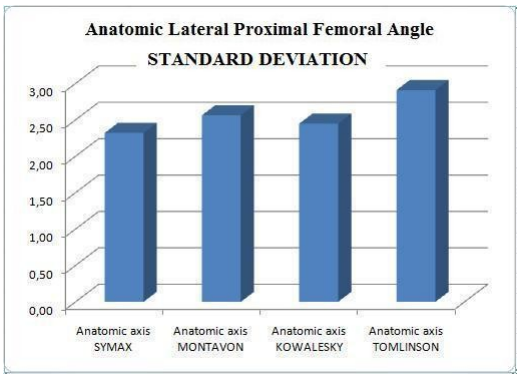

Figure 5.2 Standard Deviation in 16 femors.
Except for Tomlinson's method, SD have values that are similar in the different methods, so three methods can be accectable

Figure 5.3 shows that mean standard difference values of aMDFA are low and similar when measured with either Symax anatomic axis, Montavon anatomic axis or Tomlinson anatomic axis. Standard deviation is acceptable for all of the three methods (figure 5.4) and the frequency is the highest (16/16) for all of them too, so we could choose either one or the other method to measure the aMDFA.

Although all of these three methods can be accepted, due to the easiest way to draw the anatomic axis using Symax method and the lower subjectivity in choosing reference points to draw this line, we prefer to suggest the use of Symax method to measure the aMDFA.

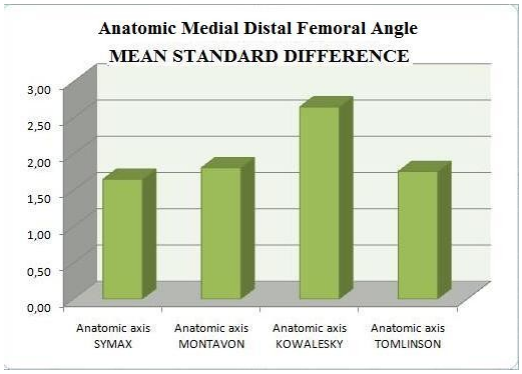

Figure 5.3 Mean of "Standard difference" in 16 femors. It is evident hoe Kowalesky's method can be exckuded as the mean value is definately higher than all of the other data

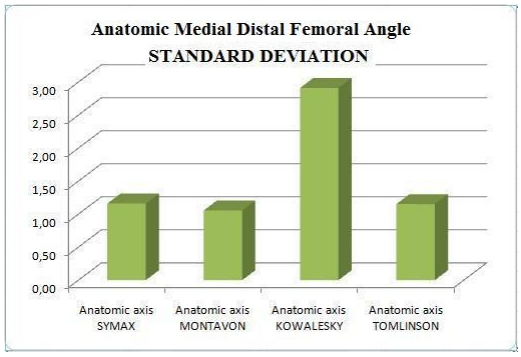

Figure 5.4 Standard Deviation in 16 femors. DS using Kowalesky's method is 2.91, much higher than all of the other methods

Femoral varus angle was measured too (results shown in figure 5.5 and 5.6). We found a difference between the 3-dimensional method and the radiographic evaluation in all of the possible measures.

The best value in measuring femoral varus was the one using Tomlinson's method to draw the anatomic axis. The mean femoral varus angle measured on radiography with this method was 4.05°. The average "Standard difference" was 4.01° that corresponded almost to 58.9% of the 3D mean value so that p was significately higher than 0.05. DS was high too (2.82) and the frequency was close to zero (1/16); the confidence interval was 4.01±2.82 so that the range of the error was extremely high (1.19 to 6.83). Due to all of these reasons we can say that this method is not acceptable.

In dogs the normal magnitude of femoral varus has not been reported. It has been recommended to correct a varus deformity if it is greater than 10° in patients with medial patellar luxation [45]. However, this is based solely on clinical experience. In the present study the mean femoral varus angle on the 3D model was 6.81°, anyway it was not our purpose to obtain a standard of reference for this angle. Future studies could evaluate the physiologic range of values for femoral varus angle using this 3D method, possibly comparing the results applying other 3D methods that have been suggested in human medicine. Furthermore we hypothesized that the difference reported in our study between the radiographic method and the 3D one could be related to a different methodology in calculating this angle. All of the angles measured in this study were calculated through axes as for the 2-dimensional method except for the femoral varus angle and the angle of torsion that were measured through planes. This change in method can create a difference in measuring and standard references.

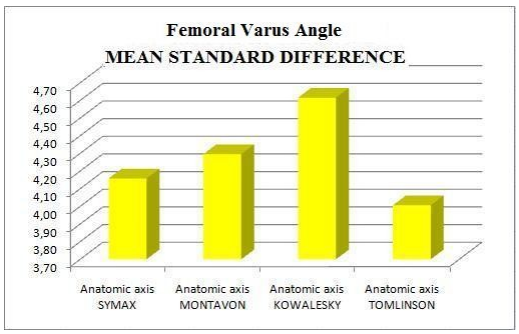

Figure 5.5 Mean of "Standard difference" in 16 femors

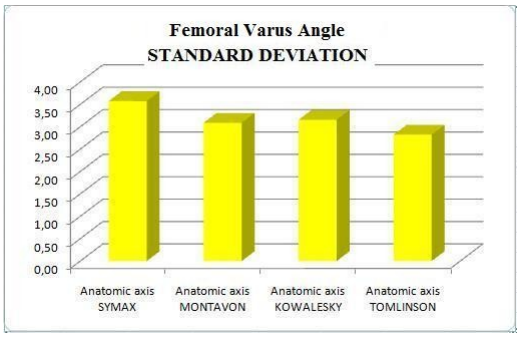

Figure 5.6 Standard Deviation in 16 femors

A difference in the values of femoral neck-shaft angles using Hauptamn A and Montavon's methods have been found too. The frequency was close to zero or zero respectively in the two methods; this difference may be related to the difference in drawing the neck axis: the 3D model considers the neck axis as the axis of the cylinder that best fit the neck related to several sections of this anatomic structure, this can be better represented in a 2-dimensional model (as a radiograph) as a line that bisects the neck. Hauptman A and Montavon's methods calculate the neck axis in a way that is different from this one so that even the average values in the population are different from the other 2-dimensional methods (140°-150° versus 130°-140°).

In our study the radiographic method that better represented the 3D model was the one using Symax method for the neck axis and Kowalesky's method for the anatomic one (high frequency, low mean standard difference and the lowest DS) as shown in figure 5.7 and 5.8 (see also table 4.3; 4.4 and 4.5)

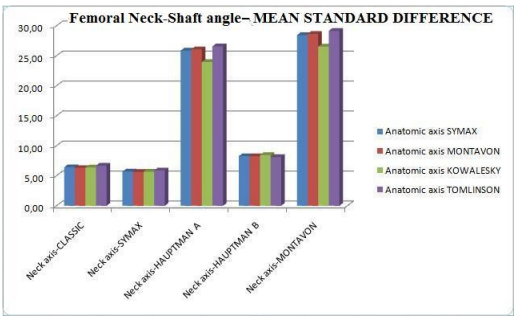

Figure 5.7 Mean of "Standard difference" in 16 femors. It is evident that Hauptman A and Montavon method can be excluded

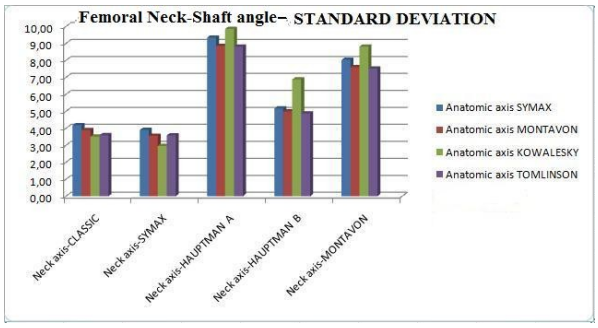

Figure 5.8 Standard Deviations in 16 femors. DS using Kowalesky method combined with Hauptman B method is higher than the other values even if the mean "Standar difference" was similar..

Dealing with the last three femoral measurements (mLPFA, mMDFA and femoral torsion) we cannot say what is the best method as we just have one 2D-method that cannot be compared with others as for the other angles. Either way we can say that no significant differences were found when comparing the radiographic method with the 3-dimensional one for both mLPFA and mMDFA (the mean standard difference and DS were acceptable with a good frequency for both mLPFA and mMDFA , see table 4.3; 4.4; 4.5). This indicates relative consistency of measurements of the radiographic method.

We could not accept the femoral angle of version as the frequency was close to zero and the mean standard difference (7.89) and DS (5.51) too high if compared with the mean 3- dimensional value (23.9). In this case p value was considerably higher than 0.05.

The magnitude of femoral torsion in normal dogs has been previously described, with a mean angle of version ranging from 13.4° to 31.3° in various studies. [6; 37; 40]. In the present study the mean femoral torsion angle of the 3D model was 23.9° ranging from 11.78° to 35.41°, the same average angle in the 2D images was 30.23° ranging from 15.86° to 37.63°. The difference detected in the present study comparing 3D and

2D models may be attributed to measurement techniques. As we previously said for the femoral varus angle, the angle of version was obtained through the creation of planes, this can change the standard values of reference reported in literature where the same angle is calculated just using standard axes instead of planes. The goal of this study was not to define normal values within dog population but future studies may be useful to further evaluate the standard of reference with the new 3D model and compare these values with those available in veterinary literature to see if any relationship exists.

No significant differences were found in tibial angles except for the measurement of MAD: the mean MAD value measured on radiography was 3.81 with a standard deviation of 2.53 and a variance of 2.03. As these values were extremely high and the frequency was close to zero (2/16) with a ranging error of 2.53±2.03 (that can be considered really high if compared to the average 3D method value that was 4.57), we cannot accept this method. It is important to notice that this angle was measured using planes as for the femoral varus angle and the angle of version so we could repeat the same considerations.

A limitation of the present study is that only a small number of femurs and tibiae was evaluated,. with evaluation of additional femurs and tibiae subtle variations between different modalities may prove to be statistically significant. It is important to note, however, that the magnitude of difference between the 3-dimensional model presented in this study, and some of the methods applied to radiography for most of femoral and tibial angles (except for femoral varus, femoral torsion and MAD or for the evaluation of neck-shaft angle using Montavon or either Hauptamn B anatomic axis) is < 5%, which is a clinically acceptable range (as we previously said).

Furthermore the small number of animals and the fact that measures were collected just by one person, does not allow to say that the method is statistically correct. We hypothesized that the 3-dimensional method was more correct than the radiographic one as the 3D image is closer to the real shape of the bone. What we know for sure is that a 3D model is the best for the evaluation of a shell in particular dealing with bones, that have complex shapes. We know that radiography has the limit to present a lack of informations about bone shape as all of the structures are superimposed in one plane.

Furthermore we know that a proper positioning is necessary to obtain a precise radiographic image because a positioning that does not satisfy the selection criteria may compromise the study suggesting erroneous alterations of skeletal alignment

measurements. We also know that proper positioning is not always possible as in case of dogs with joint pain related to common pathologies. If we take into consideration dogs with hind limb deformities we can also find out that other problems exist: radiographic images are usually evaluated for proper positioning through the examination of several parameters such as the patellar position related to the trochlear solcus, the fabellar position in relation to the femoral cortices and so on [5; 30; 59]; with a hind limb deformity these reference points can be lost so we will have no way to evaluate the positioning having a higher risk of error in an eventual preoperative planning for a corrective osteotomy.

So 3-dimensional models are definitely better then the 2-dimensional images but the problem was not on considering just the comparison between a 3-dimension and a 2-dimension, the limit is on the method applied in the evaluation of the axes.

In the last decade different methods have been proposed in human medicine to determine angles using 3D models [25; 26-29; 34; 62]. To our knowledge our method has never been suggested before, except for the evaluation of the anatomic axes and the center of the femoral head. Future studies on a larger number of dogs and/or different operators (at least three) applying this method, could allow the use of a statistical test analysis, such as t-test or ANOVA for example, to define the repeatability, reproducibility and variance of our 3-dimensional model.

Furthermore dogs admitted in this study were mixed-breed dogs with different anatomic characteristics, future studies may be conducted on a larger number of animals possibly of a single breed, this kind of study may allow to obtain a possible ranging value for each angle.

However this study has been useful for a first comparison between our method and the radiographic methods, in the evaluation of the femoral neck axis, the anatomic axis, the mechanical axis, the distal femoral long axis, the transcondylar axis and the distal and proximal tibial joint orientation lines. Based on our previous analysis of the biomechanic in considering which method could better represent these axes in the 3D model, and the results that showed an average error < 5% using most of the radiographic methods, we feel that the reported methodology may be correct except for the evaluation of the planes used to determine femoral varus angle, femoral torsion and MAD.

6. CONCLUSIONS

The goal of our study was to determine the accuracy of the conventional 2-dimensional methods (based on radiography) available up till now to measure femoral and tibial angles comparing the results with a new 3-dimensional model that we suggested.

Even if future studies may be necessary to assess the repeatability , reproducibility and variance of our 3D method, our close analysis of the biomechanic in performing the method and our results can possibly confirm that the reported methodology may be correct exctept for the evaluation of the planes used to determine femoral varus angle, angle of torsion and MAD.

This study showed that the average error in assessing mLPFA , mMDFA , mMPTA and mMDTA, was less than 5% comparing the 2-dimensional method with our 3-dimensional model. Based on these findings, we feel that the reported radiographic methodologies and values may be used to diagnose and quantify hindlimb deformities with a good accuracy.

We obtained the same results, with a p value < 0.05 even for most of the available methods to evaluate aLPFA, aMDFA and neck-shaft angle.

In particular dealing with the aLPFA our results were acceptable for three of the four methods (using Symax, Montavon and Kowalesky anatomic axis). Altough three methods can be acceptable we feel to suggest the application of Kowalesky anatomic axis in the evaluation of aLPFA as this was the method with the highest frequency (12/16).

If we take into consideration the anatomic medial distal femoral angle (aMDFA) our results showed that mean standard difference values were low and similar when measured with either Symax anatomic axis, Montavon anatomic axis or Tomlinson anatomic axis. Although all of these three methods can be accepted, due to the easiest way to draw the anatomic axis using Symax method and the lower subjectivity in choosing reference points to draw this line, we prefer to suggest the use of Symax method to measure the aMDFA.

For the determination of femoral neck-shaft angle we found out that methods applying Hauptman A and Montavon neck axes cannot be acceptable at all. To evaluate

this angle the best methology was the combination of Symax method for the neck axis and Kowalesky's method for the anatomic one but even the application of other anatomic axis could be acceptable even if with a lower accuracy.

We could also observe that femoral varus and torsio values and MAD had a p value significantly > 0.1 , for the angle of version it was higher than 0.05. Due to these results we should not recommend the applycation of the 2-dimensional model in the evaluation of these angle; however we strogly believe that the difference detected in the present study comparing 3D and 2D models may be attributed to the difference in measurement techniques.

Future studies are indicated to determine the repeatability and reproducibility of our 3D method and to possibly obtain ranging values in different breeds.

Even if some of the 2 dimensional methods can be applied with a good accuracy, we strongly believe that the future in the evaluation of hind limb deformities is in preoperative plannings performed on 3D models as they are the best in representing complex shapes such as in the medical field.

7. REFERENCES

1. Abel S.B., Hammer D.L., Shott S.: Use of the proximal portion of the tibia for measurement of the tibial plateau angle in dogs. Am J Vet Res 2003; 64 (9): 1117-1123
2. Apelt D, Kowaleski MP, Dyce J: Comparison of Computed Tomographic and standard radiographic determination of tibial torsion in the dog. Vet Surg, 2005, 34(5): 457-462
3. Arnoczy SP: Meccanica patologica dei traumi a carico dei legamenti crociati e dei menischi. In: Boyrab M.J.: Le basi patogenetiche delle malattie chirurgiche nei piccoli animali. S. Lazzaro di Savena-Bologna: Giraldi Editore, 2001, 1023-1038
4. Arnockzy SP, Torzilli PA. Biomechanical analysis of the forces acting about the canine hip. Am J Vet Res, 1981. 42:1581
5. Ballatori C.: Le patologie legate ai difetti di allineamento dell'arto posteriore del cane. Tesi di dottorato, Università degli studi di Pisa, Facoltà di Medicina Veterinaria, Anni Accademici 2004-2006
6. Bardet JF, Rudy RL, Hohn RB. Measurement of femoral torsion in dogs using a biplanar method. Vet Surg 1983; 12:1-6
7. Baroni E., Matthias R.R., Marcellin-Little D.J., Vezzoni A., Stebbins M.E.: Comparison of radiographic assessments of the tibial plateau slope in dogs. Am J Vet Res 2003; 64 (5): 586-589
8. Baroni T: Allineamento dell'arto pelvico nel cane: analisi comparativa tra valutazione radiografica e ricostruzione 3D della deviazione angolare della tibia. Tesi di laurea, Università degli studi di Padova, Facoltà di Medicina Veterinaria, AnnoAccademico 2007-2008
9. Caylor K.B., Zumpano C.A., Evans L.M., Moore R.W.: Intra- and interobserver measurement variability of tibial plateau slope from lateral radiographs in dogs. J Am Anim Hosp Assoc 2001; 37(3): 263-268
10. Ciffo M: Analisi comparativa tra valutazione radiografica e ricostruzione 3D della deviazione angolare nel femore del cane. Tesi di laurea, Università degli studi di Padova, Facoltà di Medicina Veterinaria, AnnoAccademico 2007-2008.

11. Dismukes DI, Fox DB, Tomlinson JL, Cook JL, Essman SC: Determination of pelvic limb alignment in the large-breed dog: a cadaveric radiographic study in the frontal plane. Vet Surg 2008; 37:674-682
12. Dismukes DI., Tomlinson J.L., Fox D.B., Cook J.L., Song KJE: Radiographic measurement of the proximal and distal mechanical joint angles in the canine tibia. . Vet Surg 2007, 36:699-704
13. Dudley RM, Kowaleski MP, Drost WMT Dyce J. Radiographic and computed tomographic determination of femoral varus and torsion in the dog. Vet Radiol Ultrasound 2006; 47(6): 546-552
14. Gibbons SE, Macias C, Tonzing MA, Pinchbeck GL, McKee WM: Patellar luxation in 70 large breed dogs. J Small Anim Pract, 2006; 47:3-9
15. Haransen G: Patellar luxation: Pathogenesis and surgical correction. CVJ, 2006, 47:1037-1039
16. Harrison OLA, Cormier DR, Marcellin-Little DJ, Jajal K: Rapid prototyping for treatment of canine limb deformities. Rapid prototyping journal, 2003 9(1): 37-42
17. Hauptam J: Articolazione dell'anca. In Slatter DH: Trattato di chirurgia dei piccoli animali, SMB (Ed), 1990, 2153-2160.
18. Hauptman J: Interobserver variation in the measurement of the femoral angle of inclination. Veterinary surgery 1983; 12; 189-191
19. Hauptman J, Prieur WD, Butler HC, et al. The angle of inclination of the canine femoral head and neck. Vet Surg, 1979, 8:74-77
20. Hayes AG, Boudrieau RJ, Hungerford LL: Frequency and distribution of medial and lateral patellar luxation in dogs: 124 cases (1982-1992). J Am Vet Med Assoc 1994; 205:716-720.
21. Hulse DA: Lussazione mediale della rotula. In: Boyrab M.J.: Le basi patogenetiche delle malattie chirurgiche nei piccoli animali. S. Lazzaro di Savena-Bologna: Giraldi Editore, 2001, 1077-1088
22. Hulse DA, Shire PK. Articolazione femoro-tibio-rotulea. In Slatter DH: Trattato di chirurgia dei piccoli animali, SBM (Ed), 1990, 2193-2235
23. Jaegger G, Marcellin-Little DJ, Levine D: Reliability of goniometry in Labrador Retrievers. Am J Vet Res 2002; 63:979-986

24. Kaiser S, Cornley D, Golder W et al. The correlation of canine patellar luxation and the anteversion angle as measured using magnetic resonance images. Vet Radiol Ultrasound 2001; 42:113-118

25. Kawakami H, Sugano N, Nagaoka T, Hagio K, Yonenobu K, Yoshikawa H, Ochi T, Hattori A, Suzuki N: 3D Analysis of the alignment of the lower extremity in high tibial osteotomy. LNCS, 2002; 2489:261-267

26. Kawakami H, Sugano N, Yonenobu K, Yoshikawa H, Ochi T, Hattori A, Suzuki N. Effects of rotation on measurement of lower limb alignment for knee osteotomy. J orthop Res 2006; 22(6): 1248-1253

27. Kim JS, Kim JSII: A new measurement method of femoral anteversion based on the 3Dmodeling. Engineering in medicine and biology society, 1997, Proceedings of the 19th Annual International Conference of the IEEE; vol1: 418-421

28. Kim JS, Park TS, Kim JS, Kim IY, Kim SI: Measurement of femoral neck anteversion in 3D . Part 1 and 2: 3D imaging method. Med Biol Eng Comput 2000; 38(6):603-616

29. Kowaleski MP. Femoral corrective osteotomy for medial patellar luxation. Proceedings of the ACVS Veterinary Symposium, Washington, DC, 2006, 473-476

30. Kowaleski MP. Patellar luxation – Preoperative evaluation and surgical planning for femoral corrective osteotomy. 13th ESVOT Congress, Monaco, September 7th-10th 2006, 87-90

31. Lee YS; Oh SH; Seon JK; Song EK; Yoon TR: 3D femoral neck anteversion measurements based on the posterior femoral plane in ORTHODOC system. Med Biol Eng Comput 2007; 45(3):325

32. Lozier S: Limb Alignment in dogs with cranial cruciate ligament injury. 12th ESVOT Congress, Munich, September 10-12th 2004, 78-79

33. Lozier SM: Proximal tibial alignment for correction of patellar luxation. 13th ESVOT Congress, Munich, September 7-10th 2006, 101-103

34. Mahaisavarya B, Sitthiseripratip K, Tongdee T, Bohez ELJ, Sloten V, Oris P: Morphological study of the proximal femur: a new method of geometrical assessment using 3-dimensional reverse engineering. Medical Engineering &physics 2002; 24(9):617-622

35. Mann FA, et al. Manual goniometric measurement of the canine pelvic limb. J am Anim Hosp Assoc 1988. 24:189
36. Martini FM, Marmiroli M, Gemmi S. Approccio diagnostico alle deviazioni dell'arto pelvico nel cane. XI congresso nazionale SICV, 10-12 giugno 2004, 87-90
37. Montavon PM, Hohn RB, Olmstead ML, et al. Inclination and anteversion angles of the femoral head and neck in the dog evaluation of a standard method of measurement. Vet Surg, 1985, 14:272-282
38. Mostafa AA, Griffon DJ, Thomas MW, Constable PD: Proximal evaluation and association with medial and lateral patellar luxation. Vet Surg 2008; 31:201-211.
39. Ness MG, Abercromby RH, May C, Turner BM, Carmichael S: A survey of orthopaedic conditions in small naimal veterinary practice in Britain. VCOT, 1996;9:43-52
40. Nunamaker DM, Beiry DN, Newton CD. Femoral neck anteversion in the dog: its radiographic measurement. Am J Vet Rad Soc 1973; 14:45-48
41. Olmstead ML: Lussazione laterale della rotula. In: Boyrab M.J.: Le basi patogenetiche delle malattie chirurgiche nei piccoli animali. S. Lazzaro di Savena-Bologna: Giraldi Editore, 2001, 1089-1092
42. Orthocrat solutions: http://www.orthocrat.com/index.html
43. Paley D, Herzenberg JE. Principles of deformity correction. (ed 1) Springer-Verlag. Berlin Heidelberg, 2002
44. Paley D, Tetsworth K Mechanical axis deviation of the lower limbs: preoperative planning of uniapical angular deformities of the tibia and femur. Clin Orthop 1992' 280:48-64
45. Palmer RH: Patellar Luxation: Femoral osteotomy and other therapeutic options in large breed dogs. Proceedings American College of Veterinary Surgeons Symposium, 2001
46. Palmer RH: Patellar Luxation: Therapeutic options in small breed dogs. ACVS Veterinary Symposium Equine and Small Animal Proceedings, October 1st, 2002.
47. Pauwels F Biomechanic of the locomotor apparatus. Springer Verlag,New York, 1980: 1-228
48. Petazzoni M., Atlante di goniometria clinica e misurazioni radiografiche dell’arto pelvico. 2008

49. Roch SP, Gemmil TJ: Treatment of mesial patellar luxation by femoral closing wedge ostectomy using a distal femoral plate in four dogs. J Small Anim Pract, 2008; 49:152-158

50. Rumph PF, Hathcock JT: A symmetric axis-based method for measuring the projected femoral angle of inclincation in dogs. Vet Surg 1990; 19(5): 328-333

51. Sabharwal S, Zhao C. Assessment of Lower Limb Alignment: Supine Fluoroscopy Compared with a Standing Full-Lenght Radiograph. J Bone Joint Surg Am 2008; 90 (1):43-51

52. Sarierler M. Comparison of femoral inclination angle measurements in dysplastic and nondysplastic dogs of different breeds Acta Vet Hung, 2004, 52:245-252;

53. Sharma L, Song J, Felson DT, Cahue S, Shamiyeh E, Dunlop D: The role of knee alignment in disease progression and functional decline in knee osteoarthritis. J Am Med Assoc 2001; 286:188-195

54. Shulz KS, Dejardin LM: Trattamento chirurgico della displasia dell'anca nel cane. In Slatter: Trattato di chirurgia dei piccoli animali, Antonio Delfino (Ed), 2005:2029-2032

55. Singleton WB: The surgical correction of stifle deformities in the dog. J Small Anim Pract 1969; 10:59

56. Slocum B, Devine T.: Cranial Tibial Thrust: a primary force in the canine stifle. J Am Vet Med Assoc 1983; 183: 456-459

57. Slocum B, Devine T.: Tibial plateau leveling osteotomy and cranial closing wedge osteotomy. http://www.slocumenterprisers.com, 1996

58. Slocum B, Devine T.: Trattamento della rottura del legamento crociato craniale mediante osteotomia livellante del plateau tibiale. In: Boyrab MJ, Ellison GW, SlocumB: Tecnica chirurgica 2- Chirurgia ortopedico-traumatologica: rachide, scheletro appendicolare. Torino: Unione Tipografico- Editrice Torinese, 2001:1152-1157.

59. Slocum B, Slocum TD: Alignment problems of the hindlimb. 10th ESVOT Congress, Monaco, March 23rd-26th 2000.

60. Slocum B, Slocum TD: Patellar luxation, a problem of alignment. www.slocumenterprises.com/Article/patellar_luxation.htm

61. Slocum B, Slocum TD.: Tibial plateau leveling osteotomy for repair of cranial cruciate ligament rupture in the canine. Vet Clin North Am Small Anim Pract. 1993; 23 (4): 777-795.
62. Subburaj K, Ravi B, Agarwal MG: Computerized Assessment of excessive femoral and tibial torsional deformation by 3D Anatomical landmarks referencing. 13th International Conference of Biomedical Engineering, Suntec Singapore, December 3rd-6th 2008: 136
63. Swiderski JK, Radecki SV, Park RD, Palmer RH. Comparison of radiographic and anatomic femoral varus angle measurements in normal dogs. Vet Surg, 2008, 37:43-48
64. Tomlinson J, Fox D, Cook JL, Keller GG. Measurement of femoral angles in four dog breeds. Vet Surg, 2007, 36:593-598.).
65. Towle HA, Griffon DJ, Thomas MW, Siegel AM, Dinning D, Johnson A. Pre- and postoperative radiographic and computed tomographic evaluation of dogs with medial patellar luxation. Vet Surg 2005; 34:265-272.
66. Vasseur PB, Arnozky SP. Collateral ligaments of the canine stifle joint: Anatomic and functional analysis. Am J Vet Res, 1981, 42:1133
67. Vezzoni A. Definizioni delle deviazioni assiali. Incontro SIOVET, Cremona, November 18th-19th 2006.
68. Weigel JP, Wasserman JF. Biomechanics of the normal and abnormal hip joint. Vet Clin North Am Small Anim Pract, 1992. 22(3):513-528.
69. Willauer CC, Vesseur PB: Clinical results of surgical correction of medial luxation of the patella in dogs. Vet Surg 1987; 16:31-36

APPENDICES

Appendix A

Table I Right femur n.1: "Standard difference" between 2D-angles obtained with different methods and3D-angles obtained in the same way. Blue: Anatomic Lateral Proximal Femoral Angle (aLPFA); grey: Mechanical Lateral Proximal Femoral Angle (mLPFA); green: Anatomic Medial Distal Femoral Angle (aMDFA); light blue: Mechanical Medial Distal Femoral Angle (mMDFA); yellow: Femoral Varus Angle; red: Angle of version; orange: Neck-Shaft Angle.
The underlined values are values whit p<0,05.

	Anatomic axis SYMAX	Anatomic axis MONTAVON	Anatomic axis KOWALESKY	Anatomic axis TOMLINSON	Mechanical axis	Angle of version
Hip joint orientation line	**5,29**	7,73	**0,56**	7,90	**5,37**	9,55
Transcondylar axis	**1,70**	**4,04**	**3,03**	**3,16**	**4,10**	
Distal femoral long axis	2,18	4,25	2,55	4,08		
Neck axis-CLASSIC	**1,94**	**4,38**	**2,79**	**4,55**		
Neck axis-SYMAX	**0,11**	**2,33**	**4,84**	**2,50**		
Neck axis-HAUPTMAN A	21,35	23,78	16,62	23,95		
Neck axis-HAUPTMAN B	**3,89**	**6,33**	**0,84**	**6,50**		
Neck axis-MONTAVON	22,96	25,40	18,23	25,57		

LEFT FEMUR N.1

Table II Left femur n.1: 2-dimensional values of the angles obtained with different methods. Blue: Anatomic Lateral Proximal Femoral Angle (aLPFA); grey: Mechanical Lateral Proximal Femoral Angle (mLPFA); green: Anatomic Medial Distal Femoral Angle (aMDFA); light blue: Mechanical Medial Distal Femoral Angle (mMDFA); yellow: Femoral Varus Angle; red: Angle of version; orange: Neck-Shaft Angle

	Anatomic axis SYMAX	Anatomic axis MONTAVON	Anatomic axis KOWALESKY	Anatomic axis TOMLINSON	Mechanical axis	Angle of version
Hip joint orientation line	111,55	112,20	117,80	111,34	105,87	31,13
Transcondylar axis	95,78	96,43	102,02	95,56	90,09	
Distal femoral long axis	5,78	6,43	12,02	5,56		
Neck axis-CLASSIC	134,54	133,89	128,30	134,76		
Neck axis-SYMAX	129,44	128,79	123,19	129,66		
Neck axis-HAUPTMAN A	157,89	157,25	151,65	158,11		
Neck axis-HAUPTMAN B	124,95	124,31	118,71	125,17		
Neck axis-MONTAVON	154,84	154,19	148,59	155,05		

Table III Left femur n.1: 3-dimensional values of the angles obtained with different methods. Blue: Anatomic Lateral Proximal Femoral Angle (aLPFA); grey: Mechanical Lateral Proximal Femoral Angle (mLPFA); green: Anatomic Medial Distal Femoral Angle (aMDFA); light blue: Mechanical Medial Distal Femoral Angle (mMDFA); yellow: Femoral Varus Angle; red: Angle of version; orange: Neck-Shaft Angle.

	Neck-shaft angle	Femoral varus angle	aMDFA	aLPFA	mLPFA	mMDFA	Angle of version
	131,92	5,30	94,80	114,14	108,81	91,48	26,45
5% of the value	*6,60*	*0,27*	*4,74*	*5,71*	*5,44*	*4,57*	*1,32*

Table IV Left femur n.1: "Standard difference" between 2D-angles obtained with different methods and3D-angles obtained in the same way. Blue: Anatomic Lateral Proximal Femoral Angle (aLPFA); grey: Mechanical Lateral Proximal Femoral Angle (mLPFA); green: Anatomic Medial Distal Femoral Angle (aMDFA); light blue: Mechanical Medial Distal Femoral Angle (mMDFA); yellow: Femoral Varus Angle; red: Angle of version; orange: Neck-Shaft Angle.
The underlined values are values whit p<0,05.

	Anatomic axis SYMAX	Anatomic axis MONTAVON	Anatomic axis KOWALESKY	Anatomic axis TOMLINSON	Mechanical axis	Angle of version
Hip joint orientation line	**2,59**	**1,94**	**3,66**	**2,80**	**2,94**	4,68
Transcondylar axis	**0,98**	**1,63**	7,22	**0,76**	**1,39**	
Distal femoral long axis	0,48	1,13	6,72	**0,26**		
Neck axis-CLASSIC	**2,62**	**1,97**	**3,62**	**2,84**		
Neck axis-SYMAX	**2,48**	**3,13**	8,73	**2,26**		
Neck axis-HAUPTMAN A	25,97	25,33	19,73	26,19		
Neck axis-HAUPTMAN B	6,97	7,61	13,21	6,75		
Neck axis-MONTAVON	22,92	22,27	16,67	23,13		

RIGHT FEMUR N.2

Table V Right femur n.2: 2-dimensional values of the angles obtained with different methods. Blue: Anatomic Lateral Proximal Femoral Angle (aLPFA); grey: Mechanical Lateral Proximal Femoral Angle (mLPFA); green: Anatomic Medial Distal Femoral Angle (aMDFA); light blue: Mechanical Medial Distal Femoral Angle (mMDFA); yellow: Femoral Varus Angle; red: Angle of version; orange: Neck-Shaft Angle

	Anatomic axis SYMAX	Anatomic axis MONTAVON	Anatomic axis KOWALESKY	Anatomic axis TOMLINSON	Mechanical axis	Angle of version
Hip joint orientation line	109,94	109,78	109,74	109,58	105,33	32,05
Transcondylar axis	84,17	84,01	83,98	83,81	79,56	
Distal femoral long axis	5,82	5,98	6,02	6,18		
Neck axis-CLASSIC	123,55	123,71	123,74	123,91		
Neck axis-SYMAX	124,56	124,72	124,76	124,92		
Neck axis-HAUPTMAN A	148,39	148,55	148,59	148,75		
Neck axis-HAUPTMAN B	106,98	107,13	107,17	107,34		
Neck axis-MONTAVON	152,03	152,19	152,22	152,39		

Table VI Right femur n.2: 3-dimensional values of the angles obtained with different methods. Blue: Anatomic Lateral Proximal Femoral Angle (aLPFA); grey: Mechanical Lateral Proximal Femoral Angle (mLPFA); green: Anatomic Medial Distal Femoral Angle (aMDFA); light blue: Mechanical Medial Distal Femoral Angle (mMDFA); yellow: Femoral Varus Angle; red: Angle of version; orange: Neck-Shaft Angle.

	Neck-shaft angle	Femoral varus angle	aMDFA	aLPFA	mLPFA	mMDFA	Angle of version
	125,3	6,79	86,59	115,45	109,07	84,36	15,99
5% of the value	*6,27*	*0,34*	*4,33*	*5,77*	*5,45*	*4,22*	*0,80*

Table VII Right femur n.2: "Standard difference" between 2D-angles obtained with different methods and3D-angles obtained in the same way. Blue: Anatomic Lateral Proximal Femoral Angle (aLPFA); grey: Mechanical Lateral Proximal Femoral Angle (mLPFA); green: Anatomic Medial Distal Femoral Angle (aMDFA); light blue: Mechanical Medial Distal Femoral Angle (mMDFA); yellow: Femoral Varus Angle; red: Angle of version; orange: Neck-Shaft Angle.
The underlined values are values whit p<0,05.

	Anatomic axis SYMAX	Anatomic axis MONTAVON	Anatomic axis KOWALESKY	Anatomic axis TOMLINSON	Mechanical axis	Angle of version
Hip joint orientation line	**5,51**	**5,67**	**5,71**	5,87	**3,74**	16,06
Transcondylar axis	**2,42**	**2,58**	**2,61**	**2,78**	4,80	
Distal femoral long axis	0,97	0,81	0,77	0,61		
Neck axis-CLASSIC	**1,75**	**1,59**	**1,56**	**1,39**		
Neck axis-SYMAX	**0,74**	**0,58**	**0,54**	**0,38**		
Neck axis-HAUPTMAN A	23,09	23,25	23,29	23,45		
Neck axis-HAUPTMAN B	18,32	18,17	18,13	17,96		
Neck axis-MONTAVON	26,73	26,89	26,92	27,09		

LEFT FEMUR N.2

Table VIII Left femur n.2: 2-dimensional values of the angles obtained with different methods. Blue: Anatomic Lateral Proximal Femoral Angle (aLPFA); grey: Mechanical Lateral Proximal Femoral Angle (mLPFA); green: Anatomic Medial Distal Femoral Angle (aMDFA); light blue: Mechanical Medial Distal Femoral Angle (mMDFA); yellow: Femoral Varus Angle; red: Angle of version; orange: Neck-Shaft Angle

	Anatomic axis SYMAX	Anatomic axis MONTAVON	Anatomic axis KOWALESKY	Anatomic axis TOMLINSON	Mechanical axis	Angle of version
Hip joint orientation line	111,94	111,54	110,53	111,02	107,55	32,28
Transcondylar axis	85,40	85,00	83,99	84,48	81,01	
Distal femoral long axis	4,60	5,00	6,01	5,52		
Neck axis-CLASSIC	123,78	124,19	125,20	124,71		
Neck axis-SYMAX	123,30	123,70	124,72	124,22		
Neck axis-HAUPTMAN A	152,95	153,35	154,36	153,87		
Neck axis-HAUPTMAN B	116,10	116,51	117,52	117,03		
Neck axis-MONTAVON	153,01	153,42	154,43	153,94		

Table IX Left femur n.2: 3-dimensional values of the angles obtained with different methods. Blue: Anatomic Lateral Proximal Femoral Angle (aLPFA); grey: Mechanical Lateral Proximal Femoral Angle (mLPFA); green: Anatomic Medial Distal Femoral Angle (aMDFA); light blue: Mechanical Medial Distal Femoral Angle (mMDFA); yellow: Femoral Varus Angle; red: Angle of version; orange: Neck-Shaft Angle.

	Neck-shaft angle	Femoral varus angle	aMDFA	aLPFA	mLPFA	mMDFA	Angle of version
	129,85	6,67	87,17	118,98	111,58	84,67	23,34
5% of the value	*6,49*	*0,33*	*4,36*	*5,95*	*5,58*	*4,23*	*1,17*

Table X Left femur n.2: "Standard difference" between 2D-angles obtained with different methods and3D-angles obtained in the same way. Blue: Anatomic Lateral Proximal Femoral Angle (aLPFA); grey: Mechanical Lateral Proximal Femoral Angle (mLPFA); green: Anatomic Medial Distal Femoral Angle (aMDFA); light blue: Mechanical Medial Distal Femoral Angle (mMDFA); yellow: Femoral Varus Angle; red: Angle of version; orange: Neck-Shaft Angle.
The underlined values are values whit p<0,05.

	Anatomic axis SYMAX	Anatomic axis MONTAVON	Anatomic axis KOWALESKY	Anatomic axis TOMLINSON	Mechanical axis	Angle of version
Hip joint orientation line	7,04	7,44	8,45	7,96	**4,03**	8,94
Transcondylar axis	**1,77**	**2,17**	**3,18**	**2,69**	**3,66**	
Distal femoral long axis	2,07	1,67	0,66	1,15		
Neck axis-CLASSIC	**6,07**	**5,66**	**4,65**	**5,14**		
Neck axis-SYMAX	6,55	**6,15**	**5,13**	**5,63**		
Neck axis-HAUPTMAN A	23,10	23,50	24,51	24,02		
Neck axis-HAUPTMAN B	13,75	13,34	12,33	12,82		
Neck axis-MONTAVON	23,16	23,57	24,58	24,09		

RIGHT FEMUR N.3

Table XI Right femur n.3: 2-dimensional values of the angles obtained with different methods. Blue: Anatomic Lateral Proximal Femoral Angle (aLPFA); grey: Mechanical Lateral Proximal Femoral Angle (mLPFA); green: Anatomic Medial Distal Femoral Angle (aMDFA); light blue: Mechanical Medial Distal Femoral Angle (mMDFA); yellow: Femoral Varus Angle; red: Angle of version; orange: Neck-Shaft Angle

	Anatomic axis SYMAX	Anatomic axis MONTAVON	Anatomic axis KOWALESKY	Anatomic axis TOMLINSON	Mechanical axis	Angle of version
Hip joint orientation line	107,00	106,39	106,56	106,35	102,43	37,63
Transcondylar axis	88,00	87,39	87,56	87,35	83,43	
Distal femoral long axis	1,63	2,24	2,07	2,27		
Neck axis-CLASSIC	123,45	124,06	123,88	124,09		
Neck axis-SYMAX	121,34	121,95	121,78	121,98		
Neck axis-HAUPTMAN A	152,04	152,65	152,47	152,68		
Neck axis-HAUPTMAN B	108,96	109,56	109,39	109,60		
Neck axis-MONTAVON	153,07	153,67	153,50	153,71		

Table XII Right femur n.3: 3-dimensional values of the angles obtained with different methods. Blue: Anatomic Lateral Proximal Femoral Angle (aLPFA); grey: Mechanical Lateral Proximal Femoral Angle (mLPFA); green: Anatomic Medial Distal Femoral Angle (aMDFA); light blue: Mechanical Medial Distal Femoral Angle (mMDFA); yellow: Femoral Varus Angle; red: Angle of version; orange: Neck-Shaft Angle.

	Neck-shaft angle	Femoral varus angle	aMDFA	aLPFA	mLPFA	mMDFA	Angle of version
	114,63	7,96	88,12	112,69	103,72	84,55	35,41
5% of the value	*5,73*	*0,40*	*4,41*	*5,63*	*5,19*	*4,23*	*1,77*

Table XIII Right femur n.3: "Standard difference" between 2D-angles obtained with different methods and3D-angles obtained in the same way. Blue: Anatomic Lateral Proximal Femoral Angle (aLPFA); grey: Mechanical Lateral Proximal Femoral Angle (mLPFA); green: Anatomic Medial Distal Femoral Angle (aMDFA); light blue: Mechanical Medial Distal Femoral Angle (mMDFA); yellow: Femoral Varus Angle; red: Angle of version; orange: Neck-Shaft Angle.
The underlined values are values whit p<0,05.

	Anatomic axis SYMAX	Anatomic axis MONTAVON	Anatomic axis KOWALESKY	Anatomic axis TOMLINSON	Mechanical axis	Angle of version
Hip joint orientation line	5,69	6,30	6,13	6,34	**1,29**	2,22
Transcondylar axis	**0,12**	**0,73**	**0,56**	**0,77**	**1,12**	
Distal femoral long axis	6,33	5,72	5,89	5,69		
Neck axis-CLASSIC	8,82	9,43	9,25	9,46		
Neck axis-SYMAX	6,71	7,32	7,15	7,35		
Neck axis-HAUPTMAN A	37,41	38,02	37,84	38,05		
Neck axis-HAUPTMAN B	**5,67**	**5,07**	**5,24**	**5,03**		
Neck axis-MONTAVON	38,44	39,04	38,87	39,08		

LEFT FEMUR N.3

Table XIV Left femur n.3: 2-dimensional values of the angles obtained with different methods. Blue: Anatomic Lateral Proximal Femoral Angle (aLPFA); grey: Mechanical Lateral Proximal Femoral Angle (mLPFA); green: Anatomic Medial Distal Femoral Angle (aMDFA); light blue: Mechanical Medial Distal Femoral Angle (mMDFA); yellow: Femoral Varus Angle; red: Angle of version; orange: Neck-Shaft Angle

	Anatomic axis SYMAX	Anatomic axis MONTAVON	Anatomic axis KOWALESKY	Anatomic axis TOMLINSON	Mechanical axis	Angle of version
Hip joint orientation line	106,71	107,67	108,87	107,26	102,07	30,58
Transcondylar axis	87,49	88,45	89,64	88,04	82,85	
Distal femoral long axis	2,51	1,55	0,35	1,96		
Neck axis-CLASSIC	119,5	118,54	117,34	118,95		
Neck axis-SYMAX	120,83	119,87	118,67	120,28		
Neck axis-HAUPTMAN A	143,88	142,92	141,72	143,33		
Neck axis-HAUPTMAN B	106,02	105,06	103,86	105,47		
Neck axis-MONTAVON	148,74	147,78	146,58	148,19		

Table XV Left femur n.3: 3-dimensional values of the angles obtained with different methods. Blue: Anatomic Lateral Proximal Femoral Angle (aLPFA); grey: Mechanical Lateral Proximal Femoral Angle (mLPFA); green: Anatomic Medial Distal Femoral Angle (aMDFA); light blue: Mechanical Medial Distal Femoral Angle (mMDFA); yellow: Femoral Varus Angle; red: Angle of version; orange: Neck-Shaft Angle.

	Neck-shaft angle	Femoral varus angle	aMDFA	aLPFA	mLPFA	mMDFA	Angle of version
	122,23	8,54	89,62	111,12	103,3	86,4	31,76
5% of the value	*6,11*	*0,43*	*4,48*	*5,56*	*5,17*	*4,32*	*1,59*

Table XVI Left femur n.3: "Standard difference" between 2D-angles obtained with different methods and3D-angles obtained in the same way. Blue: Anatomic Lateral Proximal Femoral Angle (aLPFA); grey: Mechanical Lateral Proximal Femoral Angle (mLPFA); green: Anatomic Medial Distal Femoral Angle (aMDFA); light blue: Mechanical Medial Distal Femoral Angle (mMDFA); yellow: Femoral Varus Angle; red: Angle of version; orange: Neck-Shaft Angle.
The underlined values are values whit p<0,05.

	Anatomic axis SYMAX	Anatomic axis MONTAVON	Anatomic axis KOWALESKY	Anatomic axis TOMLINSON	Mechanical axis	Angle of version
Hip joint orientation line	4,41	3,45	2,25	3,86	1,23	1,18
Transcondylar axis	2,13	1,17	0,02	1,58	3,55	
Distal femoral long axis	6,03	6,99	8,19	6,58		
Neck axis-CLASSIC	2,73	3,69	4,89	3,28		
Neck axis-SYMAX	1,40	2,36	3,56	1,95		
Neck axis-HAUPTMAN A	21,65	20,69	19,49	21,10		
Neck axis-HAUPTMAN B	16,21	17,17	18,37	16,76		
Neck axis-MONTAVON	26,51	25,55	24,35	25,96		

RIGHT FEMUR N.4

Table XVII Right femur n.4: 2-dimensional values of the angles obtained with different methods. Blue: Anatomic Lateral Proximal Femoral Angle (aLPFA); grey: Mechanical Lateral Proximal Femoral Angle (mLPFA); green: Anatomic Medial Distal Femoral Angle (aMDFA); light blue: Mechanical Medial Distal Femoral Angle (mMDFA); yellow: Femoral Varus Angle; red: Angle of version; orange: Neck-Shaft Angle

	Anatomic axis SYMAX	Anatomic axis MONTAVON	Anatomic axis KOWALESKY	Anatomic axis TOMLINSON	Mechanical axis	Angle of version
Hip joint orientation line	118,01	120,93	121,58	120,98	113,29	32,87
Transcondylar axis	90,82	93,74	94,39	93,78	86,09	
Distal femoral long axis	0,81	3,73	4,38	3,78		
Neck axis-CLASSIC	125,59	122,67	122,02	122,63		
Neck axis-SYMAX	128,43	125,52	124,87	125,47		
Neck axis-HAUPTMAN A	152,40	149,48	148,83	149,43		
Neck axis-HAUPTMAN B	120,70	117,78	117,13	117,74		
Neck axis-MONTAVON	154,60	151,68	151,03	151,63		

Table XVIII Right femur n.4: 3-dimensional values of the angles obtained with different methods. Blue: Anatomic Lateral Proximal Femoral Angle (aLPFA); grey: Mechanical Lateral Proximal Femoral Angle (mLPFA); green: Anatomic Medial Distal Femoral Angle (aMDFA); light blue: Mechanical Medial Distal Femoral Angle (mMDFA); yellow: Femoral Varus Angle; red: Angle of version; orange: Neck-Shaft Angle.

	Neck-shaft angle	Femoral varus angle	aMDFA	aLPFA	mLPFA	mMDFA	Angle of version
	112,95	0,03	94,5	123,88	114,55	90,43	24,35
5% of the value	*5,65*	*0,00*	*4,73*	*6,19*	*5,73*	*4,52*	*1,22*

Table XIX Right femur n.4: "Standard difference" between 2D-angles obtained with different methods and3D-angles obtained in the same way. Blue: Anatomic Lateral Proximal Femoral Angle (aLPFA); grey: Mechanical Lateral Proximal Femoral Angle (mLPFA); green: Anatomic Medial Distal Femoral Angle (aMDFA); light blue: Mechanical Medial Distal Femoral Angle (mMDFA); yellow: Femoral Varus Angle; red: Angle of version; orange: Neck-Shaft Angle.
The underlined values are values whit p<0,05.

	Anatomic axis SYMAX	Anatomic axis MONTAVON	Anatomic axis KOWALESKY	Anatomic axis TOMLINSON	Mechanical axis	Angle of version
Hip joint orientation line	5,87	2,95	2,30	2,90	1,26	8,52
Transcondylar axis	3,68	0,76	0,11	0,72	4,34	
Distal femoral long axis	0,78	3,70	4,35	3,75		
Neck axis-CLASSIC	12,64	9,72	9,07	9,68		
Neck axis-SYMAX	15,48	12,57	11,92	12,52		
Neck axis-HAUPTMAN A	39,45	36,53	35,88	36,48		
Neck axis-HAUPTMAN B	7,75	4,83	4,18	4,79		
Neck axis-MONTAVON	41,65	38,73	38,08	38,68		

LEFT FEMUR N.4

Table XX Left femur n.4: 2-dimensional values of the angles obtained with different methods. Blue: Anatomic Lateral Proximal Femoral Angle (aLPFA); grey: Mechanical Lateral Proximal Femoral Angle (mLPFA); green: Anatomic Medial Distal Femoral Angle (aMDFA); light blue: Mechanical Medial Distal Femoral Angle (mMDFA); yellow: Femoral Varus Angle; red: Angle of version; orange: Neck-Shaft Angle

	Anatomic axis SYMAX	Anatomic axis MONTAVON	Anatomic axis KOWALESKY	Anatomic axis TOMLINSON	Mechanical axis	Angle of version
Hip joint orientation line	115,12	116,44	115,98	116,29	110,65	35,18
Transcondylar axis	91,05	92,37	91,91	92,22	86,58	
Distal femoral long axis	1,05	2,38	1,91	2,23		
Neck axis-CLASSIC	126,93	125,61	126,08	125,76		
Neck axis-SYMAX	123,53	122,21	122,68	122,36		
Neck axis-HAUPTMAN A	151,50	150,18	150,64	150,33		
Neck axis-HAUPTMAN B	123,95	122,63	123,09	122,77		
Neck axis-MONTAVON	151,02	149,70	150,17	149,85		

Table XXI Left femur n.4: 3-dimensional values of the angles obtained with different methods. Blue: Anatomic Lateral Proximal Femoral Angle (aLPFA); grey: Mechanical Lateral Proximal Femoral Angle (mLPFA); green: Anatomic Medial Distal Femoral Angle (aMDFA); light blue: Mechanical Medial Distal Femoral Angle (mMDFA); yellow: Femoral Varus Angle; red: Angle of version; orange: Neck-Shaft Angle.

	Neck-shaft angle	Femoral varus angle	aMDFA	aLPFA	mLPFA	mMDFA	Angle of version
	116,36	0,19	94,69	122,42	114,41	89,5	20,98
5% of the value	*5,82*	*0,01*	*4,73*	*6,12*	*5,72*	*4,48*	*1,05*

Table XXII Left femur n.4: "Standard difference" between 2D-angles obtained with different methods and3D-angles obtained in the same way. Blue: Anatomic Lateral Proximal Femoral Angle (aLPFA); grey: Mechanical Lateral Proximal Femoral Angle (mLPFA); green: Anatomic Medial Distal Femoral Angle (aMDFA); light blue: Mechanical Medial Distal Femoral Angle (mMDFA); yellow: Femoral Varus Angle; red: Angle of version; orange: Neck-Shaft Angle.
The underlined values are values whit p<0,05.

	Anatomic axis SYMAX	Anatomic axis MONTAVON	Anatomic axis KOWALESKY	Anatomic axis TOMLINSON	Mechanical axis	Angle of version
Hip joint orientation line	7,30	**5,98**	**6,44**	**6,13**	**3,76**	14,20
Transcondylar axis	**3,64**	**2,32**	**2,78**	**2,47**	**2,92**	
Distal femoral long axis	0,86	2,19	1,72	2,04		
Neck axis-CLASSIC	10,57	9,25	9,72	9,40		
Neck axis-SYMAX	7,17	5,85	6,32	6,00		
Neck axis-HAUPTMAN A	35,14	33,82	34,28	33,97		
Neck axis-HAUPTMAN B	7,59	6,27	6,73	6,41		
Neck axis-MONTAVON	34,66	33,34	33,81	33,49		

RIGHT FEMUR N.5

Table XXIII Right femur n.5: 2-dimensional values of the angles obtained with different methods. Blue: Anatomic Lateral Proximal Femoral Angle (aLPFA); grey: Mechanical Lateral Proximal Femoral Angle (mLPFA); green: Anatomic Medial Distal Femoral Angle (aMDFA); light blue: Mechanical Medial Distal Femoral Angle (mMDFA); yellow: Femoral Varus Angle; red: Angle of version; orange: Neck-Shaft Angle

	Anatomic axis SYMAX	Anatomic axis MONTAVON	Anatomic axis KOWALESKY	Anatomic axis TOMLINSON	Mechanical axis	Angle of version
Hip joint orientation line	103,18	102,38	104,43	101,19	97,75	39,01
Transcondylar axis	88,25	87,45	89,50	86,26	82,82	
Distal femoral long axis	1,75	2,55	0,50	3,74		
Neck axis-CLASSIC	123,39	124,19	122,14	125,38		
Neck axis-SYMAX	123,80	124,60	122,55	125,79		
Neck axis-HAUPTMAN A	148,42	149,22	147,17	150,41		
Neck axis-HAUPTMAN B	122,28	123,08	121,03	124,27		
Neck axis-MONTAVON	150,57	151,37	149,32	152,56		

Table XXIV Right femur n.5: 3-dimensional values of the angles obtained with different methods. Blue: Anatomic Lateral Proximal Femoral Angle (aLPFA); grey: Mechanical Lateral Proximal Femoral Angle (mLPFA); green: Anatomic Medial Distal Femoral Angle (aMDFA); light blue: Mechanical Medial Distal Femoral Angle (mMDFA); yellow: Femoral Varus Angle; red: Angle of version; orange: Neck-Shaft Angle.

	Neck-shaft angle	Femoral varus angle	aMDFA	aLPFA	mLPFA	mMDFA	Angle of version
	115,47	0,39	88,55	111,57	106,14	85,21	35,31
5% of the value	*5,77*	*0,02*	*4,43*	*5,58*	*5,31*	*4,26*	*1,77*

Table XXV Right femur n.5: "Standard difference" between 2D-angles obtained with different methods and3D-angles obtained in the same way. Blue: Anatomic Lateral Proximal Femoral Angle (aLPFA); grey: Mechanical Lateral Proximal Femoral Angle (mLPFA); green: Anatomic Medial Distal Femoral Angle (aMDFA); light blue: Mechanical Medial Distal Femoral Angle (mMDFA); yellow: Femoral Varus Angle; red: Angle of version; orange: Neck-Shaft Angle.
The underlined values are values whit p<0,05.

	Anatomic axis SYMAX	Anatomic axis MONTAVON	Anatomic axis KOWALESKY	Anatomic axis TOMLINSON	Mechanical axis	Angle of version
Hip joint orientation line	8,39	9,19	7,14	10,38	8,39	3,70
Transcondylar axis	**0,30**	**1,10**	**0,95**	**2,29**	**2,39**	
Distal femoral long axis	1,36	2,16	0,11	3,35		
Neck axis-CLASSIC	7,92	8,72	6,67	9,91		
Neck axis-SYMAX	8,33	9,13	7,08	10,32		
Neck axis-HAUPTMAN A	32,95	33,75	31,70	34,94		
Neck axis-HAUPTMAN B	6,81	7,61	**5,56**	8,80		
Neck axis-MONTAVON	35,10	35,90	33,85	37,09		

LEFT FEMUR N.5

Table XXVI Left femur n.5: 2-dimensional values of the angles obtained with different methods. Blue: Anatomic Lateral Proximal Femoral Angle (aLPFA); grey: Mechanical Lateral Proximal Femoral Angle (mLPFA); green: Anatomic Medial Distal Femoral Angle (aMDFA); light blue: Mechanical Medial Distal Femoral Angle (mMDFA); yellow: Femoral Varus Angle; red: Angle of version; orange: Neck-Shaft Angle

	Anatomic axis SYMAX	Anatomic axis MONTAVON	Anatomic axis KOWALESKY	Anatomic axis TOMLINSON	Mechanical axis	Angle of version
Hip joint orientation line	102,27	103,86	103,64	100,57	97,30	26,93
Transcondylar axis	87,90	89,49	89,27	86,20	82,93	
Distal femoral long axis	2,10	0,51	0,73	3,80		
Neck axis-CLASSIC	122,90	121,31	121,54	124,60		
Neck axis-SYMAX	124,20	122,60	122,83	125,90		
Neck axis-HAUPTMAN A	146,66	145,07	145,30	148,36		
Neck axis-HAUPTMAN B	119,08	117,48	117,71	120,78		
Neck axis-MONTAVON	149,64	148,04	148,27	151,34		

Table XXVII Left femur n.5: 3-dimensional values of the angles obtained with different methods. Blue: Anatomic Lateral Proximal Femoral Angle (aLPFA); grey: Mechanical Lateral Proximal Femoral Angle (mLPFA); green: Anatomic Medial Distal Femoral Angle (aMDFA); light blue: Mechanical Medial Distal Femoral Angle (mMDFA); yellow: Femoral Varus Angle; red: Angle of version; orange: Neck-Shaft Angle.

	Neck-shaft angle	Femoral varus angle	aMDFA	aLPFA	mLPFA	mMDFA	Angle of version
	119,73	10,4	88,89	110,24	102,56	85,39	31,41
5% of the value	*5,99*	*0,52*	*4,44*	*5,51*	*5,13*	*4,27*	*1,57*

Table XXVIII Left femur n.5: "Standard difference" between 2D-angles obtained with different methods and3D-angles obtained in the same way. Blue: Anatomic Lateral Proximal Femoral Angle (aLPFA); grey: Mechanical Lateral Proximal Femoral Angle (mLPFA); green: Anatomic Medial Distal Femoral Angle (aMDFA); light blue: Mechanical Medial Distal Femoral Angle (mMDFA); yellow: Femoral Varus Angle; red: Angle of version; orange: Neck-Shaft Angle.
The underlined values are values whit p<0,05.

	Anatomic axis SYMAX	Anatomic axis MONTAVON	Anatomic axis KOWALESKY	Anatomic axis TOMLINSON	Mechanical axis	Angle of version
Hip joint orientation line	7,97	6,38	6,60	9,67	5,26	4,48
Transcondylar axis	**0,99**	**0,60**	**0,38**	**2,69**	**2,46**	
Distal femoral long axis	8,30	9,89	9,67	6,60		
Neck axis-CLASSIC	**3,17**	**1,58**	**1,81**	**4,87**		
Neck axis-SYMAX	**4,47**	**2,87**	**3,10**	6,17		
Neck axis-HAUPTMAN A	26,93	25,34	25,57	28,63		
Neck axis-HAUPTMAN B	**0,65**	**2,25**	**2,02**	**1,05**		
Neck axis-MONTAVON	29,91	28,31	28,54	31,61		

RIGHT FEMUR N.6

Table XXIX Right femur n.6: 2-dimensional values of the angles obtained with different methods. Blue: Anatomic Lateral Proximal Femoral Angle (aLPFA); grey: Mechanical Lateral Proximal Femoral Angle (mLPFA); green: Anatomic Medial Distal Femoral Angle (aMDFA); light blue: Mechanical Medial Distal Femoral Angle (mMDFA); yellow: Femoral Varus Angle; red: Angle of version; orange: Neck-Shaft Angle

	Anatomic axis SYMAX	Anatomic axis MONTAVON	Anatomic axis KOWALESKY	Anatomic axis TOMLINSON	Mechanical axis	Angle of version
Hip joint orientation line	114,89	112,12	113,15	113,19	110,62	23,66
Transcondylar axis	85,43	82,65	83,69	83,73	81,16	
Distal femoral long axis	4,57	7,35	6,31	6,27		
Neck axis-CLASSIC	129,53	132,30	131,27	131,22		
Neck axis-SYMAX	128,26	131,04	130,00	129,96		
Neck axis-HAUPTMAN A	155,16	157,93	156,90	156,85		
Neck axis-HAUPTMAN B	124,07	126,85	125,82	125,77		
Neck axis-MONTAVON	158,36	161,13	160,10	160,05		

Table XXX Right femur n.6: 3-dimensional values of the angles obtained with different methods. Blue: Anatomic Lateral Proximal Femoral Angle (aLPFA); grey: Mechanical Lateral Proximal Femoral Angle (mLPFA); green: Anatomic Medial Distal Femoral Angle (aMDFA); light blue: Mechanical Medial Distal Femoral Angle (mMDFA); yellow: Femoral Varus Angle; red: Angle of version; orange: Neck-Shaft Angle.

	Neck-shaft angle	Femoral varus angle	aMDFA	aLPFA	mLPFA	mMDFA	Angle of version
	120,78	15,85	84,71	111,92	109,28	82,15	27,73
5% of the value	*6,04*	*0,79*	*4,24*	*5,60*	*5,46*	*4,11*	*1,39*

Table XXXI Right femur n.6: "Standard difference" between 2D-angles obtained with different methods and3D-angles obtained in the same way. Blue: Anatomic Lateral Proximal Femoral Angle (aLPFA); grey: Mechanical Lateral Proximal Femoral Angle (mLPFA); green: Anatomic Medial Distal Femoral Angle (aMDFA); light blue: Mechanical Medial Distal Femoral Angle (mMDFA); yellow: Femoral Varus Angle; red: Angle of version; orange: Neck-Shaft Angle.
The underlined values are values whit p<0,05.

	Anatomic axis SYMAX	Anatomic axis MONTAVON	Anatomic axis KOWALESKY	Anatomic axis TOMLINSON	Mechanical axis	Angle of version
Hip joint orientation line	**2,97**	**0,20**	**1,23**	**1,27**	**1,34**	4,07
Transcondylar axis	**0,72**	**2,06**	**1,02**	**0,98**	**0,99**	
Distal femoral long axis	11,28	8,50	9,54	9,58		
Neck axis-CLASSIC	8,75	11,52	10,49	10,44		
Neck axis-SYMAX	7,48	10,26	9,22	9,18		
Neck axis-HAUPTMAN A	34,38	37,15	36,12	36,07		
Neck axis-HAUPTMAN B	**3,29**	**6,07**	**5,04**	**4,99**		
Neck axis-MONTAVON	37,58	40,35	39,32	39,27		

LEFT FEMUR N.6

Table XXXII Left femur n.6: 2-dimensional values of the angles obtained with different methods. Blue: Anatomic Lateral Proximal Femoral Angle (aLPFA); grey: Mechanical Lateral Proximal Femoral Angle (mLPFA); green: Anatomic Medial Distal Femoral Angle (aMDFA); light blue: Mechanical Medial Distal Femoral Angle (mMDFA); yellow: Femoral Varus Angle; red: Angle of version; orange: Neck-Shaft Angle

	Anatomic axis SYMAX	Anatomic axis MONTAVON	Anatomic axis KOWALESKY	Anatomic axis TOMLINSON	Mechanical axis	Angle of version
Hip joint orientation line	116,91	117,56	118,71	116,67	111,90	15,86
Transcondylar axis	87,30	87,95	89,10	87,06	82,29	
Distal femoral long axis	2,70	2,05	0,90	2,94		
Neck axis-CLASSIC	124,90	124,25	123,10	125,14		
Neck axis-SYMAX	125,46	124,81	123,66	125,70		
Neck axis-HAUPTMAN A	148,35	147,70	146,55	148,59		
Neck axis-HAUPTMAN B	126,38	125,73	124,58	126,62		
Neck axis-MONTAVON	151,38	150,74	149,59	151,63		

Table XIII Left femur n.6: 3-dimensional values of the angles obtained with different methods. Blue: Anatomic Lateral Proximal Femoral Angle (aLPFA); grey: Mechanical Lateral Proximal Femoral Angle (mLPFA); green: Anatomic Medial Distal Femoral Angle (aMDFA); light blue: Mechanical Medial Distal Femoral Angle (mMDFA); yellow: Femoral Varus Angle; red: Angle of version; orange: Neck-Shaft Angle.

	Neck-shaft angle	Femoral varus angle	aMDFA	aLPFA	mLPFA	mMDFA	Angle of version
	121,84	2,39	87,01	116,63	113,19	84,66	18,65
5% of the value	*6,09*	*0,12*	*4,35*	*5,83*	*5,66*	*4,23*	*0,93*

Table XXXIV Left femur n.6: "Standard difference" between 2D-angles obtained with different methods and3D-angles obtained in the same way. Blue: Anatomic Lateral Proximal Femoral Angle (aLPFA); grey: Mechanical Lateral Proximal Femoral Angle (mLPFA); green: Anatomic Medial Distal Femoral Angle (aMDFA); light blue: Mechanical Medial Distal Femoral Angle (mMDFA); yellow: Femoral Varus Angle; red: Angle of version; orange: Neck-Shaft Angle.
The underlined values are values whit p<0,05.

	Anatomic axis SYMAX	Anatomic axis MONTAVON	Anatomic axis KOWALESKY	Anatomic axis TOMLINSON	Mechanical axis	Angle of version
Hip joint orientation line	0,28	0,93	2,08	0,04	1,29	2,79
Transcondylar axis	0,29	0,94	2,09	0,05	2,37	
Distal femoral long axis	0,31	0,34	1,49	0,55		
Neck axis-CLASSIC	3,06	2,41	1,26	3,30		
Neck axis-SYMAX	3,62	2,97	1,82	3,86		
Neck axis-HAUPTMAN A	26,51	25,86	24,71	26,75		
Neck axis-HAUPTMAN B	4,54	3,89	2,74	4,78		
Neck axis-MONTAVON	29,54	28,90	27,75	29,79		

RIGHT FEMUR N.7

Table XXXV Right femur n.7: 2-dimensional values of the angles obtained with different methods. Blue: Anatomic Lateral Proximal Femoral Angle (aLPFA); grey: Mechanical Lateral Proximal Femoral Angle (mLPFA); green: Anatomic Medial Distal Femoral Angle (aMDFA); light blue: Mechanical Medial Distal Femoral Angle (mMDFA); yellow: Femoral Varus Angle; red: Angle of version; orange: Neck-Shaft Angle

	Anatomic axis SYMAX	Anatomic axis MONTAVON	Anatomic axis KOWALESKY	Anatomic axis TOMLINSON	Mechanical axis	Angle of version
Hip joint orientation line	102,46	101,7	110,2	100,75	97,06	30,46
Transcondylar axis	87,88	87,11	95,61	86,16	82,47	
Distal femoral long axis	2,12	2,89	5,61	3,84		
Neck axis-CLASSIC	128,9	129,66	121,17	130,61		
Neck axis-SYMAX	133,3	134,06	125,57	135,01		
Neck axis-HAUPTMAN A	147,96	148,72	140,23	149,67		
Neck axis-HAUPTMAN B	112,91	113,67	105,18	114,62		
Neck axis-MONTAVON	151,54	152,3	143,81	153,25		

Table XXXVI Right femur n.7: 3-dimensional values of the angles obtained with different methods. Blue: Anatomic Lateral Proximal Femoral Angle (aLPFA); grey: Mechanical Lateral Proximal Femoral Angle (mLPFA); green: Anatomic Medial Distal Femoral Angle (aMDFA); light blue: Mechanical Medial Distal Femoral Angle (mMDFA); yellow: Femoral Varus Angle; red: Angle of version; orange: Neck-Shaft Angle.

	Neck-shaft angle	Femoral varus angle	aMDFA	aLPFA	mLPFA	mMDFA	Angle of version
	128,71	11,49	85,53	106,97	101,04	82,55	23,54
5% of the value	*6,44*	*0,57*	*4,28*	*5,35*	*5,05*	*4,13*	*1,18*

Table XXXVII Right femur n.7: "Standard difference" between 2D-angles obtained with different methods and3D-angles obtained in the same way. Blue: Anatomic Lateral Proximal Femoral Angle (aLPFA); grey: Mechanical Lateral Proximal Femoral Angle (mLPFA); green: Anatomic Medial Distal Femoral Angle (aMDFA); light blue: Mechanical Medial Distal Femoral Angle (mMDFA); yellow: Femoral Varus Angle; red: Angle of version; orange: Neck-Shaft Angle.
The underlined values are values whit p<0,05.

	Anatomic axis SYMAX	Anatomic axis MONTAVON	Anatomic axis KOWALESKY	Anatomic axis TOMLINSON	Mechanical axis	Angle of version
Hip joint orientation line	**4,51**	**5,27**	**3,23**	6,22	**3,98**	6,92
Transcondylar axis	**2,35**	**1,58**	10,08	**0,63**	**0,08**	
Distal femoral long axis	9,37	8,60	5,88	7,65		
Neck axis-CLASSIC	**0,19**	**0,95**	7,54	**1,90**		
Neck axis-SYMAX	**4,59**	**5,35**	**3,14**	**6,30**		
Neck axis-HAUPTMAN A	19,25	20,01	11,52	20,96		
Neck axis-HAUPTMAN B	15,80	15,04	23,53	14,09		
Neck axis-MONTAVON	22,83	23,59	15,10	24,54		

LEFT FEMUR N.7

Table XXXVIII Left femur n.7: 2-dimensional values of the angles obtained with different methods. Blue: Anatomic Lateral Proximal Femoral Angle (aLPFA); grey: Mechanical Lateral Proximal Femoral Angle (mLPFA); green: Anatomic Medial Distal Femoral Angle (aMDFA); light blue: Mechanical Medial Distal Femoral Angle (mMDFA); yellow: Femoral Varus Angle; red: Angle of version; orange: Neck-Shaft Angle

	Anatomic axis SYMAX	Anatomic axis MONTAVON	Anatomic axis KOWALESKY	Anatomic axis TOMLINSON	Mechanical axis	Angle of version
Hip joint orientation line	107,79	107,48	112,08	106,83	102,53	29,54
Transcondylar axis	88,04	87,72	92,32	87,08	82,77	
Distal femoral long axis	1,96	2,28	2,32	2,92		
Neck axis-CLASSIC	128,36	128,67	124,07	129,32		
Neck axis-SYMAX	127,61	127,92	123,32	128,56		
Neck axis-HAUPTMAN A	148,01	148,32	143,72	148,96		
Neck axis-HAUPTMAN B	123,05	123,36	118,76	124,01		
Neck axis-MONTAVON	150,4	150,72	146,12	151,36		

Table XXXIX Left femur n.7: 3-dimensional values of the angles obtained with different methods. Blue: Anatomic Lateral Proximal Femoral Angle (aLPFA); grey: Mechanical Lateral Proximal Femoral Angle (mLPFA); green: Anatomic Medial Distal Femoral Angle (aMDFA); light blue: Mechanical Medial Distal Femoral Angle (mMDFA); yellow: Femoral Varus Angle; red: Angle of version; orange: Neck-Shaft Angle.

	Neck-shaft angle	Femoral varus angle	aMDFA	aLPFA	mLPFA	mMDFA	Angle of version
	116,93	9,39	85,88	109,95	105,22	82,68	23,24
5% of the value	*5,85*	*0,47*	*4,29*	*5,50*	*5,26*	*4,13*	*1,16*

Table XL Left femur n.7: "Standard difference" between 2D-angles obtained with different methods and3D-angles obtained in the same way. Blue: Anatomic Lateral Proximal Femoral Angle (aLPFA); grey: Mechanical Lateral Proximal Femoral Angle (mLPFA); green: Anatomic Medial Distal Femoral Angle (aMDFA); light blue: Mechanical Medial Distal Femoral Angle (mMDFA); yellow: Femoral Varus Angle; red: Angle of version; orange: Neck-Shaft Angle.
The underlined values are values whit p<0,05.

	Anatomic axis SYMAX	Anatomic axis MONTAVON	Anatomic axis KOWALESKY	Anatomic axis TOMLINSON	Mechanical axis	Angle of version
Hip joint orientation line	**2,16**	**2,47**	**2,13**	**3,12**	**2,69**	6,30
Transcondylar axis	**2,16**	**1,84**	6,44	**1,20**	**0,09**	
Distal femoral long axis	7,43	7,11	7,07	6,47		
Neck axis-CLASSIC	11,43	11,74	7,14	12,39		
Neck axis-SYMAX	10,68	10,99	6,39	11,63		
Neck axis-HAUPTMAN A	31,08	31,39	26,79	32,03		
Neck axis-HAUPTMAN B	6,12	6,43	**1,83**	7,08		
Neck axis-MONTAVON	33,47	33,79	29,19	34,43		

RIGHT FEMUR N.8

Table XLI Right femur n.8: 2-dimensional values of the angles obtained with different methods. Blue: Anatomic Lateral Proximal Femoral Angle (aLPFA); grey: Mechanical Lateral Proximal Femoral Angle (mLPFA); green: Anatomic Medial Distal Femoral Angle (aMDFA); light blue: Mechanical Medial Distal Femoral Angle (mMDFA); yellow: Femoral Varus Angle; red: Angle of version; orange: Neck-Shaft Angle

	Anatomic axis SYMAX	Anatomic axis MONTAVON	Anatomic axis KOWALESKY	Anatomic axis TOMLINSON	Mechanical axis	Angle of version
Hip joint orientation line	112,9	111,61	113,75	111,48	107,68	23,58
Transcondylar axis	83,95	82,66	84,8	82,53	78,73	
Distal femoral long axis	6,05	7,34	5,2	7,47		
Neck axis-CLASSIC	118,9	120,19	118,05	120,32		
Neck axis-SYMAX	123,4	124,69	122,55	124,82		
Neck axis-HAUPTMAN A	135,8	137,09	134,96	137,22		
Neck axis-HAUPTMAN B	119,75	121,04	118,9	121,17		
Neck axis-MONTAVON	143,22	144,51	142,37	144,64		

Table XLII Right femur n.8: 3-dimensional values of the angles obtained with different methods. Blue: Anatomic Lateral Proximal Femoral Angle (aLPFA); grey: Mechanical Lateral Proximal Femoral Angle (mLPFA); green: Anatomic Medial Distal Femoral Angle (aMDFA); light blue: Mechanical Medial Distal Femoral Angle (mMDFA); yellow: Femoral Varus Angle; red: Angle of version; orange: Neck-Shaft Angle.

	Neck-shaft angle	Femoral varus angle	aMDFA	aLPFA	mLPFA	mMDFA	Angle of version
	130,28	9,91	86,71	115,15	108,65	82,53	11,78
5% of the value	*6,51*	*0,50*	*4,34*	*5,76*	*5,43*	*4,13*	*0,59*

Table XLIII Right femur n.8: "Standard difference" between 2D-angles obtained with different methods and3D-angles obtained in the same way. Blue: Anatomic Lateral Proximal Femoral Angle (aLPFA); grey: Mechanical Lateral Proximal Femoral Angle (mLPFA); green: Anatomic Medial Distal Femoral Angle (aMDFA); light blue: Mechanical Medial Distal Femoral Angle (mMDFA); yellow: Femoral Varus Angle; red: Angle of version; orange: Neck-Shaft Angle.
The underlined values are values whit p<0,05.

	Anatomic axis SYMAX	Anatomic axis MONTAVON	Anatomic axis KOWALESKY	Anatomic axis TOMLINSON	Mechanical axis	Angle of version
Hip joint orientation line	**2,25**	**3,54**	**1,40**	**3,67**	**0,97**	11,80
Transcondylar axis	**2,76**	**4,05**	**1,91**	**4,18**	**3,80**	
Distal femoral long axis	3,86	2,57	4,71	2,44		
Neck axis-CLASSIC	11,38	10,09	12,23	9,96		
Neck axis-SYMAX	6,88	**5,59**	7,73	**5,46**		
Neck axis-HAUPTMAN A	**5,52**	6,81	**4,68**	6,94		
Neck axis-HAUPTMAN B	10,53	9,24	11,38	9,11		
Neck axis-MONTAVON	12,94	14,23	12,09	14,36		

LEFT FEMUR N.8

Table XLIV Left femur n.8 2-dimensional values of the angles obtained with different methods. Blue: Anatomic Lateral Proximal Femoral Angle (aLPFA); grey: Mechanical Lateral Proximal Femoral Angle (mLPFA); green: Anatomic Medial Distal Femoral Angle (aMDFA); light blue: Mechanical Medial Distal Femoral Angle (mMDFA); yellow: Femoral Varus Angle; red: Angle of version; orange: Neck-Shaft Angle

	Anatomic axis SYMAX	Anatomic axis MONTAVON	Anatomic axis KOWALESKY	Anatomic axis TOMLINSON	Mechanical axis	Angle of version
Hip joint orientation line	114,16	112,35	113,77	112,54	109,12	34,08
Transcondylar axis	85,66	83,85	85,28	84,05	80,62	
Distal femoral long axis	4,34	6,15	4,72	5,95		
Neck axis-CLASSIC	117,91	119,73	118,3	119,53		
Neck axis-SYMAX	123,32	125,14	123,71	124,94		
Neck axis-HAUPTMAN A	138,19	140,01	138,58	139,81		
Neck axis-HAUPTMAN B	123,32	125,14	123,71	124,94		
Neck axis-MONTAVON	144,9	146,71	145,29	146,52		

Table XLV Left femur n.8: 3-dimensional values of the angles obtained with different methods. Blue: Anatomic Lateral Proximal Femoral Angle (aLPFA); grey: Mechanical Lateral Proximal Femoral Angle (mLPFA); green: Anatomic Medial Distal Femoral Angle (aMDFA); light blue: Mechanical Medial Distal Femoral Angle (mMDFA); yellow: Femoral Varus Angle; red: Angle of version; orange: Neck-Shaft Angle.

	Neck-shaft angle	Femoral varus angle	aMDFA	aLPFA	mLPFA	mMDFA	Angle of version
	127,92	9,25	85,25	117,69	110,71	81,27	13,21
5% of the value	6,4	0,46	4,26	5,88	5,54	4,06	0,66

Table XLVI Left femur n.8: "Standard difference" between 2D-angles obtained with different methods and3D-angles obtained in the same way. Blue: Anatomic Lateral Proximal Femoral Angle (aLPFA); grey: Mechanical Lateral Proximal Femoral Angle (mLPFA); green: Anatomic Medial Distal Femoral Angle (aMDFA); light blue: Mechanical Medial Distal Femoral Angle (mMDFA); yellow: Femoral Varus Angle; red: Angle of version; orange: Neck-Shaft Angle.
The underlined values are values whit p<0,05.

	Anatomic axis SYMAX	Anatomic axis MONTAVON	Anatomic axis KOWALESKY	Anatomic axis TOMLINSON	Mechanical axis	Angle of version
Hip joint orientation line	**3,53**	**5,34**	**3,92**	**5,15**	**1,59**	20,87
Transcondylar axis	**0,41**	**1,40**	**0,03**	**1,20**	**0,65**	
Distal femoral long axis	4,91	3,10	4,53	3,30		
Neck axis-CLASSIC	10,01	8,19	9,62	8,39		
Neck axis-SYMAX	**4,60**	**2,78**	**4,21**	**2,98**		
Neck axis-HAUPTMAN A	10,27	12,09	10,66	11,89		
Neck axis-HAUPTMAN B	**4,60**	**2,78**	**4,21**	**2,98**		
Neck axis-MONTAVON	16,98	18,79	17,37	18,60		

Table XLVII Variance in 16 femora. Blue: Anatomic Lateral Proximal Femoral Angle (aLPFA); grey: Mechanical Lateral Proximal Femoral Angle (mLPFA); green: Anatomic Medial Distal Femoral Angle (aMDFA); light blue: Mechanical Medial Distal Femoral Angle (mMDFA); yellow: Femoral Varus Angle; red: Angle of version; orange: Neck-Shaft Angle.
Red underlined values are values are the best values.

	Anatomic axis SYMAX	Anatomic axis MONTAVON	Anatomic axis KOWALESKY	Anatomic axis TOMLINSON	Mechanical axis	Angle of version
Hip joint orientation line	5,39	6,57	5,99	8,46	4,25	30,35
Transcondylar axis	1,35	1,11	8,47	1,33	2,40	
Distal femoral long axis	12,77	9,55	9,97	7,97		
Neck axis-CLASSIC	17,51	15,25	12,42	12,92		
Neck axis-SYMAX	15,25	12,67	8,81	12,88		
Neck axis-HAUPTMAN A	87,31	78,35	97,07	77,64		
Neck axis-HAUPTMAN B	26,75	24,95	47,40	23,81		
Neck axis-MONTAVON	64,52	57,88	77,75	56,56		

Appendix B

Table I 2-dimensional values of the tibial angles obtained in 16 different bones

DATI 2D	TIBIA 1dx	TIBIA 1sx	TIBIA 2dx	TIBIA 2sx	TIBIA 3dx	TIBIA 3sx	TIBIA 4dx	TIBIA 4sx
mMPTA	93,70	94,00	95,00	96,40	92,40	91,40	91,00	96,20
mMDTA	93,70	95,80	91,30	90,60	92,80	91,60	95,60	96,60
MAD	3,70	4,00	5,00	6,40	2,40	1,40	1,00	6,20

	TIBIA 5dx	TIBIA 5sx	TIBIA 6dx	TIBIA 6sx	TIBIA 7dx	TIBIA 7sx	TIBIA 8dx	TIBIA 8sx
mMPTA	94,91	94,22	94,73	95,68	92,18	92,12	94,62	92,40
mMDTA	95,20	95,85	93,47	98,14	95,93	98,48	94,55	93,84
MAD	4,91	4,22	4,73	5,68	2,18	2,12	4,62	2,40

Table II 3-dimensional values of the tibial angles obtained in 16 different bones

DATI 3D	TIBIA 1dx	TIBIA 1sx	TIBIA 2dx	TIBIA 2sx	TIBIA 3dx	TIBIA 3sx	TIBIA 4dx	TIBIA 4sx
mMPTA	93,50	93,20	91,80	90,90	94,10	94,60	93,60	97,20
mMDTA	96,00	97,30	90,50	95,30	95,90	95,40	92,60	96,00
MAD	3,50	3,20	1,80	0,90	4,10	4,60	3,60	7,20

	TIBIA 5dx	TIBIA 5sx	TIBIA 6dx	TIBIA 6sx	TIBIA 7dx	TIBIA 7sx	TIBIA 8dx	TIBIA 8sx
mMPTA	94,21	92,68	101,06	99,62	92,35	98,34	92,38	93,83
mMDTA	102,72	103,12	94,35	96,85	105,53	95,07	95,44	96,95
MAD	4,21	2,68	11,06	9,38	2,35	8,34	2,38	3,83